



Studies of new Higgs boson interactions through nonresonant HH production in the $b\bar{b}\gamma\gamma$ final state in pp collisions at $\sqrt{s} = 13$ TeV with the ATLAS detector

The ATLAS Collaboration

A search for nonresonant Higgs boson pair production in the $b\bar{b}\gamma\gamma$ final state is performed using 140 fb^{-1} of proton–proton collisions at a centre-of-mass energy of 13 TeV recorded by the ATLAS detector at the CERN Large Hadron Collider. This analysis supersedes and expands upon the previous nonresonant ATLAS results in this final state based on the same data sample. The analysis strategy is optimised to probe anomalous values not only of the Higgs (H) boson self-coupling modifier κ_λ but also of the quartic $HHVV$ ($V = W, Z$) coupling modifier κ_{2V} . No significant excess above the expected background from Standard Model processes is observed. An observed upper limit $\mu_{HH} < 4.0$ is set at 95% confidence level on the Higgs boson pair production cross-section normalised to its Standard Model prediction. The 95% confidence intervals for the coupling modifiers are $-1.4 < \kappa_\lambda < 6.9$ and $-0.5 < \kappa_{2V} < 2.7$, assuming all other Higgs boson couplings except the one under study are fixed to the Standard Model predictions. The results are interpreted in the Standard Model effective field theory and Higgs effective field theory frameworks in terms of constraints on the couplings of anomalous Higgs boson (self-)interactions.

Contents

1	Introduction	2
2	The ATLAS detector	5
3	Data and simulation samples	6
4	Event selection and classification	7
4.1	Event preselection	7
4.2	Event categories	8
5	Signal and background modelling of the diphoton mass spectrum	10
6	Systematic uncertainties	11
7	Results	13
8	Effective field theory interpretation	16
9	Conclusion	21

1 Introduction

Since the discovery of a Higgs boson (H) in 2012 [1, 2], the ATLAS and CMS collaborations at the Large Hadron Collider (LHC) have pursued an intense programme of measurements of its properties. All results obtained so far, such as the spin [3, 4], intrinsic width [5, 6], production and decay rates [7, 8] of this particle, are consistent with the predictions of the Standard Model (SM) [9–17] for a Higgs boson with an observed mass m_H near 125 GeV [18, 19].

The current measurements provide constraints on the strengths of the couplings of the Higgs boson to the heaviest of the SM elementary particles, and on the Higgs boson mass m_H . The latter is one of the parameters of the Higgs boson potential $V(H) = \frac{1}{2}m_H^2 H^2 + \lambda_{HHH}vH^3 + \frac{1}{4}\lambda_{HHHH}H^4$, where $v \approx 246$ GeV is the vacuum expectation value of the Higgs field. Among the SM predictions of the Higgs sector that still remain to be verified are those for the coupling strengths of the interactions involving multiple Higgs bosons, such as the trilinear and quartic Higgs boson self-couplings, λ_{HHH} and λ_{HHHH} , as well as the quartic couplings between two Higgs bosons and two W or Z bosons, g_{HHVV} ($V = W, Z$). In the SM, the trilinear and quartic self-couplings have the value $\lambda_{HHH}^{\text{SM}} = \lambda_{HHHH}^{\text{SM}} = m_H^2/2v^2$, while the couplings g_{HHVV} are related to the HWW and HZZ couplings g_{HVV} through $g_{HHVV}^{\text{SM}} = g_{HVV}^{\text{SM}}/2v$.

A significant effort has been dedicated by the ATLAS and CMS collaborations to search for processes that are particularly sensitive to λ_{HHH} and g_{HHVV} , such as Higgs boson pair production in gluon–gluon fusion (ggF) and vector-boson fusion (VBF). In the SM, ggF HH production proceeds through the destructive interference of two leading Feynman diagrams: one for the process $gg \rightarrow H^* \rightarrow HH$, involving an intermediate virtual Higgs boson (H^*) and a HHH vertex (Figure 1(a)), and a second one describing a loop-mediated process in which two Higgs bosons are radiated off a virtual quark (Figure 1(b)). VBF HH production is induced at tree level in the SM by three Feynman diagrams in which the two vector bosons

radiated by the scattering quarks either fuse into a virtual Higgs boson H^* decaying into two Higgs bosons via a HHH vertex (Figure 2(a)), fuse into two Higgs bosons via a $HHVV$ vertex (Figure 2(b)), or produce two Higgs bosons via t -channel scattering through two HVV interactions (Figure 2(c)). The amplitudes of diagrams involving a HHH vertex are proportional to λ_{HHH} , while those of diagrams involving a $HHVV$ vertex are proportional to g_{HHVV} . For this reason, the results of the searches for HH production can be used to infer the values of the coupling modifiers $\kappa_\lambda \equiv \lambda_{HHH}/\lambda_{HHH}^{\text{SM}}$ and $\kappa_{2V} = g_{HHVV}/g_{HHVV}^{\text{SM}}$. An observed value of these coupling modifiers significantly different from unity would provide a proof of non-SM Higgs boson interactions [20].

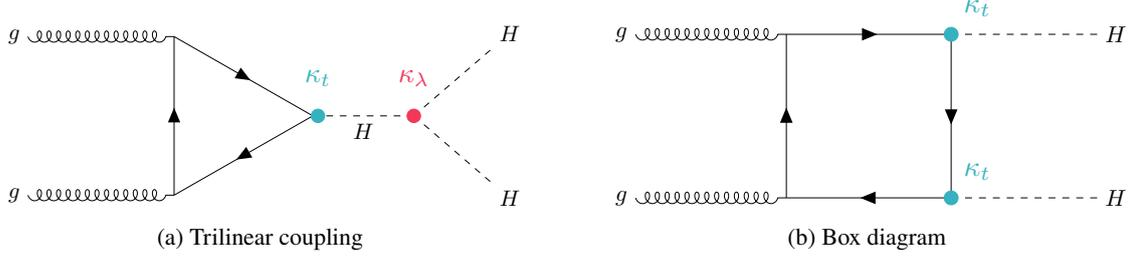


Figure 1: The Feynman diagrams for the dominant gluon–gluon fusion production processes. In the SM, the (a) trilinear coupling process, (b) box diagram, and the destructive interference between the two processes, contribute to the total cross-section. In the figure, κ_λ represents the Higgs boson trilinear coupling modifier. The quark content in the diagram is dominated by the top-quark contribution due to the large top-quark Yukawa coupling to the Higgs boson. The corresponding coupling strength modifier is denoted by κ_t .

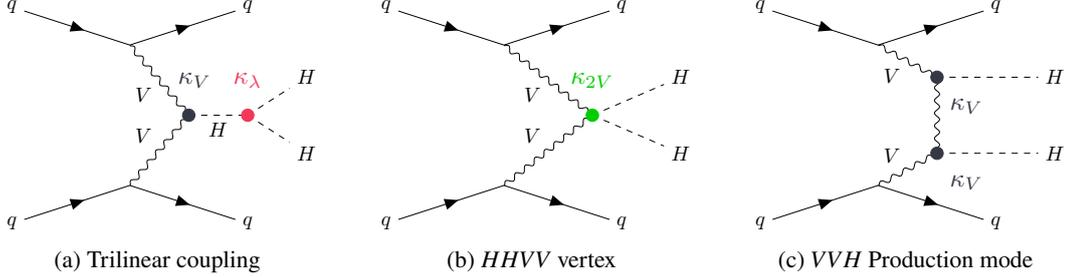


Figure 2: The VBF production of Higgs boson pairs via (a) the trilinear coupling, (b) the $HHVV$ vertex, and (c) the VVH production mode. In the figure, κ_V and κ_{2V} denote the HVV and $HHVV$ coupling strength modifiers.

In the SM, these processes are expected to be rare, with cross-sections that are about three orders of magnitude smaller than those of single Higgs boson production: $\sigma_{\text{ggF}}^{HH} = 31.1^{+2.1}_{-7.2}$ fb [21–28] and $\sigma_{\text{VBF}}^{HH} = 1.73 \pm 0.04$ fb [29–31] for $m_H = 125$ GeV and a proton-proton centre-of-mass energy of $\sqrt{s} = 13$ TeV. It is thus crucial to analyse the latest available data sample and reconstruct as many decay final states of the Higgs boson pairs as possible. The most stringent constraints on κ_λ and κ_{2V} exploit the entire sample of proton–proton (pp) collisions provided by the LHC during its second phase of data-taking (Run 2, 2015–2018), and a multitude of Higgs boson decay channels. In particular, the ATLAS experiment recently released the results of searches based on the full Run 2 data in the three most sensitive channels, $b\bar{b}\gamma\gamma$ [32], $b\bar{b}\tau^+\tau^-$ [33], and $b\bar{b}b\bar{b}$ [34], and their combination [35]. No excess over the SM background was observed, and constraints on the coupling modifiers κ_λ and κ_{2V} were set at the 95% confidence level (CL). The observed (expected for $\kappa_\lambda = 1$) 95% confidence interval for κ_λ when all other coupling strength modifiers are set to unity is $-0.6 < \kappa_\lambda < 6.6$ ($-2.1 < \kappa_\lambda < 7.8$) after combining the three HH decay

channels. For κ_{2V} , the observed (expected) 95% confidence interval when all other coupling strength modifiers are set to unity is $0.1 < \kappa_{2V} < 2.0$ ($0.0 < \kappa_{2V} < 2.1$). With a similar data sample, CMS also reported similar results in their $b\bar{b}\gamma\gamma$ [36], $b\bar{b}\tau^+\tau^-$ [37], and $b\bar{b}b\bar{b}$ [38, 39] channels, observing 95% CL intervals of $-1.2 < \kappa_\lambda < 6.5$ and $0.7 < \kappa_{2V} < 1.4$, based on a different statistical procedure [8].

The $b\bar{b}\gamma\gamma$ final state has an expected branching ratio (0.26%) that is significantly smaller than that of $b\bar{b}b\bar{b}$ (34%) and $b\bar{b}\tau^+\tau^-$ (7.3%). However, the larger expected signal-to-background (S/B) ratio and the higher trigger efficiency and thus larger acceptance in phase-space regions (e.g., at small values of the HH invariant mass), where potential deviations from the SM are expected to be enhanced, compensate for the lower expected event yield and lead to a sensitivity similar to that of the other two decay modes. The latest results for $HH \rightarrow b\bar{b}\gamma\gamma$ with the full Run 2 ATLAS data, based on the event selection and classification of Ref. [32] but using the statistical procedures of Ref. [35] and of this analysis, yields the following observed (expected) one-dimensional 95% confidence intervals: $-1.4 < \kappa_\lambda < 6.5$ ($-3.2 < \kappa_\lambda < 8.1$) and $-0.8 < \kappa_{2V} < 3.0$ ($-1.6 < \kappa_{2V} < 3.7$).

This paper presents an updated search for nonresonant Higgs boson pair production in the $b\bar{b}\gamma\gamma$ final state using the full Run 2 ATLAS data, superseding and expanding upon the nonresonant results of Ref. [32]. Compared to the previous publication, an identical event selection and a similar analysis strategy are used, but a reoptimised classification of events in categories with different S/B leads to a higher sensitivity to the κ_λ and κ_{2V} coupling modifiers. The new event classification relies on improved multivariate classifiers, also exploiting the kinematic features of VBF HH production for SM and anomalous values of κ_λ and κ_{2V} . After the events are classified in mutually orthogonal event categories, the signal cross-section is estimated through a simultaneous maximum-likelihood fit to the diphoton invariant mass spectrum of the selected events in each category. The fit probes an enhancement in event yields around the experimental value of the Higgs boson mass over the predicted background, consisting of the sum of a monotonically decreasing distribution from continuum photon and jet production and a peak from singly produced Higgs bosons decaying into two photons.

Another novelty compared to the previous publication is the interpretation of the results in two effective field theory (EFT) extensions to the SM, the Higgs effective field theory (HEFT) [40, 41] and the SM effective field theory (SMEFT) [42, 43]. The data are used to set constraints on the Wilson coefficients of operators of the EFT Lagrangians describing anomalous Higgs boson interactions in both frameworks. HEFT and SMEFT describe the same effective interactions, but with different bases of operators. One advantage of HEFT compared with SMEFT is that it provides a one-to-one relation between operators (and corresponding Wilson coefficients) and effective interactions, which allows single- and di-Higgs boson couplings to be separated, leading to simplified HH interpretations.

This paper is organised as follows. Section 2 describes the experimental apparatus. The data and simulated event samples used for the measurements are summarised in Section 3. Section 4 is devoted to the event selection and classification, with an emphasis on the novelties of the latter compared to the previous publication. The $m_{\gamma\gamma}$ signal and background models used in the final fit are described in Section 5. The systematic uncertainties in the measurement and the results are given in Sections 6 and 7, respectively. Finally, the procedure and results of the EFT interpretation are detailed in Section 8. Section 9 provides the conclusions.

2 The ATLAS detector

The ATLAS detector [44] at the LHC covers nearly the entire solid angle around the collision point.¹ It consists of an inner tracking detector surrounded by a thin superconducting solenoid, electromagnetic and hadron calorimeters, and a muon spectrometer incorporating three large superconducting air-core toroidal magnets.

The inner-detector system (ID) is immersed in a 2 T axial magnetic field and provides charged-particle tracking in the range of $|\eta| < 2.5$. The high-granularity silicon pixel detector covers the vertex region and typically provides four measurements per track, the first hit normally being in the insertable B-layer (IBL) installed before Run 2 [45, 46]. It is followed by the silicon microstrip tracker (SCT), which usually provides eight measurements per track. These silicon detectors are complemented by the transition radiation tracker (TRT), which enables radially extended track reconstruction up to $|\eta| = 2.0$. The TRT also provides electron identification information based on the fraction of hits (typically 30 in total) above a higher energy-deposit threshold corresponding to transition radiation.

The calorimeter system covers the pseudorapidity range of $|\eta| < 4.9$. In the region $|\eta| < 3.2$, electromagnetic calorimetry is provided by barrel and endcap high-granularity lead/liquid-argon (LAr) calorimeters, with an additional thin LAr presampler covering $|\eta| < 1.8$ to correct for energy loss in material upstream of the calorimeters. Hadron calorimetry is provided by the steel/scintillator-tile calorimeter, segmented into three barrel structures with $|\eta| < 1.7$, and two copper/LAr hadron endcap calorimeters. The solid angle coverage is completed with forward copper/LAr and tungsten/LAr calorimeter modules optimised for electromagnetic and hadronic energy measurements respectively.

The muon spectrometer (MS) comprises separate trigger and high-precision tracking chambers measuring the deflection of muons in a magnetic field generated by the superconducting air-core toroidal magnets. The field integral of the toroids ranges between 2.0 and 6.0 T m across most of the detector. Three layers of precision chambers, each consisting of layers of monitored drift tubes, cover the region $|\eta| < 2.7$, complemented by cathode-strip chambers in the forward region, where the background is highest. The muon trigger system covers the range of $|\eta| < 2.4$ with resistive-plate chambers in the barrel, and thin-gap chambers in the endcap regions.

Interesting events are selected by the first-level trigger system implemented in custom hardware, followed by selections made by algorithms implemented in software in the high-level trigger [47]. The first-level trigger accepts events from the 40 MHz bunch crossings at a rate below 100 kHz, which the high-level trigger further reduces in order to record events to disk at about 1 kHz.

An extensive software suite [48] is used in data simulation, in the reconstruction and analysis of real and simulated data, in detector operations, and in the trigger and data acquisition systems of the experiment.

¹ ATLAS uses a right-handed coordinate system with its origin at the nominal interaction point (IP) in the centre of the detector and the z -axis along the beam pipe. The x -axis points from the IP to the centre of the LHC ring, and the y -axis points upwards. Cylindrical coordinates (r, ϕ) are used in the transverse plane, ϕ being the azimuthal angle around the z -axis. The pseudorapidity is defined in terms of the polar angle θ as $\eta = -\ln \tan(\theta/2)$. The rapidity y is defined in terms of the energy, the momentum and the polar angle θ : $y = \frac{1}{2} \ln \left(\frac{E+p \cdot \cos \theta}{E-p \cdot \cos \theta} \right)$. The angular distance is measured in units of $\Delta R \equiv \sqrt{(\Delta\eta)^2 + (\Delta\phi)^2}$.

3 Data and simulation samples

The measurements presented in this paper use pp collision data collected by the ATLAS experiment during the LHC Run 2 at $\sqrt{s} = 13$ TeV. After data quality requirements [49], the integrated luminosity of the data sample is $140.1 \pm 1.2 \text{ fb}^{-1}$ [50].

The simulated event samples used in this study are summarised in Table 1. Besides the samples already used in Ref. [32], VBF HH samples were produced for additional κ_{2V} and κ_V variations (where $\kappa_V = g_{HVV}/g_{HVV}^{\text{SM}}$ is the HVV coupling modifier), and a dedicated diphoton + two b -jet sample was generated.

Table 1: Summary of the nominal Higgs boson pair signal, single Higgs boson background and continuum background event samples used in this analysis. The generator used in the simulation, the parton distribution function (PDF) set, and the set of tuned parameters (tune) are also provided. The final two columns list the accuracy in QCD of the event generator and the order in QCD of the calculated cross-section for the HH signal and the single Higgs boson background (LO: leading order, NLO: next-to-leading order, NNLO: next-to-next-to-leading order, N³LO: next-to-next-to-next-to-leading order). More details are given in the text and in Ref. [32]. The accuracy and cross-sections for the nonresonant background processes are omitted since their shape parameters and overall normalisation are determined from fits to the data.

Process	Generator	PDF set	Showering	Tune	Accuracy	Order of σ calculation
ggF HH	POWHEG Box v2 [51–55]	PDF4LHC15NLO [56]	PYTHIA 8.2 [57]	A14 [58]	NLO	NNLO
VBF HH	MADGRAPH5_AMC@NLO [59]	NNPDF3.0NLO [60]	PYTHIA 8.2	A14	LO	N ³ LO
ggF H	NNLOPS [51–53, 61, 62]	PDF4LHC15NLO	PYTHIA 8.2	AZNLO [63]	NNLO	N ³ LO
VBF H	POWHEG Box v2 [51–53, 64]	PDF4LHC15NLO	PYTHIA 8.2	AZNLO	NLO	NNLO
WH	POWHEG Box v2 [51–53, 65]	PDF4LHC15NLO	PYTHIA 8.2	AZNLO	NLO	NNLO
$qq \rightarrow ZH$	POWHEG Box v2 [51–53, 65]	PDF4LHC15NLO	PYTHIA 8.2	AZNLO	NLO	NNLO
$gg \rightarrow ZH$	POWHEG Box v2 [51–53, 65]	PDF4LHC15NLO	PYTHIA 8.2	AZNLO	LO	NLO
$t\bar{t}H$	POWHEG Box v2 [51–53, 66]	NNPDF3.0NLO	PYTHIA 8.2	A14	NLO	NNLO
$b\bar{b}H$	POWHEG Box v2 [51–53, 67]	NNPDF3.0NLO	PYTHIA 8.2	A14	NLO	NNLO
tHq	MADGRAPH5_AMC@NLO	NNPDF3.0NLO	PYTHIA 8.2	A14	NLO	NLO
tHW	MADGRAPH5_AMC@NLO	NNPDF3.0NLO	PYTHIA 8.2	A14	NLO	NLO
$\gamma\gamma$ +jets	SHERPA 2.2.4 [68]	NNPDF3.0NNLO	SHERPA 2.2.4	–	–	–
$\gamma\gamma b\bar{b}$	SHERPA 2.2.12 [68]	NNPDF3.0NNLO	SHERPA 2.2.12	–	–	–
$t\bar{t}\gamma\gamma$	MADGRAPH5_AMC@NLO	NNPDF2.3LO	PYTHIA 8.2	A14	–	–

Signal samples consist of simulated events from nonresonant ggF and VBF production of Higgs boson pairs, with one Higgs boson decaying into $b\bar{b}$ and the other one into $\gamma\gamma$. In addition to the samples in Table 1, a ggF HH sample was generated with the same settings as the nominal sample but with the non-SM value of the self-coupling modifier $\kappa_\lambda = 10$, and then passed through the detector simulation and the reconstruction algorithms. A reweighting technique based on the particle-level invariant mass m_{HH} of the Higgs boson pair is applied to the $\kappa_\lambda = 1$ sample to determine the ggF HH signal yield and kinematic distributions for any value of κ_λ [69]. The particle-level m_{HH} spectrum for any generic value of κ_λ is calculated from the m_{HH} distributions of three ggF HH samples generated at particle level for $\kappa_\lambda = 0, 1, \text{ and } 20$. To determine the potential ‘non-closure’ in the reweighting process from residual kinematic effects, the procedure is validated by comparing the predicted event yields and kinematic distributions of the simulated sample generated with $\kappa_\lambda = 1$ and reweighted to $\kappa_\lambda = 10$ with those of the simulated sample generated under the hypothesis $\kappa_\lambda = 10$. Furthermore, 12 additional VBF HH samples were generated and simulated with the same set-up and settings as the nominal VBF sample but using non-SM combinations of the coupling strength scale factors $\kappa_\lambda, \kappa_{2V}$ and κ_V . A linear combination of a ‘basis’ formed by the

SM sample and five of the other 12 samples, corresponding to the combinations of the κ_λ , κ_{2V} , and κ_V couplings (1, 1.5, 1), (0, 1, 1), (10, 1, 1), (1, 3, 1), (-5, 1, 0.5), is used to determine the expected yields and distributions for any value of κ_λ , κ_{2V} , and κ_V . The remaining seven samples are compared with the corresponding predictions from the interpolation procedure for validation purposes. The same procedure was used in the measurements presented in Refs. [34, 35].

Background samples include simulated events of single Higgs bosons decaying into $\gamma\gamma$ produced by ggF, VBF, in association with a W or Z boson, with a $t\bar{t}$ or $b\bar{b}$ pair, or with a single top-quark t . Simulated event samples of continuum diphoton production in association with top quark pairs ($t\bar{t}\gamma\gamma$) or with jets from quarks of other flavours ($\gamma\gamma$ +jets) were also produced, to optimise the event classification described in Section 4.2. In addition to the previous samples, shared with Ref. [32], a sample of simulated continuum diphoton plus two b -jets events ($\gamma\gamma b\bar{b}$) was generated with SHERPA 2.2.12 [68] using NLO matrix elements for the production of the two photons and the two b -quarks in the four-flavour scheme, with additional jets produced in the parton shower. Due to the increased efficiency from generator-level requirements on the b -quarks, the use of this new sample reduces the statistical uncertainty in the main component of the nonresonant background originating from $b\bar{b}\gamma\gamma$ events by a factor of two, despite containing about 60 times fewer simulated events than the inclusive diphoton sample. This sample was used to study the background diphoton invariant mass distribution, as described in Section 5.

All generated samples were passed through a detailed simulation of the ATLAS detector response [70] based on GEANT4 [71], except for the inclusive diphoton sample, which was interfaced to a fast detector simulation based on a parametric description of the calorimeter response [72], and for the ggF HH particle-level samples used for the m_{HH} -based reweighting procedure, for which the detector response was not simulated. The generation of the simulated event samples includes the effect of multiple inelastic pp interactions per bunch crossing, and the effect on the detector response of interactions from bunch crossings before or after the one containing the hard interaction. The inelastic pp events were generated with PYTHIA 8.186 using the NNPDF2.3LO PDF set and the A3 tune [73]. The Higgs boson mass was assumed to be 125 GeV in both simulation and the analysis of the data. The impacts of the differences relative to the best-fit values of the m_H measurements reported in Refs. [18, 19], and the effects of the corresponding experimental uncertainties in m_H , are negligible.

4 Event selection and classification

The same preselection as described in Ref. [32] is used to suppress the background while providing good signal efficiency. It is briefly summarised in Section 4.1. The selected events are then classified into orthogonal categories based on multivariate discriminants using several input kinematic quantities. The definition of the event categories, described in Section 4.2, is chosen in order to optimise the expected constraints on the coupling modifiers κ_λ and κ_{2V} .

4.1 Event preselection

To identify $H \rightarrow \gamma\gamma$ decays, events were collected with diphoton triggers [74] with nominal transverse momentum (p_T) thresholds of 35 GeV and 25 GeV for the leading- and subleading- p_T candidates, respectively. Selected events are required to contain two photon candidates in the acceptance of the finely segmented part of the electromagnetic calorimeter ($|\eta| < 1.37$ or $1.52 < |\eta| < 2.37$). The candidates must

be identified as photons by an algorithm based on the shower shapes reconstructed in the calorimeter. Of all potential reconstructed collision vertices, the primary diphoton vertex (PV) is selected by a neural-network algorithm using extrapolated photon trajectories and tracks associated with the candidate vertices [75]. The photon candidates must also meet the requirements of an isolation algorithm based on the energy flow in the calorimeter and the total transverse momentum of charged particle tracks from the PV in the inner detector, in cones surrounding the photon direction [76]. The two leading photons passing these selections are then required to have an invariant mass $m_{\gamma\gamma}$ between 105 and 160 GeV and transverse momenta above 35% and 25% of $m_{\gamma\gamma}$.

Jets are reconstructed from particle-flow objects built from noise-suppressed positive-energy topological clusters in the calorimeter and reconstructed tracks using the anti- k_t clustering algorithm with the parameter $R = 0.4$ [77, 78]. Jet candidates are required to have $p_T > 25$ GeV and $|y| < 4.4$. Jets in the fiducial acceptance of the inner detector ($|\eta| < 2.4$) and with $p_T < 60$ GeV must be identified by a ‘jet-vertex tagger’ as originating from the PV [79]. To target $H \rightarrow b\bar{b}$ decays, events are required to contain exactly two *b-tagged* jets, defined as *central* jets (those in the acceptance of the inner detector ($|\eta| < 2.5$)) that satisfy the criteria of the ‘DL1r’ *b*-tagging algorithm with a nominal efficiency of 77% for *b*-jets and a misidentification rate of 1/170 (1/5) for light-flavour (charm) jets in $t\bar{t}$ simulated events [80]. A correction factor is applied to the energy of the two *b*-tagged jets to account for possible contributions from muons originating from semileptonic *b*-hadron decays and undetected energy from neutrinos and out-of-cone effects [32]. Jets failing to satisfy the *b*-tagging requirement are ranked from first to last based on a discrete *b*-tagging score defined by three bins, corresponding to central jets with DL1r efficiencies of 77%–85% and 85%–100%, and non-central jets. Jets with the same score are ranked by p_T .

Events with six or more central jets, or with one or more isolated lepton (electron or muon) candidates with $p_T > 10$ GeV and passing the lepton identification criteria are rejected in order to suppress background from $t\bar{t}H(\gamma\gamma)$ and inclusive $t\bar{t}$ production. No requirements are made on the number of non-central jets.

The efficiency of the event preselection is 13% (9%) for SM ggF (VBF) HH events. The number of events selected in data in this inclusive signal region is 1874. With this selection, approximately 45% of the continuum background consists of events with two genuine *b*-jets and two prompt photons, 40% consists of events with two genuine prompt photons and at least one misidentified *b*-jet, and 15% consists of events with at least one misidentified photon.

4.2 Event categories

The kinematic properties of Higgs boson pair production, especially m_{HH} , are significantly affected by the values of κ_λ and κ_{2V} . In particular, ggF and VBF HH production with values of κ_λ close to the SM expectation lead to rather large values of m_{HH} , while for κ_λ significantly different from one the HH invariant mass spectrum is relatively soft. Anomalous values of κ_{2V} also lead to events, produced via VBF, with a large invariant mass of the Higgs boson pair. The events are therefore classified in two regions based on the modified four-body invariant mass $m_{b\bar{b}\gamma\gamma}^* = m_{b\bar{b}\gamma\gamma} - (m_{b\bar{b}} - 125 \text{ GeV}) - (m_{\gamma\gamma} - 125 \text{ GeV})$: a *high mass* ($m_{b\bar{b}\gamma\gamma}^* > 350$ GeV) region and a *low mass* ($m_{b\bar{b}\gamma\gamma}^* \leq 350$ GeV) region. The use of $m_{b\bar{b}\gamma\gamma}^*$ over $m_{b\bar{b}\gamma\gamma}$ improves the signal mass resolution due to the cancellation of detector resolution effects [32].

In each of the two $m_{b\bar{b}\gamma\gamma}^*$ regions, a dedicated boosted-decision-tree (BDT) discriminant is trained to distinguish HH signals from the background arising from $H \rightarrow \gamma\gamma$ decays in single Higgs boson production events and from the continuum diphoton background from $t\bar{t}\gamma\gamma$ and $\gamma\gamma$ +jets events. The training is

performed with the XGBoost program [81] using only simulated event samples. In the high mass region, the signal samples used for training include SM ggF and VBF HH events, as well as the five non-SM samples of the VBF HH basis. In the low mass region, the signal samples consist of non-SM ggF HH events corresponding to $\kappa_\lambda = 10$ and $\kappa_\lambda = 5.6$, plus the same five non-SM VBF HH basis samples. The choice of $\kappa_\lambda = 5.6$ corresponds to a large anomalous value of κ_λ that is not yet excluded with a high confidence level by the previous search in this channel. However, it is observed that the training is relatively stable for variations of the order of unity on the κ_λ value used in training.

The BDT discriminant uses the same input variables that were used for the analogous multivariate discriminant in Ref. [32] (denoted by *baseline* variables), complemented by a set of additional observables that provide further discrimination between the background and the signal, mainly from VBF HH production. The baseline variables include kinematic properties of the two photon and the two b -jet candidates, the scalar sum H_T of the p_T of all the jets, and the magnitude E_T^{miss} and direction ϕ^{miss} of the missing transverse momentum vector \vec{p}_T^{miss} [82]. Another baseline variable is the *single-topness* χ_{Wt} , quantifying how likely any three-jet combination in the event is to originate from a $t \rightarrow Wb \rightarrow q\bar{q}'b$ decay:

$$\chi_{Wt} = \min \sqrt{\left(\frac{m_{j_1 j_2} - m_W}{m_W}\right)^2 + \left(\frac{m_{j_1 j_2 j_3} - m_t}{m_t}\right)^2}, \quad (1)$$

where m_W and m_t are the masses of the W boson and of the top quark, and the minimum is evaluated over all combinations of any three jets in the event, with no requirements on whether they are b -tagged.

The additional variables include, for events with at least four jets, the p_T , η , ϕ , and discrete b -tagging score of the third and fourth jets. Events with at least four jets can arise from VBF HH production, in which the scattered quarks responsible for the VBF process hadronise after having radiated a weak boson and produce two forward, high-momentum jets ('VBF jets'). In events with exactly four selected jets, the two non b -tagged jets are considered as VBF-jet candidates. In events with at least five selected jets (about 25% of the VBF HH events passing the previous requirements according to the simulation), the two non b -tagged jets that are considered as VBF-jet candidates are determined by means of a BDT classifier ('VBF-jet tagger'). The inputs of the VBF-jet tagger consist of: (i) for each non b -tagged jet j , its p_T , η , and $\Delta\eta$ and ΔR separations from the $\gamma\gamma b\bar{b}$ system; (ii) for each jj pair, its invariant mass, $\Delta\eta$ between the two jets, $\Delta\eta$ and ΔR separations from the $\gamma\gamma b\bar{b}$ system, and p_T , η , and invariant mass of the $\gamma\gamma b\bar{b}jj$ system. The BDT is trained on simulated SM VBF HH events using the pair of jets matched to the scattered quarks as signal, and all other pairs of jets as background. After training, the VBF-jet tagger is applied to all possible jet pair combinations in data and simulated events, and the jets belonging to the pair with the highest tagger score are considered as VBF-jet candidates. Their invariant mass and pseudorapidity difference are then used as input variables for the event classification BDTs. In simulated VBF HH events with at least three non b -tagged jets, the VBF-jet tagger is able to correctly identify the VBF-jet pair in 95% of events.

A second set of additional variables used as input to the event classification BDTs consists of event-level kinematic quantities such as $m_{b\bar{b}\gamma\gamma}^*$ and the angular separation $\Delta R(\gamma, \gamma)$ ($\Delta R(b, \bar{b})$) between the two photon (b -tagged jet) candidates. Finally, three event-shape observables are also used: the transverse sphericity S_\perp [83], the planar flow Pf [84], and the transverse momentum balance, defined as

$$p_T^{\text{balance}} = \frac{|\vec{p}_T^{\gamma_1} + \vec{p}_T^{\gamma_2} + \vec{p}_T^{b_1} + \vec{p}_T^{b_2}|}{|\vec{p}_T^{\gamma_1}| + |\vec{p}_T^{\gamma_2}| + |\vec{p}_T^{b_1}| + |\vec{p}_T^{b_2}|}. \quad (2)$$

The relative weights of the training samples, as well as the values of the XGBoost hyperparameters, are tuned using a Bayesian optimisation algorithm that maximises the expected combined number-counting significance Z [85] of a benchmark signal using the signal and background yields in each category in the diphoton invariant mass range $120 \text{ GeV} < m_{\gamma\gamma} < 130 \text{ GeV}$, as described below.

After training, three categories (labelled ‘High Mass i ’, $i = 1..3$) in the high mass region and four categories (labelled ‘Low Mass i ’, $i = 1..4$) in the low mass region are defined based on the high mass region and low mass region BDT discriminants, with a higher category index i corresponding to higher BDT scores and more signal-like events. Events from the inclusive signal region are thus classified in seven orthogonal exclusive signal regions based on the value of $m_{b\bar{b}\gamma\gamma}^*$ and of the BDT scores. Events with a BDT score lower than the threshold defining the category with the lowest index in the corresponding low or high mass region are discarded. The values of the BDT scores used to define the categories are chosen by maximising the combined number-counting significance of all categories in a region for a benchmark signal using expected signal and background yields in the diphoton invariant mass range $120 \text{ GeV} < m_{\gamma\gamma} < 130 \text{ GeV}$. During this optimisation process, each category must contain at least nine expected continuum background events in the $m_{\gamma\gamma}$ sidebands, *i.e.* excluding the region $120 \text{ GeV} < m_{\gamma\gamma} < 130 \text{ GeV}$, in order to have sufficient events to constrain the shape of the diphoton invariant mass distribution of the continuum background when the selection is evaluated on the data. In the high mass region, the signal yield is computed from the sum of the expected SM ggF and VBF HH contributions, while in low mass region, the signal yield is computed from the ggF HH $\kappa_\lambda = 5.6$ and VBF HH $\kappa_\lambda = 10$ predictions.

The BDT discriminant distributions in the low and high mass regions observed in data in the $m_{\gamma\gamma}$ sidebands are shown in Figure 3. Also illustrated for comparison are the expected BDT score distributions for the dominant nonresonant background from the $\gamma\gamma + \text{jets}$ sample, the resonant single Higgs boson background, and the ggF and VBF HH signals for different values of κ_λ and κ_{2V} . The values of the BDT scores that define the categories are represented by vertical dashed lines. In total, 340 events in the range of $105 \text{ GeV} < m_{\gamma\gamma} < 160 \text{ GeV}$ are retained from the 1874 passing the initial preselection.

5 Signal and background modelling of the diphoton mass spectrum

The signal, resonant and nonresonant background yields in each category are determined from unbinned fits to the diphoton invariant mass distributions in the signal regions, as described in Section 7. The signal and background $m_{\gamma\gamma}$ distributions in each category are independently modelled by means of analytical functions chosen as follows.

The $m_{\gamma\gamma}$ distributions of signal events and resonant background events from single Higgs bosons decaying into $\gamma\gamma$ are described by double-sided Crystal Ball functions [75, 86]. The shape parameters are obtained from fits to simulated SM HH events, and then either fixed in the final fits (parameters describing the tail of the distribution) or constrained around the initial values within the uncertainties resulting from the photon energy calibration. The same model is found to describe selected single Higgs boson and Higgs boson pair events well for both SM and non-SM coupling values. Signal + background fits performed on a combination of signal and resonant background events from simulation and the expected nonresonant background distribution show negligible signal yield non-closure resulting from this assumption.

The $m_{\gamma\gamma}$ distributions of the nonresonant diphoton background are modelled with exponential functions, whose normalisation and shape parameters are obtained from the fit to the data. The chosen exponential model in each category has two degrees of freedom and is found to describe the data well in the $m_{\gamma\gamma}$

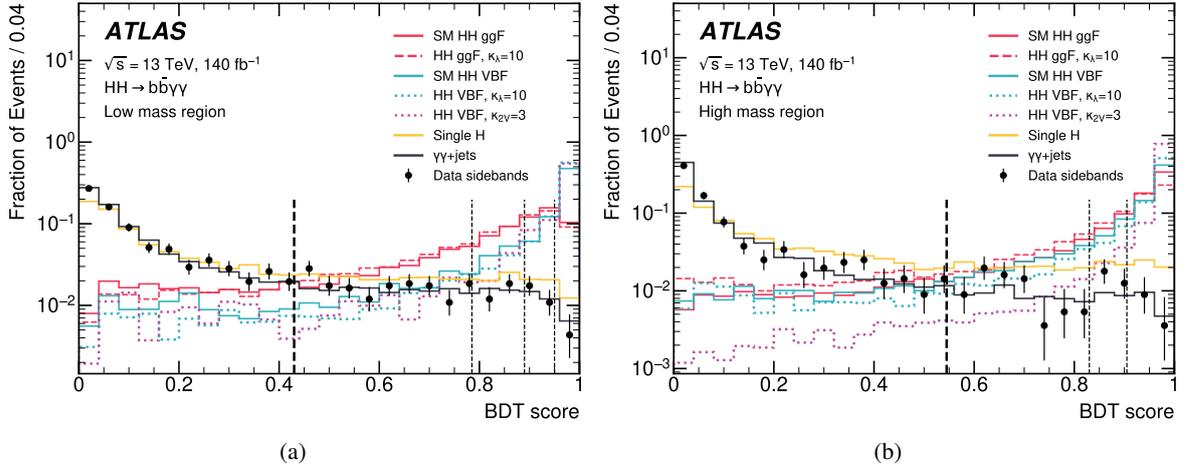


Figure 3: BDT score distributions for simulated ggF and VBF $HH \rightarrow b\bar{b}\gamma\gamma$ signal events and simulated background events from nonresonant $\gamma\gamma + \text{jets}$ and singly produced Higgs bosons decaying into $\gamma\gamma$ for the (a) low and (b) high mass regions. The data in the $m_{\gamma\gamma}$ sidebands, which are not expected to be populated by single nor double Higgs boson events, are also shown compared with the $\gamma\gamma + \text{jets}$ sample. The latter comprises the majority of the nonresonant diphoton background and is used in the training of the BDT. All distributions are normalised to unity. The vertical dashed lines correspond to the thresholds used to define the event categories. Events with a BDT score between 0 and the lowest threshold (thick dashed line) are discarded. Events satisfying the lowest threshold are categorised as Low Mass i , $i = 1..4$ (High Mass i , $i = 1..3$), with a higher category index i corresponding to higher BDT scores and more signal-like events.

sidebands, as well as the background-only template obtained with the SHERPA 2.2.12 $\gamma\gamma b\bar{b}$ sample normalised to the data in the $m_{\gamma\gamma}$ sidebands. The *spurious signal* [75, 87] is defined as the maximum absolute value of the bias on the fitted signal yield in multiple signal+background fits to the background-only template, performed with varying mass assumptions on $m_H \in [123, 127]$ GeV in intervals of 0.5 GeV. For each of the exponential models, the spurious signal is smaller than 20% of the statistical uncertainty in the expected fitted signal yield, plus twice the statistical uncertainty in the spurious signal itself. Alternative models with the same numbers of degrees of freedom, such as power functions of $m_{\gamma\gamma}$, performed similarly to the exponential model. While the nominal templates are constructed with simulated $\gamma\gamma b\bar{b}$ events only, alternative templates accounting for potential shape differences due to other background components such as $\gamma\gamma q\bar{q}$ ($q \neq b$), γj , and jj do not significantly alter the spurious signal value or the quality of the exponential fit.

6 Systematic uncertainties

Systematic uncertainties affect the shape and normalisation of the diphoton invariant mass distributions of the Higgs boson pair signal and single Higgs boson backgrounds. Nevertheless, due to the limited number of events and the small signal-to-background ratio, the impact of the systematic uncertainties is small compared with that of the statistical uncertainties.

The systematic uncertainties are computed separately for the ggF and VBF HH production modes and for the various single Higgs boson production modes. Those from the same source are correlated between processes. For the ggF (VBF) HH signal, for each source of uncertainty the corresponding estimate is

obtained by taking the envelope of values computed using both the SM and the $\kappa_\lambda = 10$ simulated event sample (using the six VBF basis simulated event samples).

The uncertainty in the full Run 2 integrated luminosity is derived from dedicated measurements [50] using the LUCID-2 [88] detector. The diphoton trigger efficiency uncertainty is evaluated using radiative Z boson decays and with events collected using prescaled lower-threshold triggers [74]. The uncertainty in the vertex selection efficiency is evaluated by comparing the reconstruction efficiency of photon-pointing vertices in $Z \rightarrow e^+e^-$ events in data with that in simulation [89].

The uncertainties in photon identification and isolation efficiencies are determined from control samples of prompt photons from photon+jet production and from radiative Z boson decays and electrons [76]. The uncertainties in the photon energy scale and resolution are determined from control samples of electrons from Z boson and J/ψ decays and of photons from radiative Z boson decays [76].

The uncertainties in the jet energy scale and resolution are determined from control samples of jets recoiling against well calibrated particles such as photons, Z bosons or already calibrated jets [90]. Additional uncertainties from the simulation account for potential differences between the response for b -jets and jets from gluons and light quarks. The uncertainties in the flavour-tagging efficiencies and misidentification rates are estimated by using $t\bar{t}$ events for b - and c -jets and Z +jets events for light-flavour jets [80, 91, 92].

Theoretical uncertainties due to missing higher-order terms in the perturbative expansion of the cross-section, the PDF set, and the value of α_s affect the total expected yields of single Higgs boson and Higgs boson pair events, and their fractional contributions to each category. These uncertainties are evaluated by considering alternative choices of factorisation and renormalisation scales, PDF sets, and the value of α_s . For SM Higgs boson pair production, the values of the QCD scale and PDF+ α_s total cross-section uncertainties are taken from Ref. [93]. For SM HH production through ggF, the QCD scale and PDF+ α_s cross-section uncertainties are further combined with the top-quark mass scale uncertainty according to the prescription described in Ref. [28]. The uncertainties in the $H \rightarrow \gamma\gamma$ and $H \rightarrow b\bar{b}$ branching ratios are also included [94].

For the signal and the ggF, VBF, and $t\bar{t}H$ single Higgs boson processes, the uncertainty due to the choice of parton shower model is evaluated by comparing the predictions of the nominal simulation using the PYTHIA 8 model with an alternative simulation in which the same generator-level events are showered with HERWIG 7. An additional 100% uncertainty in the yields of single Higgs boson ggF, VBF and WH production modes is applied, motivated by studies of heavy-flavour production in association with top-quark pairs [95, 96] and W boson production in association with b -jets [97].

For the ggF HH process with $\kappa_\lambda \neq 1$, a systematic uncertainty is assigned to the κ_λ reweighting procedure by computing for each category the maximum deviation between the expected yields determined from the ggF HH sample generated with $\kappa_\lambda = 10$ and the sample generated with $\kappa_\lambda = 1$ and reweighted to $\kappa_\lambda = 10$. For the VBF HH process, a similar uncertainty for the potential non-closure of the procedure used to calculate the expected yield for any value of κ_λ and κ_{2V} from a linear combination of the six basis samples is determined for each category. It is calculated as the maximum difference, for the seven validation samples described in Section 3, between the expected yield calculated with the validation sample and that obtained from the linear combination approach.

An additional uncertainty in the signal yield is due to the choice of the background model and is assumed to be equal to the spurious signal described in Section 5. The larger equivalent integrated luminosity of the SHERPA 2.2.12 $\gamma\gamma b\bar{b}$ sample used to create the background-only template, compared with that of the SHERPA 2.2.4 $\gamma\gamma$ +jets sample used in the previous search published in Ref. [32], is more

effective at suppressing statistical fluctuations in the template that would otherwise lead to overestimated spurious signals. As a consequence, the spurious signal obtained with the background template from the SHERPA 2.2.12 $\gamma\gamma b\bar{b}$ sample in each category ranges between 10% and 50% of that from the background template produced with the SHERPA 2.2.4 $\gamma\gamma$ +jets sample. Its impact on the expected upper limit on the HH signal strength μ_{HH} , defined as the ratio of the Higgs boson pair production cross-section to its SM prediction, is thus at the permille level, compared to 3% in the previous analysis.

The impacts of the systematic uncertainties in the expected 95% CL upper limit on μ_{HH} , determined with the statistical interpretation described in the next section, are listed in Table 2.

Table 2: Breakdown of the dominant systematic uncertainties in the expected μ_{HH} upper limit at 95% CL. The impact of the uncertainties corresponds to the relative variation of the expected upper limit when re-evaluating the profile likelihood ratio after fixing the nuisance parameter in question to its best-fit value, while all remaining nuisance parameters remain free to float. Only systematic uncertainties with an impact of at least 0.1% are shown.

Systematic uncertainty source	Relative impact [%]
Experimental	
Photon energy resolution	0.4
Photon energy scale	0.1
Flavour tagging	0.1
Theoretical	
Factorisation and renormalisation scale	4.8
$\mathcal{B}(H \rightarrow \gamma\gamma, b\bar{b})$	0.2
Parton showering model	0.2
Heavy-flavour content	0.1
Background model (spurious signal)	0.1

7 Results

The results are derived using the statistical procedures outlined in Refs. [32, 35, 98] from the global likelihood function $L(\alpha, \theta)$. The set α contains the parameters of interest (POI) of the measurement, while θ is the ensemble of nuisance parameters, corresponding to systematic uncertainties constrained by auxiliary measurements in control regions or by theoretical predictions, or to parameters such as the continuum background yields that are *a priori* unconstrained. The function $L(\alpha, \theta)$ is the product of the likelihood functions in each of the seven orthogonal categories, and of constraint terms for the nuisance parameters that are not freely floating in the fit. For each category, the likelihood function is determined from the corresponding signal and background models of the $m_{\gamma\gamma}$ probability density functions described in Section 5, the signal and background yield expectations for given values of α and θ , and the observed $m_{\gamma\gamma}$ distribution in data.

The constraints on the coupling strength parameters, expressed as 68% and 95% CL intervals, are determined with the same procedure as that of Ref. [35], using a profile-likelihood-ratio test statistic

$\Lambda(\alpha, \theta)$ computed from the likelihood function in the asymptotic approximation [85], where the POIs in α are the coupling strength modifiers κ . Signal strength upper limits are derived as in Ref. [32] using the CL_s approach [99] from a separate test statistic \tilde{q}_α that evaluates to zero when the parameter of interest $\alpha = \mu_{HH}$ corresponding to the cross-section under study is lower than its maximum likelihood estimate (MLE) $\hat{\mu}_{HH}$. The allowed κ_λ interval published in Ref. [32] was determined in a different way, from the range of κ_λ values for which the predicted HH cross-sections are lower than the observed upper limits. The expected results are obtained with Asimov datasets [85] generated from the likelihood function after setting all nuisance parameters to their MLE in the fit to the data and fixing the POIs to the values corresponding to the hypothesis under test. The asymptotic results are found to agree within 10% with values obtained using pseudo-experiments.

Figure 4 shows the result of a background-only fit to the data, using the likelihood function L after fixing the parameters of interest corresponding to setting the signal cross-sections to zero. Table 3 compares the number of events in the observed data to the expected values in each category. No significant excess over the expected background is found, and a 95% CL upper limit of 4.0 on the total HH production signal strength μ_{HH} (where only ggF and VBF processes are considered) is set, to be compared with an expected limit of 5.0 (6.4) in the background-only $\mu_{HH} = 0$ (SM $\mu_{HH} = 1$) hypothesis. If the VBF (ggF) HH signal strength is fixed to the SM prediction, the observed upper limit on the ggF (VBF) HH signal strength is 4.1 (96), while the expected upper limit, computed assuming $\mu_{\text{ggF}} = 0$ ($\mu_{\text{VBF}} = 0$), is 5.3 (145). The observed limits are tighter than the expected ones due to deficits in the signal regions of the most sensitive categories, as shown in Table 3. The compatibility between the best-fit value of μ_{HH} and the SM expectation is approximately 1.3 standard deviations.

The values of $-2 \ln \Lambda$ as a function of the coupling strength factor κ_λ or κ_{2V} under the hypothesis that all other coupling modifiers are equal to their SM predictions are shown in Figure 5. The observed (expected) constraints under this hypothesis are $-1.4 < \kappa_\lambda < 6.9$ ($-2.8 < \kappa_\lambda < 7.8$) and $-0.5 < \kappa_{2V} < 2.7$ ($-1.1 < \kappa_{2V} < 3.3$) at 95% CL. Two-dimensional constraints at 68% and 95% CL in the $(\kappa_\lambda, \kappa_{2V})$ plane are also shown in Figure 6, when all the other coupling modifiers are fixed to their SM predictions.

The impact of the systematic uncertainties on the results is small, leading to an increase of the upper limits on the signal strengths by 6%–7% and to a widening of 95% CL confidence intervals for the coupling modifiers by 2%–3% relative to the case in which systematic uncertainties are neglected.

Compared to the previous analysis of Ref. [32, 35], the new event classification procedure leads to a reduction in the expected upper limit on μ_{HH} by 12% and a reduction in the width of the expected one-dimensional confidence interval for κ_λ (κ_{2V}) by 6% (17%), based on a consistent statistical procedure for evaluating the 95% confidence interval as described at the beginning of this section. The observed upper limit on μ_{HH} is reduced by 5%, while the observed one-dimensional confidence interval for κ_λ (κ_{2V}) is increased by 5% (reduced by 16%).

The increase in the width of the observed κ_λ confidence interval arises from the fact that this new analysis favours larger, less negative values of the signal strength, corresponding to larger magnitudes of the coupling strength modifier κ_λ . The compatibility, considering only statistical uncertainties, between the allowed κ_λ interval at 95% CL from this study and that of Ref. [32] is evaluated using a bootstrap technique [100], based on the data events passing the selection of either the previous analysis, or that of the current one, or both. The compatibility between the two results is at the level of 0.3 standard deviations.

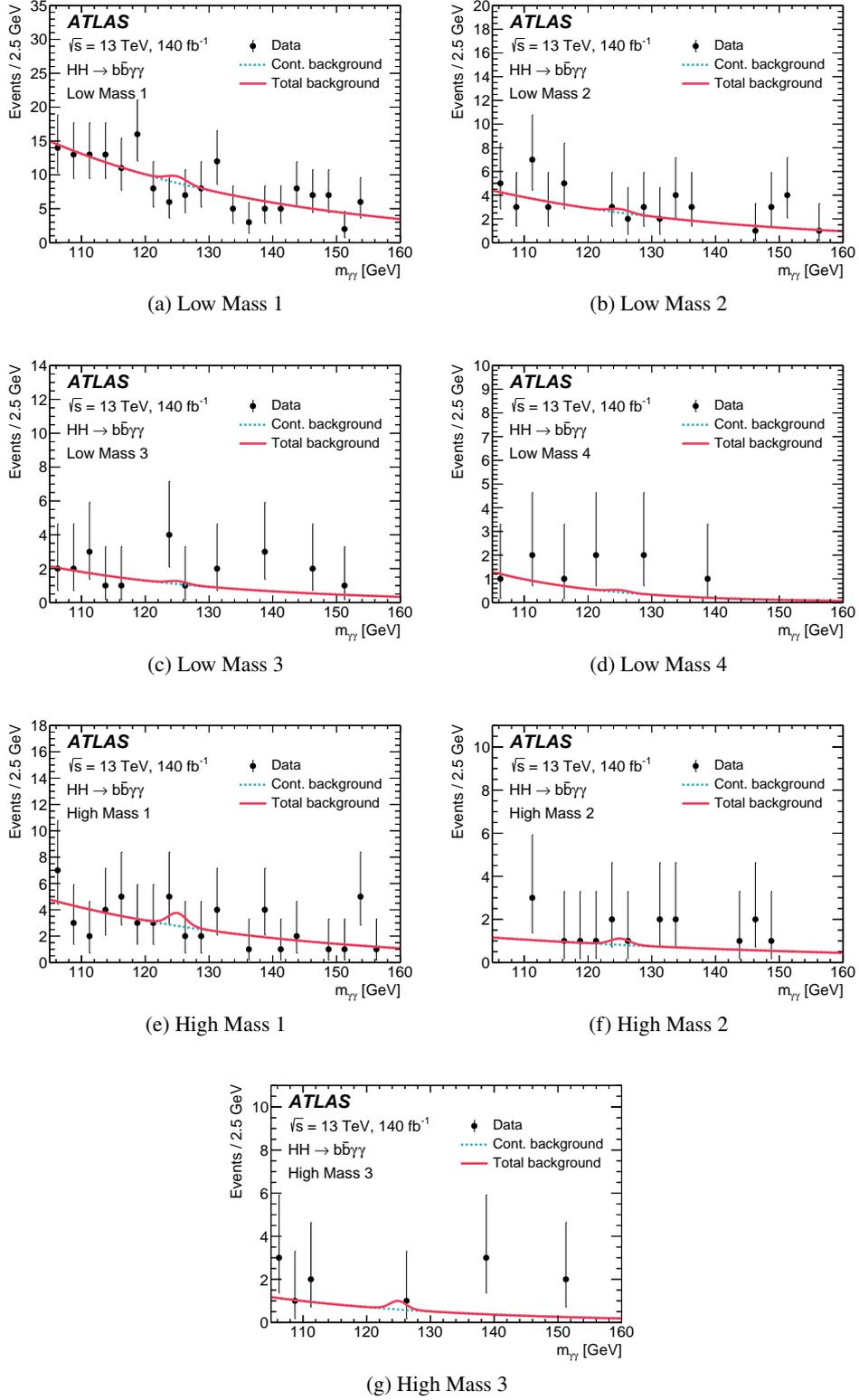


Figure 4: Comparison between the diphoton invariant mass distribution in data (points with error bars) and the background-only fit (solid line) for the four low mass (a–d) and three high mass (e–g) categories of the $HH \rightarrow b\bar{b}\gamma\gamma$ search. In each of the regions, a higher category index corresponds to higher BDT scores and more signal-like events. The solid line peaks near 125 GeV are due to single Higgs boson production.

Table 3: The expected number of events (estimated by using simulation) from HH signals with various κ_λ and κ_{2V} hypotheses and single Higgs boson production, and the expected number of events from the continuum background, evaluated in the $120 \text{ GeV} < m_{\gamma\gamma} < 130 \text{ GeV}$ window. For comparison, the number of observed data events is also shown. The uncertainties in the HH signals and single Higgs boson backgrounds include the systematic uncertainties discussed in Section 6. Asymmetric uncertainties arise primarily from the theory calculation of the SM ggF HH cross-section and the large uncertainty in the yield of single Higgs bosons produced in ggF events in association with heavy-flavour jets, parameterised by a lognormal distribution. The uncertainty in the continuum background is given by the sum in quadrature of the statistical uncertainty from the fit to the data and the spurious signal uncertainty.

	High Mass 1	High Mass 2	High Mass 3	Low Mass 1	Low Mass 2	Low Mass 3	Low Mass 4
SM $HH(\kappa_\lambda = 1)$ signal	$0.26^{+0.03}_{-0.04}$	$0.194^{+0.021}_{-0.032}$	$0.84^{+0.10}_{-0.14}$	$0.048^{+0.007}_{-0.008}$	$0.038^{+0.004}_{-0.006}$	$0.039^{+0.004}_{-0.006}$	$0.032^{+0.004}_{-0.004}$
ggF	$0.25^{+0.03}_{-0.04}$	$0.188^{+0.021}_{-0.032}$	$0.81^{+0.10}_{-0.14}$	$0.046^{+0.007}_{-0.008}$	$0.036^{+0.004}_{-0.006}$	$0.037^{+0.004}_{-0.006}$	$0.025^{+0.004}_{-0.004}$
VBF [10^{-3}]	$7.9^{+0.6}_{-0.5}$	$5.3^{+0.5}_{-0.4}$	29^{+4}_{-3}	$1.98^{+0.28}_{-0.24}$	$1.71^{+0.16}_{-0.14}$	$1.96^{+0.21}_{-0.19}$	$7.4^{+0.6}_{-0.5}$
Alternative $HH(\kappa_\lambda = 10)$ signal	$2.5^{+0.4}_{-0.3}$	$1.81^{+0.25}_{-0.20}$	$6.2^{+0.8}_{-0.6}$	$5.0^{+1.2}_{-0.9}$	$3.8^{+0.7}_{-0.5}$	$3.7^{+0.7}_{-0.6}$	$3.6^{+0.4}_{-0.4}$
ggF	$2.3^{+0.4}_{-0.3}$	$1.64^{+0.25}_{-0.19}$	$4.9^{+0.8}_{-0.6}$	$4.7^{+1.0}_{-0.8}$	$3.6^{+0.7}_{-0.6}$	$3.3^{+0.7}_{-0.5}$	$2.04^{+0.34}_{-0.27}$
VBF	$0.231^{+0.019}_{-0.017}$	$0.170^{+0.019}_{-0.017}$	$1.29^{+0.15}_{-0.14}$	$0.28^{+0.20}_{-0.11}$	$0.23^{+0.23}_{-0.12}$	$0.36^{+0.10}_{-0.08}$	$1.57^{+0.17}_{-0.16}$
Alternative VBF $HH(\kappa_{2V} = 3)$ signal	$0.23^{+0.04}_{-0.04}$	$0.20^{+0.05}_{-0.04}$	$3.8^{+0.7}_{-0.6}$	$0.03^{+0.04}_{-0.02}$	$0.03^{+0.06}_{-0.02}$	$0.048^{+0.023}_{-0.015}$	$0.17^{+0.04}_{-0.03}$
Single Higgs boson background	$1.5^{+0.5}_{-0.3}$	$0.48^{+0.21}_{-0.10}$	$0.57^{+0.25}_{-0.14}$	$1.72^{+0.31}_{-0.19}$	$0.53^{+0.08}_{-0.06}$	$0.29^{+0.14}_{-0.07}$	$0.16^{+0.06}_{-0.03}$
ggF	$0.5^{+0.5}_{-0.2}$	$0.14^{+0.21}_{-0.09}$	$0.25^{+0.25}_{-0.12}$	$0.29^{+0.31}_{-0.15}$	$0.08^{+0.08}_{-0.04}$	$0.07^{+0.13}_{-0.06}$	$0.04^{+0.06}_{-0.03}$
$t\bar{t}H$	$0.302^{+0.034}_{-0.032}$	$0.069^{+0.009}_{-0.008}$	$0.063^{+0.008}_{-0.007}$	$0.77^{+0.09}_{-0.08}$	$0.214^{+0.029}_{-0.026}$	$0.100^{+0.012}_{-0.012}$	$0.048^{+0.005}_{-0.005}$
ZH	$0.61^{+0.06}_{-0.05}$	$0.174^{+0.020}_{-0.016}$	$0.188^{+0.035}_{-0.029}$	$0.49^{+0.05}_{-0.04}$	$0.149^{+0.028}_{-0.025}$	$0.069^{+0.033}_{-0.023}$	$0.028^{+0.010}_{-0.007}$
Rest	$0.17^{+0.08}_{-0.04}$	$0.089^{+0.030}_{-0.016}$	$0.07^{+0.04}_{-0.02}$	$0.181^{+0.030}_{-0.019}$	$0.089^{+0.016}_{-0.009}$	$0.046^{+0.007}_{-0.004}$	$0.039^{+0.008}_{-0.004}$
Continuum background	$11.3^{+1.5}_{-1.6}$	$3.2^{+0.8}_{-0.8}$	$2.8^{+0.8}_{-0.8}$	$37.2^{+2.9}_{-2.9}$	$10.8^{+1.5}_{-1.5}$	$4.4^{+0.9}_{-1.0}$	$1.1^{+0.5}_{-0.5}$
Total background	$12.8^{+1.6}_{-1.6}$	$3.7^{+0.9}_{-0.8}$	$3.4^{+0.8}_{-0.8}$	$38.9^{+2.9}_{-2.9}$	$11.3^{+1.5}_{-1.5}$	$4.7^{+0.9}_{-1.0}$	$1.3^{+0.5}_{-0.5}$
Data	12	4	1	29	8	5	4

8 Effective field theory interpretation

Anomalous Higgs boson self-interactions or interactions with the other gauge fields and fermions can alter the Higgs boson pair production cross-section and kinematics, as well as the Higgs boson decay rates. The results of the previous section are thus interpreted in the context of two effective field theories to set constraints on the Wilson coefficients of the operators describing these anomalous interactions.

The approach used here follows closely that described in Ref. [34], probing a similar set of operators and benchmark points that directly affect HH production: three Wilson coefficients (c_{hhh} , c_{tthh} , c_{gghh}) and seven benchmark points [101] of the Higgs effective field theory, and two Wilson coefficients (c_H , $c_{H\Box}$) of the $(H^\dagger H)^3$ and $(H^\dagger H)\Box(H^\dagger H)$ operators of the ‘Warsaw’ basis [102] of the SM effective field theory. In the SMEFT Lagrangian, the operators \mathcal{O}_i are multiplied by coefficients c_i/Λ^2 , where Λ is the energy scale that bounds from above the range of validity of the EFT approach. In this study, a value of $\Lambda = 1 \text{ TeV}$ is assumed. In the HEFT interpretation, the only considered coefficient affecting VBF HH production is c_{hhh} , and thus this production mode is always subdominant relative to ggF HH . In the SMEFT interpretation, the effects of the operators on VBF HH production are similarly expected to be small, since the SMEFT preserves the Higgs doublet structure of the SM and the corresponding cancellation between the VVH and $VVHH$ diagrams involved in VBF HH production. Consequently both interpretations consider only ggF HH production while VBF HH is assumed to be negligible.

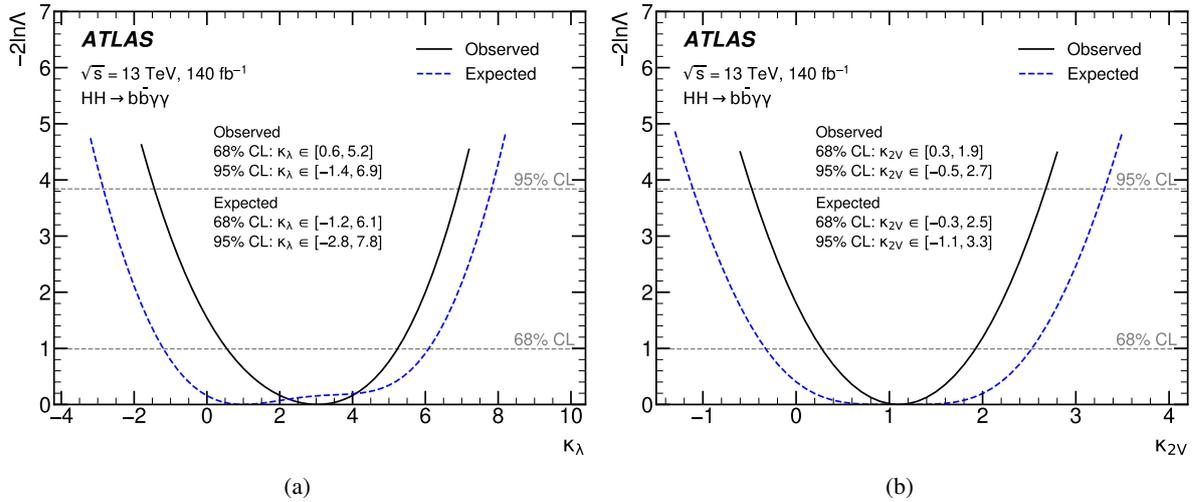


Figure 5: Observed (solid line) and expected (dashed line) value of $-2 \ln \Lambda$ as a function of (a) κ_λ and (b) κ_{2V} , when all other coupling modifiers (including, respectively, κ_{2V} or κ_λ) are fixed to their SM predictions.

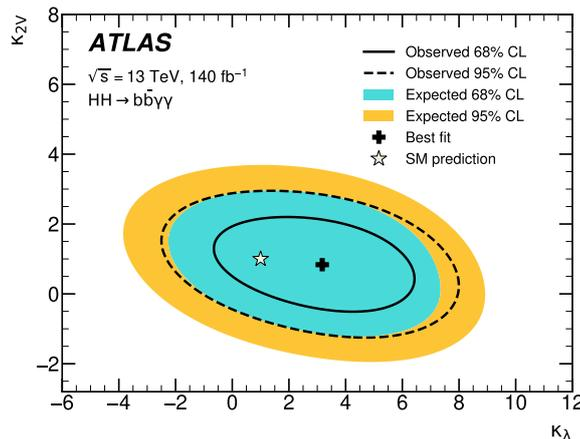


Figure 6: Likelihood contours at 68% (solid line) and 95% (dashed line) CL in the $(\kappa_\lambda, \kappa_{2V})$ parameter space, when all other coupling modifiers are fixed to their SM predictions. The corresponding expected contours are shown by the inner and outer shaded regions. The SM prediction is indicated by the star, while the best-fit value is denoted by the cross.

Predictions for ggF HH production for various values of the Wilson coefficients under study are obtained by applying an event reweighting technique to the SM ggF HH sample, similar to the method described in Section 3 to emulate samples with anomalous values of κ_λ . The reweighting functions are based on the particle-level m_{HH} distributions predicted at NLO accuracy in the strong coupling constant for alternative values of the EFT coefficients. For the HEFT interpretation, the functions are taken directly from Ref. [103], while for the SMEFT interpretation, they are computed using POWHEG BOX v2 with the SMEFT@NLO model [104]. For the SMEFT interpretation, a similar reweighting function is also derived for single Higgs boson processes, but instead using the differential distribution of the Higgs boson transverse momentum.

Uncertainties related to PDF, α_s , and missing higher-order terms in the prediction are included by taking for each analysis category the envelope of the uncertainties from each source, determined with the same

procedure as that described in Section 6. In addition, a non-closure uncertainty is estimated by comparing the expected yields from dedicated samples corresponding to specific values of the anomalous couplings to those from the reweighting procedure described above in categories reproducing the analysis selections at generator level. These uncertainties in the expected yield are generally of the order of 10% or less in each category and have a small impact on the results.

In the HEFT interpretation, constraints on the coefficients c_{hhh} , c_{tthh} , and c_{gghh} that describe Higgs boson self-interactions as well as effective $t\bar{t}HH$ and $ggHH$ interactions are determined from the data from one-dimensional scans of the profile likelihood function as a function of the coefficients. The operators corresponding to these coefficients do not impact single Higgs boson production and decay at tree level and their effect on the resonant background and on the Higgs boson branching ratios is therefore neglected. The one-dimensional constraints on the three HEFT coefficients c_{hhh} , c_{tthh} and c_{gghh} are summarised in Table 4. The difference between the c_{hhh} constraint and the κ_λ constraint previously presented in Figure 5 is mainly due to the lack of VBF production in the former. In addition, the observed constraints are comparable with those of Ref. [34], when evaluated using the same statistical procedure of Ref. [34]. The width of the allowed 95% CL interval for c_{gghh} is 20% narrower, while that of the c_{tthh} interval is the same. Figure 7 shows two-dimensional profile log-likelihood contours for the simultaneous variation of the (c_{gghh}, c_{hhh}) and (c_{tthh}, c_{hhh}) HEFT coefficients, with the remaining coefficient fixed to its SM value.

Table 4: The observed and expected 95% CL constraints on the HEFT Wilson coefficients, obtained from one-dimensional scans of the profile log-likelihood assuming that all other Wilson coefficients are fixed to their SM values. The contribution from VBF HH production is subdominant to that from ggF and is neglected.

Wilson coefficient	95% CL Observed	95% CL Expected
c_{hhh}	[−1.7 , 7.7]	[−3.4 , 8.9]
c_{tthh}	[−0.28, 0.73]	[−0.48, 0.94]
c_{gghh}	[−0.42, 0.52]	[−0.59, 0.69]

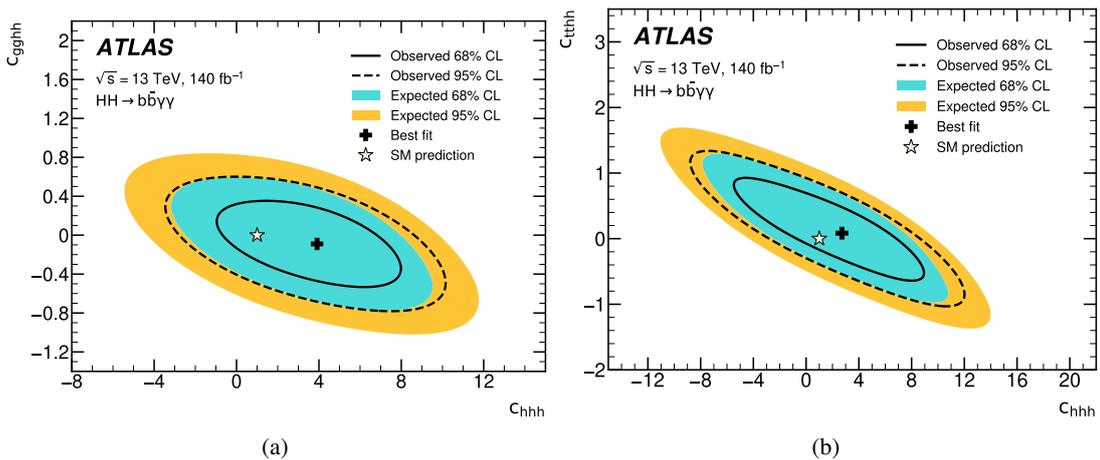


Figure 7: Likelihood contours at 68% (solid line) and 95% (dashed line) CL in the (a) c_{gghh} versus c_{hhh} and (b) c_{tthh} versus c_{hhh} HEFT parameter space, with the remaining coefficient fixed to its SM value. The corresponding expected contours are shown by the inner and outer shaded regions. The SM prediction is indicated by the star, while the best-fit value is denoted by the cross.

In addition, upper limits are set on the Higgs boson pair production cross-section for seven benchmark

points [101] corresponding to different values of the five coefficients c_{hhh} , c_{tthh} , c_{gghh} , c_{ggh} , and c_{tth} , where the latter two correspond to an effective Higgs–gluon interaction and to the Higgs–top Yukawa interaction. The impact of these coefficients on single Higgs boson production and decay is expected to be small compared to the signal and is thus neglected. Defined in Table 5, the benchmark points describe representative signal kinematics and m_{HH} shape features, and have sensitivities that can vary significantly between one point and another. For example, benchmark 1 results in a very soft m_{HH} distribution while benchmark 5 produces a more SM-like m_{HH} distribution with an enhanced tail.

The resulting upper limits on the Higgs boson pair production cross-section through gluon–gluon fusion are shown in Figure 8. For benchmark points 3, 5 and 7, this analysis sets upper limits similar to those set by the search for $HH \rightarrow 4b$ events [34], and, in an analogous way, excludes these scenarios at 95% CL. The remaining benchmarks (1, 2, 4, and 6) have updated definitions compared to those used in Ref. [34] and therefore the results cannot be directly compared. Benchmark 4 is excluded for the first time at 95% CL by this study, while the other three scenarios are compatible with the data.

Table 5: The definitions of the seven HEFT benchmark points described in Ref. [101].

Benchmark	c_{hhh}	c_{tth}	c_{ggh}	c_{gghh}	c_{tthh}
SM	1.00	1.00	0	0	0
1	5.11	1.10	0	0	0
2	6.84	1.03	$-1/3$	0	$1/6$
3	2.21	1.05	$1/2$	$1/2$	$-1/3$
4	2.79	0.90	$-1/3$	$-1/2$	$-1/6$
5	3.95	1.17	$1/6$	$-1/2$	$-1/3$
6	-0.68	0.90	$1/2$	$1/4$	$-1/6$
7	-0.10	0.94	$1/6$	$-1/6$	1

In the SMEFT interpretation, one-dimensional constraints are derived on the Wilson coefficients after fixing all other coefficients to zero. The results are obtained by including the contributions to the HH and H cross-sections from both linear and quadratic terms in the Wilson coefficient expansion. An interpretation in which the expansion is truncated at linear order is poorly constrained due to the dominance of the quadratic term and can yield negative signal cross-sections. The impact of the operators under study on ggF HH production parameterised as a function of m_{HH} and on single Higgs boson production parameterised as a function of the Higgs boson transverse momentum are included in the interpretation. As in the case of HEFT, the coefficients do not impact the Higgs boson decay branching ratios. The one-dimensional constraints on the SMEFT Wilson coefficients in the scenario where the other parameters are fixed to zero, as expected in the SM, are summarised in Table 6. When using the same statistical procedure of Ref. [34] to determine the constraints on the SMEFT Wilson coefficients, the results are only mildly affected, and the size of the 95% CL interval for c_H ($c_{H\Box}$) is 38% (10%) smaller than that in Ref. [34]. Furthermore, Figure 9 shows two-dimensional likelihood scans as a function of the couplings $c_{H\Box}$ and c_H .

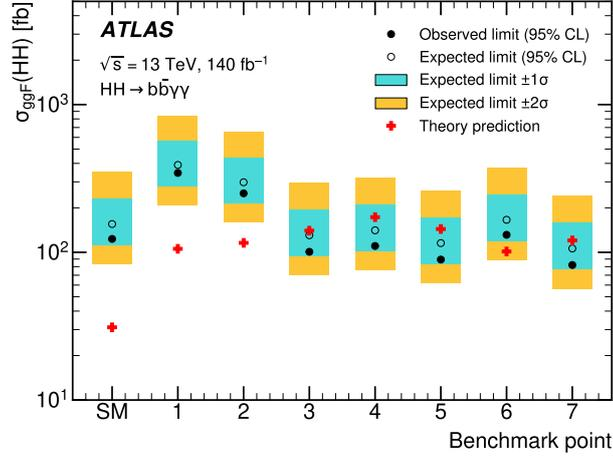


Figure 8: The observed (filled circles) and expected (hollow circles) 95% CL upper limits on the HH ggF production cross-section in the SM and for seven HEFT benchmark points defined in Ref. [101]. The expected constraints are obtained from a background hypothesis with $\sigma_{HH} = 0$. The predicted cross-sections of each of the models under consideration are shown by the crosses. Benchmarks where the filled circles are below the crosses are excluded. The inner and outer shaded bands indicate the $\pm 1\sigma$ and $\pm 2\sigma$ variations on the expected limit due to statistical and systematic uncertainties. The contribution from VBF production to the total HH production cross-section is neglected.

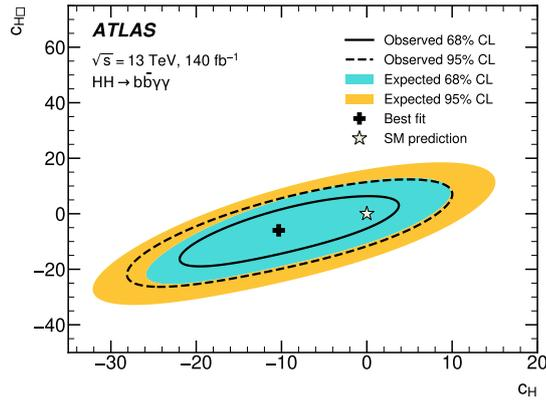


Figure 9: Likelihood contours at 68% (solid line) and 95% (dashed line) CL in the $c_{H\Box}$ versus c_H SMEFT parameter space. The corresponding expected contours are shown by the inner and outer shaded regions. The SM prediction is indicated by the star, while the best-fit value is denoted by the cross.

Table 6: The observed and expected 95% CL constraints on the SMEFT Wilson coefficients, obtained from one dimensional scans of the profile log-likelihood assuming that all other Wilson coefficients are fixed to their SM values. The contribution from VBF production is neglected.

Wilson coefficient	95% CL Observed	95% CL Expected
c_H	[-14.4, 6.2]	[-16.8, 9.7]
$c_{H\Box}$	[-9.4, 10.2]	[-12.4, 13.7]

9 Conclusion

An updated search for nonresonant Higgs boson pair production in the $b\bar{b}\gamma\gamma$ final state is performed using the full Run 2 ATLAS data, corresponding to 140 fb^{-1} of 13 TeV pp collisions. The results supersede and expand upon those of a previous nonresonant search based on the same data sample. Compared to the previous publication, the classification of events in orthogonal event categories is reoptimised to increase the sensitivity to HH production in the main production modes, ggF and VBF, and to the Higgs boson self-coupling and quartic coupling to W, Z bosons. The sensitivity is increased by 6%–17% depending on the parameter of interest. The statistical procedure for the interpretation of the observed yields in terms of the signal coupling strength modifiers has also been updated. In addition, the results are interpreted in the context of the Higgs and SM effective field theory frameworks to constrain the Wilson coefficients of operators describing anomalous Higgs boson interactions.

No evidence of signal is found. In the most sensitive categories of the analysis a small deficit of events in the signal region leads to a 95% CL upper limit on the HH production signal strength $\mu_{HH} < 4.0$ that is lower than the expected value of 5.0 (6.4) in the background-only $\mu_{HH} = 0$ (SM $\mu_{HH} = 1$) hypothesis. The corresponding observed (expected) one-dimensional intervals at 95% CL for the self-coupling modifier κ_λ and the quartic coupling modifier κ_{2V} are $-1.4 < \kappa_\lambda < 6.9$ ($-2.8 < \kappa_\lambda < 7.8$) and $-0.5 < \kappa_{2V} < 2.7$ ($-1.1 < \kappa_{2V} < 3.3$), respectively. From these results, one-dimensional limits on the Wilson coefficients of operators affecting Higgs boson pair production in the Higgs effective field theory ($c_{hhh}, c_{tthh}, c_{ggghh}$) and SM effective field theory ($c_H, c_{H\Box}$) frameworks are inferred. In the former, the comparison between the predicted gluon–gluon fusion HH cross-sections and the corresponding upper limits set by the analysis excludes four of the seven benchmark points considered at 95% CL. While three of these were already excluded by a similar interpretation of the results in the ATLAS search for HH production in the $4b$ final state, one newly proposed benchmark is excluded for the first time by the results presented in this paper. The one-dimensional constraints on the Wilson coefficients considered in this analysis are up to 38% tighter than those reported previously by ATLAS when evaluated using the same statistical procedure.

Acknowledgements

We thank CERN for the very successful operation of the LHC, as well as the support staff from our institutions without whom ATLAS could not be operated efficiently.

We acknowledge the support of ANPCyT, Argentina; YerPhI, Armenia; ARC, Australia; BMWFW and FWF, Austria; ANAS, Azerbaijan; CNPq and FAPESP, Brazil; NSERC, NRC and CFI, Canada; CERN; ANID, Chile; CAS, MOST and NSFC, China; Minciencias, Colombia; MEYS CR, Czech Republic; DNRF and DNSRC, Denmark; IN2P3-CNRS and CEA-DRF/IRFU, France; SRNSFG, Georgia; BMBF,

HGF and MPG, Germany; GSRI, Greece; RGC and Hong Kong SAR, China; ISF and Benozziyo Center, Israel; INFN, Italy; MEXT and JSPS, Japan; CNRST, Morocco; NWO, Netherlands; RCN, Norway; MEiN, Poland; FCT, Portugal; MNE/IFA, Romania; MESTD, Serbia; MSSR, Slovakia; ARRS and MIZŠ, Slovenia; DSI/NRF, South Africa; MICINN, Spain; SRC and Wallenberg Foundation, Sweden; SERI, SNSF and Cantons of Bern and Geneva, Switzerland; MOST, Taiwan; TENMAK, Türkiye; STFC, United Kingdom; DOE and NSF, United States of America. In addition, individual groups and members have received support from BCKDF, CANARIE, Compute Canada and CRC, Canada; PRIMUS 21/SCI/017 and UNCE SCI/013, Czech Republic; COST, ERC, ERDF, Horizon 2020, ICSC-NextGenerationEU and Marie Skłodowska-Curie Actions, European Union; Investissements d’Avenir Labex, Investissements d’Avenir IDEX and ANR, France; DFG and AvH Foundation, Germany; Herakleitos, Thales and Aristeia programmes co-financed by EU-ESF and the Greek NSRF, Greece; BSF-NSF and MINERVA, Israel; Norwegian Financial Mechanism 2014-2021, Norway; NCN and NAWA, Poland; La Caixa Banking Foundation, CERCA Programme Generalitat de Catalunya and PROMETEO and GenT Programmes Generalitat Valenciana, Spain; Göran Gustafssons Stiftelse, Sweden; The Royal Society and Leverhulme Trust, United Kingdom.

The crucial computing support from all WLCG partners is acknowledged gratefully, in particular from CERN, the ATLAS Tier-1 facilities at TRIUMF (Canada), NDGF (Denmark, Norway, Sweden), CC-IN2P3 (France), KIT/GridKA (Germany), INFN-CNAF (Italy), NL-T1 (Netherlands), PIC (Spain), ASGC (Taiwan), RAL (UK) and BNL (USA), the Tier-2 facilities worldwide and large non-WLCG resource providers. Major contributors of computing resources are listed in Ref. [105].

References

- [1] ATLAS Collaboration, *Observation of a new particle in the search for the Standard Model Higgs boson with the ATLAS detector at the LHC*, *Phys. Lett. B* **716** (2012) 1, arXiv: [1207.7214 \[hep-ex\]](#).
- [2] CMS Collaboration, *Observation of a new boson at a mass of 125 GeV with the CMS experiment at the LHC*, *Phys. Lett. B* **716** (2012) 30, arXiv: [1207.7235 \[hep-ex\]](#).
- [3] ATLAS Collaboration, *Study of the spin and parity of the Higgs boson in diboson decays with the ATLAS detector*, *Eur. Phys. J. C* **75** (2015) 476, arXiv: [1506.05669 \[hep-ex\]](#), Erratum: *Eur. Phys. J. C* **76** (2016) 152.
- [4] CMS Collaboration, *Constraints on the spin-parity and anomalous HVV couplings of the Higgs boson in proton collisions at 7 and 8 TeV*, *Phys. Rev. D* **92** (2015) 012004, arXiv: [1411.3441 \[hep-ex\]](#).
- [5] ATLAS Collaboration, *Evidence of off-shell Higgs boson production from ZZ leptonic decay channels and constraints on its total width with the ATLAS detector*, *Phys. Lett. B* **846** (2023) 138223, arXiv: [2304.01532 \[hep-ex\]](#).
- [6] CMS Collaboration, *Measurement of the Higgs boson width and evidence of its off-shell contributions to ZZ production*, *Nature Phys.* **18** (2022) 1329, arXiv: [2202.06923 \[hep-ex\]](#).

- [7] ATLAS Collaboration, *A detailed map of Higgs boson interactions by the ATLAS experiment ten years after the discovery*, *Nature* **607** (2022) 52, arXiv: 2207.00092 [hep-ex].
- [8] CMS Collaboration, *A portrait of the Higgs boson by the CMS experiment ten years after the discovery*, *Nature* **607** (2022) 60, arXiv: 2207.00043 [hep-ex].
- [9] F. Englert and R. Brout, *Broken Symmetry and the Mass of Gauge Vector Mesons*, *Phys. Rev. Lett.* **13** (9 1964) 321.
- [10] P. W. Higgs, *Broken symmetries, massless particles and gauge fields*, *Phys. Lett.* **12** (1964) 132.
- [11] P. W. Higgs, *Broken Symmetries and the Masses of Gauge Bosons*, *Phys. Rev. Lett.* **13** (16 1964) 508.
- [12] G. S. Guralnik, C. R. Hagen and T. W. B. Kibble, *Global Conservation Laws and Massless Particles*, *Phys. Rev. Lett.* **13** (1964) 585.
- [13] P. W. Higgs, *Spontaneous Symmetry Breakdown without Massless Bosons*, *Phys. Rev.* **145** (1966) 1156.
- [14] T. W. B. Kibble, *Symmetry Breaking in Non-Abelian Gauge Theories*, *Phys. Rev.* **155** (1967) 1554.
- [15] S. L. Glashow, *Partial-symmetries of Weak Interactions*, *Nucl. Phys.* **22** (1961) 579.
- [16] A. Salam, *Weak and Electromagnetic Interactions*, *Conf. Proc. C* **680519** (1968) 367.
- [17] S. Weinberg, *A Model of Leptons*, *Phys. Rev. Lett.* **19** (1967) 1264.
- [18] ATLAS and CMS Collaborations, *Combined Measurement of the Higgs Boson Mass in pp Collisions at $\sqrt{s} = 7$ and 8 TeV with the ATLAS and CMS Experiments*, *Phys. Rev. Lett.* **114** (2015) 191803, arXiv: 1503.07589 [hep-ex].
- [19] ATLAS Collaboration, *Combined measurement of the Higgs boson mass from the $H \rightarrow \gamma\gamma$ and $H \rightarrow ZZ^* \rightarrow 4\ell$ decay channels with the ATLAS detector using $\sqrt{s} = 7, 8$ and 13 TeV pp collision data*, CERN-EP-2023-156 (2023), arXiv: 2308.04775 [hep-ex].
- [20] P. Agrawal, D. Saha, L.-X. Xu, J.-H. Yu and C.-P. Yuan, *Determining the shape of the Higgs potential at future colliders*, *Phys. Rev. D* **101** (2020) 075023, arXiv: 1907.02078 [hep-ph].
- [21] M. Grazzini et al., *Higgs boson pair production at NNLO with top quark mass effects*, *JHEP* **05** (2018) 059, arXiv: 1803.02463 [hep-ph].
- [22] S. Dawson, S. Dittmaier and M. Spira, *Neutral Higgs-boson pair production at hadron colliders: QCD corrections*, *Phys. Rev. D* **58** (1998) 115012, arXiv: hep-ph/9805244 [hep-ph].
- [23] S. Borowka et al., *Higgs Boson Pair Production in Gluon Fusion at Next-to-Leading Order with Full Top-Quark Mass Dependence*, *Phys. Rev. Lett.* **117** (2016) 012001, [Erratum: *Phys. Rev. Lett.* **117** (2016) 079901], arXiv: 1604.06447 [hep-ph].
- [24] J. Baglio et al., *Gluon fusion into Higgs pairs at NLO QCD and the top mass scheme*, *Eur. Phys. J. C* **79** (2019) 459, arXiv: 1811.05692 [hep-ph].

- [25] D. de Florian and J. Mazzitelli, *Higgs Boson Pair Production at Next-to-Next-to-Leading Order in QCD*, [Phys. Rev. Lett. **111** \(2013\) 201801](#), arXiv: [1309.6594 \[hep-ph\]](#).
- [26] D. Y. Shao, C. S. Li, H. T. Li and J. Wang, *Threshold resummation effects in Higgs boson pair production at the LHC*, [JHEP **07** \(2013\) 169](#), arXiv: [1301.1245 \[hep-ph\]](#).
- [27] D. de Florian and J. Mazzitelli, *Higgs pair production at next-to-next-to-leading logarithmic accuracy at the LHC*, [JHEP **09** \(2015\) 053](#), arXiv: [1505.07122 \[hep-ph\]](#).
- [28] J. Baglio et al., *gg \rightarrow HH: Combined uncertainties*, [Phys. Rev. D **103** \(2021\) 056002](#), arXiv: [2008.11626 \[hep-ph\]](#).
- [29] F. A. Dreyer and A. Karlberg, *Vector-boson fusion Higgs pair production at N³LO*, [Phys. Rev. D **98** \(11 2018\) 114016](#), arXiv: [1811.07906](#).
- [30] J. Baglio et al., *The measurement of the Higgs self-coupling at the LHC: theoretical status*, [JHEP **04** \(2013\) 151](#), arXiv: [1212.5581](#).
- [31] L.-S. Ling et al., *NNLO QCD corrections to Higgs pair production via vector boson fusion at hadron colliders*, [Phys. Rev. D **89** \(2014\) 073001](#), arXiv: [1401.7754](#).
- [32] ATLAS Collaboration, *Search for Higgs boson pair production in the two bottom quarks plus two photons final state in pp collisions at $\sqrt{s} = 13$ TeV with the ATLAS detector*, [Phys. Rev. D **106** \(2022\) 052001](#), arXiv: [2112.11876 \[hep-ex\]](#).
- [33] ATLAS Collaboration, *Search for resonant and non-resonant Higgs boson pair production in the $b\bar{b}\tau^+\tau^-$ decay channel using 13 TeV pp collision data from the ATLAS detector*, [JHEP **07** \(2023\) 040](#), arXiv: [2209.10910 \[hep-ex\]](#).
- [34] ATLAS Collaboration, *Search for nonresonant pair production of Higgs bosons in the $b\bar{b}b\bar{b}$ final state in pp collisions at $\sqrt{s} = 13$ TeV with the ATLAS detector*, [Phys. Rev. D **108** \(2023\) 052003](#), arXiv: [2301.03212 \[hep-ex\]](#).
- [35] ATLAS Collaboration, *Constraints on the Higgs boson self-coupling from single- and double-Higgs production with the ATLAS detector using pp collisions at $\sqrt{s} = 13$ TeV*, [Phys. Lett. B **843** \(2023\) 137745](#), arXiv: [2211.01216 \[hep-ex\]](#).
- [36] CMS Collaboration, *Search for nonresonant Higgs boson pair production in final states with two bottom quarks and two photons in proton–proton collisions at $\sqrt{s} = 13$ TeV*, [JHEP **03** \(2021\) 257](#), arXiv: [2011.12373 \[hep-ex\]](#).
- [37] CMS Collaboration, *Search for nonresonant Higgs boson pair production in final state with two bottom quarks and two tau leptons in proton–proton collisions at $\sqrt{s} = 13$ TeV*, [Phys. Lett. B **842** \(2022\) 137531](#), arXiv: [2206.09401 \[hep-ex\]](#).
- [38] CMS Collaboration, *Search for Higgs Boson Pair Production in the Four b Quark Final State in Proton–Proton Collisions at $\sqrt{s} = 13$ TeV*, [Phys. Rev. Lett. **129** \(2022\) 081802](#), arXiv: [2202.09617 \[hep-ex\]](#).
- [39] CMS Collaboration, *Search for nonresonant pair production of highly energetic Higgs bosons decaying to bottom quarks*, (2022), arXiv: [2205.06667 \[hep-ex\]](#).

- [40] R. Alonso, M. B. Gavela, L. Merlo, S. Rigolin and J. Yepes, *The effective chiral Lagrangian for a light dynamical "Higgs particle"*, [Phys. Lett. B **722** \(2013\) 330](#), [Erratum: [Phys. Lett. B **726** \(2013\) 926](#)], arXiv: [1212.3305 \[hep-ph\]](#).
- [41] G. Buchalla, O. Catà and C. Krause, *Complete electroweak chiral Lagrangian with a light Higgs at NLO*, [Nucl. Phys. B **880** \(2014\) 552](#), [Erratum: [Nucl. Phys. B **913** \(2016\) 475](#)], arXiv: [1307.5017 \[hep-ph\]](#).
- [42] W. Buchmüller and D. Wyler, *Effective lagrangian analysis of new interactions and flavour conservation*, [Nucl. Phys. B **268** \(1986\) 621](#).
- [43] I. Brivio and M. Trott, *The standard model as an effective field theory*, [Phys. Rept. **793** \(2019\) 1](#), arXiv: [1706.08945 \[hep-ph\]](#).
- [44] ATLAS Collaboration, *The ATLAS Experiment at the CERN Large Hadron Collider*, [JINST **3** \(2008\) S08003](#).
- [45] ATLAS Collaboration, *ATLAS Insertable B-Layer: Technical Design Report*, ATLAS-TDR-19; CERN-LHCC-2010-013, 2010, URL: <https://cds.cern.ch/record/1291633>, Addendum: ATLAS-TDR-19-ADD-1; CERN-LHCC-2012-009, 2012, URL: <https://cds.cern.ch/record/1451888>.
- [46] B. Abbott et al., *Production and integration of the ATLAS Insertable B-Layer*, [JINST **13** \(2018\) T05008](#), arXiv: [1803.00844 \[physics.ins-det\]](#).
- [47] ATLAS Collaboration, *Performance of the ATLAS trigger system in 2015*, [Eur. Phys. J. C **77** \(2017\) 317](#), arXiv: [1611.09661 \[hep-ex\]](#).
- [48] ATLAS Collaboration, *The ATLAS Collaboration Software and Firmware*, ATL-SOFT-PUB-2021-001, 2021, URL: <https://cds.cern.ch/record/2767187>.
- [49] ATLAS Collaboration, *ATLAS data quality operations and performance for 2015–2018 data-taking*, [JINST **15** \(2020\) P04003](#), arXiv: [1911.04632 \[physics.ins-det\]](#).
- [50] ATLAS Collaboration, *Luminosity determination in pp collisions at $\sqrt{s} = 13$ TeV using the ATLAS detector at the LHC*, CERN-EP-2022-281 (2022), arXiv: [2212.09379 \[hep-ex\]](#).
- [51] P. Nason, *A new method for combining NLO QCD with shower Monte Carlo algorithms*, [JHEP **11** \(2004\) 040](#), arXiv: [hep-ph/0409146](#).
- [52] S. Frixione, P. Nason and C. Oleari, *Matching NLO QCD computations with parton shower simulations: the POWHEG method*, [JHEP **11** \(2007\) 070](#), arXiv: [0709.2092 \[hep-ph\]](#).
- [53] S. Alioli, P. Nason, C. Oleari and E. Re, *A general framework for implementing NLO calculations in shower Monte Carlo programs: the POWHEG BOX*, [JHEP **06** \(2010\) 043](#), arXiv: [1002.2581 \[hep-ph\]](#).
- [54] G. Heinrich, S. P. Jones, M. Kerner, G. Luisoni and E. Vryonidou, *NLO predictions for Higgs boson pair production with full top quark mass dependence matched to parton showers*, [JHEP **08** \(2017\) 088](#), arXiv: [1703.09252 \[hep-ph\]](#).

- [55] G. Heinrich, S. P. Jones, M. Kerner, G. Luisoni and L. Scyboz, *Probing the trilinear Higgs boson coupling in di-Higgs production at NLO QCD including parton shower effects*, *JHEP* **06** (2019) 066, arXiv: [1903.08137 \[hep-ph\]](#).
- [56] J. Butterworth et al., *PDF4LHC recommendations for LHC Run II*, *J. Phys. G* **43** (2016) 023001, arXiv: [1510.03865 \[hep-ph\]](#).
- [57] T. Sjöstrand et al., *An introduction to PYTHIA 8.2*, *Comput. Phys. Commun.* **191** (2015) 159, arXiv: [1410.3012 \[hep-ph\]](#).
- [58] ATLAS Collaboration, *ATLAS Pythia 8 tunes to 7 TeV data*, ATL-PHYS-PUB-2014-021, 2014, URL: <https://cds.cern.ch/record/1966419>.
- [59] J. Alwall et al., *The automated computation of tree-level and next-to-leading order differential cross sections, and their matching to parton shower simulations*, *JHEP* **07** (2014) 079, arXiv: [1405.0301 \[hep-ph\]](#).
- [60] The NNPDF Collaboration, R. D. Ball et al., *Parton distributions for the LHC run II*, *JHEP* **04** (2015) 040, arXiv: [1410.8849 \[hep-ph\]](#).
- [61] K. Hamilton, P. Nason, E. Re and G. Zanderighi, *NNLOPS simulation of Higgs boson production*, *JHEP* **10** (2013) 222, arXiv: [1309.0017 \[hep-ph\]](#).
- [62] K. Hamilton, P. Nason and G. Zanderighi, *Finite quark-mass effects in the NNLOPS POWHEG+MiNLO Higgs generator*, *JHEP* **05** (2015) 140, arXiv: [1501.04637 \[hep-ph\]](#).
- [63] ATLAS Collaboration, *Measurement of the Z/γ^* boson transverse momentum distribution in pp collisions at $\sqrt{s} = 7$ TeV with the ATLAS detector*, *JHEP* **09** (2014) 145, arXiv: [1406.3660 \[hep-ex\]](#).
- [64] P. Nason and C. Oleari, *NLO Higgs boson production via vector-boson fusion matched with shower in POWHEG*, *JHEP* **02** (2010) 037, arXiv: [0911.5299 \[hep-ph\]](#).
- [65] G. Luisoni, P. Nason, C. Oleari and F. Tramontano, *$HW^\pm/HZ + 0$ and 1 jet at NLO with the POWHEG BOX interfaced to GoSam and their merging within MiNLO*, *JHEP* **10** (2013) 083, arXiv: [1306.2542 \[hep-ph\]](#).
- [66] H. B. Hartanto, B. Jäger, L. Reina and D. Wackerroth, *Higgs boson production in association with top quarks in the POWHEG BOX*, *Phys. Rev. D* **91** (2015) 094003, arXiv: [1501.04498 \[hep-ph\]](#).
- [67] B. Jäger, L. Reina and D. Wackerroth, *Higgs boson production in association with b jets in the POWHEG BOX*, *Phys. Rev. D* **93** (2016) 014030, arXiv: [1509.05843 \[hep-ph\]](#).
- [68] E. Bothmann et al., *Event generation with Sherpa 2.2*, *SciPost Phys.* **7** (2019) 034, arXiv: [1905.09127 \[hep-ph\]](#).
- [69] ATLAS Collaboration, *Validation of signal Monte Carlo event generation in searches for Higgs boson pairs with the ATLAS detector*, ATL-PHYS-PUB-2019-007, 2019, URL: <https://cds.cern.ch/record/2665057>.
- [70] ATLAS Collaboration, *The ATLAS Simulation Infrastructure*, *Eur. Phys. J. C* **70** (2010) 823, arXiv: [1005.4568 \[physics.ins-det\]](#).
- [71] S. Agostinelli et al., *GEANT4 – a simulation toolkit*, *Nucl. Instrum. Meth. A* **506** (2003) 250.

- [72] ATLAS Collaboration, *The simulation principle and performance of the ATLAS fast calorimeter simulation FastCaloSim*, ATL-PHYS-PUB-2010-013, 2010, URL: <https://cds.cern.ch/record/1300517>.
- [73] ATLAS Collaboration, *The Pythia 8 A3 tune description of ATLAS minimum bias and inelastic measurements incorporating the Donnachie–Landshoff diffractive model*, ATL-PHYS-PUB-2016-017, 2016, URL: <https://cds.cern.ch/record/2206965>.
- [74] ATLAS Collaboration, *Performance of electron and photon triggers in ATLAS during LHC Run 2*, *Eur. Phys. J. C* **80** (2020) 47, arXiv: [1909.00761](https://arxiv.org/abs/1909.00761) [hep-ex].
- [75] ATLAS Collaboration, *Measurement of Higgs boson production in the diphoton decay channel in pp collisions at center-of-mass energies of 7 and 8 TeV with the ATLAS detector*, *Phys. Rev. D* **90** (2014) 112015, arXiv: [1408.7084](https://arxiv.org/abs/1408.7084) [hep-ex].
- [76] ATLAS Collaboration, *Electron and photon performance measurements with the ATLAS detector using the 2015–2017 LHC proton–proton collision data*, *JINST* **14** (2019) P12006, arXiv: [1908.00005](https://arxiv.org/abs/1908.00005) [hep-ex].
- [77] M. Cacciari, G. P. Salam and G. Soyez, *FastJet user manual*, *Eur. Phys. J. C* **72** (2012) 1896, arXiv: [1111.6097](https://arxiv.org/abs/1111.6097) [hep-ph].
- [78] M. Cacciari, G. P. Salam and G. Soyez, *The anti- k_t jet clustering algorithm*, *JHEP* **04** (2008) 063, arXiv: [0802.1189](https://arxiv.org/abs/0802.1189) [hep-ph].
- [79] ATLAS Collaboration, *Tagging and suppression of pileup jets with the ATLAS detector*, ATL-CONF-2014-018, 2014, URL: <https://cds.cern.ch/record/1700870>.
- [80] ATLAS Collaboration, *ATLAS flavour-tagging algorithms for the LHC Run 2 pp collision dataset*, *Eur. Phys. J. C* **83** (2023) 681, arXiv: [2211.16345](https://arxiv.org/abs/2211.16345) [physics.data-an].
- [81] T. Chen and C. Guestrin, ‘XGBoost: A Scalable Tree Boosting System’, *KDD 16*, (2016), 785, arXiv: [1603.02754](https://arxiv.org/abs/1603.02754) [cs.LG].
- [82] ATLAS Collaboration, *Performance of missing transverse momentum reconstruction with the ATLAS detector using proton–proton collisions at $\sqrt{s} = 13$ TeV*, *Eur. Phys. J. C* **78** (2018) 903, arXiv: [1802.08168](https://arxiv.org/abs/1802.08168) [hep-ex].
- [83] ATLAS Collaboration, *Measurement of event shapes at large momentum transfer with the ATLAS detector in pp collisions at $\sqrt{s} = 7$ TeV*, *Eur. Phys. J. C* **72** (2012) 2211, arXiv: [1206.2135](https://arxiv.org/abs/1206.2135) [hep-ex].
- [84] L. G. Almeida et al., *Substructure of high- p_T jets at the LHC*, *Phys. Rev. D* **79** (2009) 074017, arXiv: [0807.0234](https://arxiv.org/abs/0807.0234) [hep-ph].
- [85] G. Cowan, K. Cranmer, E. Gross and O. Vitells, *Asymptotic formulae for likelihood-based tests of new physics*, *Eur. Phys. J. C* **71** (2011) 1554, arXiv: [1007.1727](https://arxiv.org/abs/1007.1727) [physics.data-an], Erratum: *Eur. Phys. J. C* **73** (2013) 2501.
- [86] M. Oreglia, *A Study of the Reactions $\psi' \rightarrow \gamma\gamma\psi$* , Appendix D. Ph.D. thesis, Stanford University, SLAC-R-0236 (1980), URL: <https://www-public.slac.stanford.edu/sciDoc/docMeta.aspx?slacPubNumber=slac-r-236>.
- [87] ATLAS Collaboration, *Recommendations for the Modeling of Smooth Backgrounds*, ATL-PHYS-PUB-2020-028, 2020, URL: <https://cds.cern.ch/record/2743717>.
- [88] G. Avoni et al., *The new LUCID-2 detector for luminosity measurement and monitoring in ATLAS*, *JINST* **13** (2018) P07017.

- [89] ATLAS Collaboration, *Measurement of the properties of Higgs boson production at $\sqrt{s} = 13$ TeV in the $H \rightarrow \gamma\gamma$ channel using 139 fb^{-1} of pp collision data with the ATLAS experiment*, [JHEP **07** \(2023\) 088](#), arXiv: [2207.00348 \[hep-ex\]](#).
- [90] ATLAS Collaboration, *Jet energy scale and resolution measured in proton–proton collisions at $\sqrt{s} = 13$ TeV with the ATLAS detector*, [Eur. Phys. J. C **81** \(2021\) 689](#), arXiv: [2007.02645 \[hep-ex\]](#).
- [91] ATLAS Collaboration, *Measurement of the c -jet mistagging efficiency in $t\bar{t}$ events using pp collision data at $\sqrt{s} = 13$ TeV collected with the ATLAS detector*, [Eur. Phys. J. C **82** \(2022\) 95](#), arXiv: [2109.10627 \[hep-ex\]](#).
- [92] ATLAS Collaboration, *Calibration of the light-flavour jet mistagging efficiency of the b -tagging algorithms with Z +jets events using 139 fb^{-1} of ATLAS proton-proton collision data at $\sqrt{s} = 13$ TeV*, [Eur. Phys. J. C **83** \(2023\) 728](#), arXiv: [2301.06319 \[hep-ex\]](#).
- [93] B. Di Micco, M. Gouzevitch, J. Mazzitelli and C. Vernieri, *Higgs boson potential at colliders: Status and perspectives*, [Reviews in Physics **5** \(2020\) 100045](#), arXiv: [1910.00012 \[hep-ph\]](#).
- [94] LHC Higgs Cross Section Working Group, D. de Florian et al., *Handbook of LHC Higgs cross sections: 4. Deciphering the nature of the Higgs sector*, [CERN-2017-002-M \(2017\)](#), arXiv: [1610.07922 \[hep-ph\]](#).
- [95] ATLAS Collaboration, *Measurements of inclusive and differential fiducial cross-sections of $t\bar{t}$ production with additional heavy-flavour jets in proton–proton collisions at $\sqrt{s} = 13$ TeV with the ATLAS detector*, [JHEP **04** \(2019\) 046](#), arXiv: [1811.12113 \[hep-ex\]](#).
- [96] ATLAS Collaboration, *Study of heavy-flavor quarks produced in association with top-quark pairs at $\sqrt{s} = 7$ TeV using the ATLAS detector*, [Phys. Rev. D **89** \(2014\) 072012](#), arXiv: [1304.6386 \[hep-ex\]](#).
- [97] ATLAS Collaboration, *Measurement of the cross-section for W boson production in association with b -jets in pp collisions at $\sqrt{s} = 7$ TeV with the ATLAS detector*, [JHEP **06** \(2013\) 084](#), arXiv: [1302.2929 \[hep-ex\]](#).
- [98] ATLAS and CMS Collaborations, *Measurements of the Higgs boson production and decay rates and constraints on its couplings from a combined ATLAS and CMS analysis of the LHC pp collision data at $\sqrt{s} = 7$ and 8 TeV*, [JHEP **08** \(2016\) 045](#), arXiv: [1606.02266 \[hep-ex\]](#).
- [99] A. L. Read, *Presentation of search results: the CL_s technique*, [J. Phys. G **28** \(2002\) 2693](#).
- [100] K. G. Hayes, M. L. Perl and B. Efron, *Application of the bootstrap statistical method to the tau-decay-mode problem*, [Phys. Rev. D **39** \(1 1989\) 274](#).
- [101] L. Alasfar et al., *Effective Field Theory descriptions of Higgs boson pair production*, (2023), arXiv: [2304.01968 \[hep-ph\]](#).
- [102] B. Grzadkowski, M. Iskrzyński, M. Misiak and J. Rosiek, *Dimension-six terms in the Standard Model Lagrangian*, [JHEP **10** \(2010\) 085](#), arXiv: [1008.4884 \[hep-ph\]](#).

- [103] R. Gröber et al., *Effective Field Theory descriptions of Higgs boson pair production*, LHCHWG-2022-004, 2022, URL: <https://cds.cern.ch/record/2843280>.
- [104] C. Degrande et al., *Automated one-loop computations in the standard model effective field theory*, *Phys. Rev. D* **103** (2021) 096024, arXiv: 2008.11743 [hep-ph].
- [105] ATLAS Collaboration, *ATLAS Computing Acknowledgements*, ATL-SOFT-PUB-2023-001, 2023, URL: <https://cds.cern.ch/record/2869272>.

The ATLAS Collaboration

G. Aad ¹⁰², B. Abbott ¹²⁰, K. Abeling ⁵⁵, N.J. Abicht ⁴⁹, S.H. Abidi ²⁹, A. Aboulhorma ^{35e}, H. Abramowicz ¹⁵¹, H. Abreu ¹⁵⁰, Y. Abulaiti ¹¹⁷, B.S. Acharya ^{69a,69b,m}, C. Adam Bourdarios ⁴, L. Adamczyk ^{86a}, S.V. Addepalli ²⁶, M.J. Addison ¹⁰¹, J. Adelman ¹¹⁵, A. Adiguzel ^{21c}, T. Adye ¹³⁴, A.A. Affolder ¹³⁶, Y. Afik ³⁶, M.N. Agaras ¹³, J. Agarwala ^{73a,73b}, A. Aggarwal ¹⁰⁰, C. Agheorghiesei ^{27c}, A. Ahmad ³⁶, F. Ahmadov ^{38,y}, W.S. Ahmed ¹⁰⁴, S. Ahuja ⁹⁵, X. Ai ^{62a}, G. Aielli ^{76a,76b}, A. Aikot ¹⁶³, M. Ait Tamlihat ^{35e}, B. Aitbenchikh ^{35a}, I. Aizenberg ¹⁶⁹, M. Akbiyik ¹⁰⁰, T.P.A. Åkesson ⁹⁸, A.V. Akimov ³⁷, D. Akiyama ¹⁶⁸, N.N. Akolkar ²⁴, S. Aktas ^{21a}, K. Al Houry ⁴¹, G.L. Alberghi ^{23b}, J. Albert ¹⁶⁵, P. Albicocco ⁵³, G.L. Albouy ⁶⁰, S. Alderweireldt ⁵², Z.L. Alegria ¹²¹, M. Aleksa ³⁶, I.N. Aleksandrov ³⁸, C. Alexa ^{27b}, T. Alexopoulos ¹⁰, F. Alfonsi ^{23b}, M. Algren ⁵⁶, M. Alhroob ¹²⁰, B. Ali ¹³², H.M.J. Ali ⁹¹, S. Ali ¹⁴⁸, S.W. Alibocus ⁹², M. Aliev ¹⁴⁵, G. Alimonti ^{71a}, W. Alkakhki ⁵⁵, C. Allaire ⁶⁶, B.M.M. Allbrooke ¹⁴⁶, J.F. Allen ⁵², C.A. Allendes Flores ^{137f}, P.P. Allport ²⁰, A. Aloisio ^{72a,72b}, F. Alonso ⁹⁰, C. Alpigiani ¹³⁸, M. Alvarez Estevez ⁹⁹, A. Alvarez Fernandez ¹⁰⁰, M. Alves Cardoso ⁵⁶, M.G. Alviggi ^{72a,72b}, M. Aly ¹⁰¹, Y. Amaral Coutinho ^{83b}, A. Ambler ¹⁰⁴, C. Amelung ³⁶, M. Amerl ¹⁰¹, C.G. Ames ¹⁰⁹, D. Amidei ¹⁰⁶, S.P. Amor Dos Santos ^{130a}, K.R. Amos ¹⁶³, V. Ananiev ¹²⁵, C. Anastopoulos ¹³⁹, T. Andeen ¹¹, J.K. Anders ³⁶, S.Y. Andrean ^{47a,47b}, A. Andreazza ^{71a,71b}, S. Angelidakis ⁹, A. Angerami ^{41,ab}, A.V. Anisenkov ³⁷, A. Annovi ^{74a}, C. Antel ⁵⁶, M.T. Anthony ¹³⁹, E. Antipov ¹⁴⁵, M. Antonelli ⁵³, F. Anulli ^{75a}, M. Aoki ⁸⁴, T. Aoki ¹⁵³, J.A. Aparisi Pozo ¹⁶³, M.A. Aparo ¹⁴⁶, L. Aperio Bella ⁴⁸, C. Appelt ¹⁸, A. Apyan ²⁶, N. Aranzabal ³⁶, S.J. Arbiol Val ⁸⁷, C. Arcangeletti ⁵³, A.T.H. Arce ⁵¹, E. Arena ⁹², J-F. Arguin ¹⁰⁸, S. Argyropoulos ⁵⁴, J.-H. Arling ⁴⁸, O. Arnaez ⁴, H. Arnold ¹¹⁴, G. Artoni ^{75a,75b}, H. Asada ¹¹¹, K. Asai ¹¹⁸, S. Asai ¹⁵³, N.A. Asbah ⁶¹, K. Assamagan ²⁹, R. Astalos ^{28a}, S. Atashi ¹⁶⁰, R.J. Atkin ^{33a}, M. Atkinson ¹⁶², H. Atmani ^{35f}, P.A. Atlasiddha ¹²⁸, K. Augsten ¹³², S. Auricchio ^{72a,72b}, A.D. Auriol ²⁰, V.A. Austrup ¹⁰¹, G. Avolio ³⁶, K. Axiotis ⁵⁶, G. Azuelos ^{108,af}, D. Babal ^{28b}, H. Bachacou ¹³⁵, K. Bachas ^{152,p}, A. Bachi ³⁴, F. Backman ^{47a,47b}, A. Badea ⁶¹, T.M. Baer ¹⁰⁶, P. Bagnaia ^{75a,75b}, M. Bahmani ¹⁸, D. Bahner ⁵⁴, A.J. Bailey ¹⁶³, V.R. Bailey ¹⁶², J.T. Baines ¹³⁴, L. Baines ⁹⁴, O.K. Baker ¹⁷², E. Bakos ¹⁵, D. Bakshi Gupta ⁸, V. Balakrishnan ¹²⁰, R. Balasubramanian ¹¹⁴, E.M. Baldin ³⁷, P. Balek ^{86a}, E. Ballabene ^{23b,23a}, F. Balli ¹³⁵, L.M. Baltes ^{63a}, W.K. Balunas ³², J. Balz ¹⁰⁰, E. Banas ⁸⁷, M. Bandieramonte ¹²⁹, A. Bandyopadhyay ²⁴, S. Bansal ²⁴, L. Barak ¹⁵¹, M. Barakat ⁴⁸, E.L. Barberio ¹⁰⁵, D. Barberis ^{57b,57a}, M. Barbero ¹⁰², M.Z. Barel ¹¹⁴, K.N. Barends ^{33a}, T. Barillari ¹¹⁰, M-S. Barisits ³⁶, T. Barklow ¹⁴³, P. Baron ¹²², D.A. Baron Moreno ¹⁰¹, A. Baroncelli ^{62a}, G. Barone ²⁹, A.J. Barr ¹²⁶, J.D. Barr ⁹⁶, L. Barranco Navarro ^{47a,47b}, F. Barreiro ⁹⁹, J. Barreiro Guimarães da Costa ^{14a}, U. Barron ¹⁵¹, M.G. Barros Teixeira ^{130a}, S. Barsov ³⁷, F. Bartels ^{63a}, R. Bartoldus ¹⁴³, A.E. Barton ⁹¹, P. Bartos ^{28a}, A. Basan ¹⁰⁰, M. Baselga ⁴⁹, A. Bassalat ^{66,b}, M.J. Basso ^{156a}, C.R. Basson ¹⁰¹, R.L. Bates ⁵⁹, S. Batlamous ^{35e}, J.R. Batley ³², B. Batool ¹⁴¹, M. Battaglia ¹³⁶, D. Battulga ¹⁸, M. Bauce ^{75a,75b}, M. Bauer ³⁶, P. Bauer ²⁴, L.T. Bazzano Hurrell ³⁰, J.B. Beacham ⁵¹, T. Beau ¹²⁷, J.Y. Beauchamp ⁹⁰, P.H. Beauchemin ¹⁵⁸, F. Becherer ⁵⁴, P. Bechtel ²⁴, H.P. Beck ^{19,o}, K. Becker ¹⁶⁷, A.J. Beddall ⁸², V.A. Bednyakov ³⁸, C.P. Bee ¹⁴⁵, L.J. Beamster ¹⁵, T.A. Beermann ³⁶, M. Begalli ^{83d}, M. Begel ²⁹, A. Behera ¹⁴⁵, J.K. Behr ⁴⁸, J.F. Beirer ³⁶, F. Beisiegel ²⁴, M. Belfkir ¹⁵⁹, G. Bella ¹⁵¹, L. Bellagamba ^{23b}, A. Bellerive ³⁴, P. Bellos ²⁰, K. Beloborodov ³⁷, D. Bencheekroun ^{35a}, F. Bendebba ^{35a}, Y. Benhammou ¹⁵¹, M. Benoit ²⁹, J.R. Bensinger ²⁶, S. Bentvelsen ¹¹⁴, L. Beresford ⁴⁸,

M. Beretta ⁵³, E. Bergeaas Kuutmann ¹⁶¹, N. Berger ⁴, B. Bergmann ¹³², J. Beringer ^{17a},
G. Bernardi ⁵, C. Bernius ¹⁴³, F.U. Bernlochner ²⁴, F. Bernon ^{36,102}, A. Berrocal Guardia ¹³,
T. Berry ⁹⁵, P. Berta ¹³³, A. Berthold ⁵⁰, I.A. Bertram ⁹¹, S. Bethke ¹¹⁰, A. Betti ^{75a,75b},
A.J. Bevan ⁹⁴, N.K. Bhalla ⁵⁴, M. Bhamjee ^{33c}, S. Bhatta ¹⁴⁵, D.S. Bhattacharya ¹⁶⁶,
P. Bhattarai ¹⁴³, V.S. Bhopatkar ¹²¹, R. Bi ^{29,ai}, R.M. Bianchi ¹²⁹, G. Bianco ^{23b,23a}, O. Biebel ¹⁰⁹,
R. Bielski ¹²³, M. Biglietti ^{77a}, M. Bindi ⁵⁵, A. Bingul ^{21b}, C. Bini ^{75a,75b}, A. Biondini ⁹²,
C.J. Birch-sykes ¹⁰¹, G.A. Bird ^{20,134}, M. Birman ¹⁶⁹, M. Biros ¹³³, S. Biryukov ¹⁴⁶,
T. Bisanz ⁴⁹, E. Bisceglie ^{43b,43a}, J.P. Biswal ¹³⁴, D. Biswas ¹⁴¹, A. Bitadze ¹⁰¹, K. Bjørke ¹²⁵,
I. Bloch ⁴⁸, A. Blue ⁵⁹, U. Blumenschein ⁹⁴, J. Blumenthal ¹⁰⁰, G.J. Bobbink ¹¹⁴,
V.S. Bobrovnikov ³⁷, M. Boehler ⁵⁴, B. Boehm ¹⁶⁶, D. Bogavac ³⁶, A.G. Bogdanchikov ³⁷,
C. Bohm ^{47a}, V. Boisvert ⁹⁵, P. Bokan ⁴⁸, T. Bold ^{86a}, M. Bomben ⁵, M. Bona ⁹⁴,
M. Boonekamp ¹³⁵, C.D. Booth ⁹⁵, A.G. Borbély ⁵⁹, I.S. Bordulev ³⁷, H.M. Borecka-Bielska ¹⁰⁸,
G. Borissov ⁹¹, D. Bortoletto ¹²⁶, D. Boscherini ^{23b}, M. Bosman ¹³, J.D. Bossio Sola ³⁶,
K. Bouaouda ^{35a}, N. Bouchhar ¹⁶³, J. Boudreau ¹²⁹, E.V. Bouhova-Thacker ⁹¹, D. Boumediene ⁴⁰,
R. Bouquet ¹⁶⁵, A. Boveia ¹¹⁹, J. Boyd ³⁶, D. Boye ²⁹, I.R. Boyko ³⁸, J. Bracinik ²⁰,
N. Brahimy ^{62d}, G. Brandt ¹⁷¹, O. Brandt ³², F. Braren ⁴⁸, B. Brau ¹⁰³, J.E. Brau ¹²³,
R. Brenner ¹⁶⁹, L. Brenner ¹¹⁴, R. Brenner ¹⁶¹, S. Bressler ¹⁶⁹, D. Britton ⁵⁹, D. Britzger ¹¹⁰,
I. Brock ²⁴, G. Brooijmans ⁴¹, W.K. Brooks ^{137f}, E. Brost ²⁹, L.M. Brown ¹⁶⁵, L.E. Bruce ⁶¹,
T.L. Bruckler ¹²⁶, P.A. Bruckman de Renstrom ⁸⁷, B. Brüers ⁴⁸, A. Bruni ^{23b}, G. Bruni ^{23b},
M. Bruschi ^{23b}, N. Bruscinò ^{75a,75b}, T. Buanes ¹⁶, Q. Buat ¹³⁸, D. Buchin ¹¹⁰, A.G. Buckley ⁵⁹,
O. Bulekov ³⁷, B.A. Bullard ¹⁴³, S. Burdin ⁹², C.D. Burgard ⁴⁹, A.M. Burger ⁴⁰,
B. Burghgrave ⁸, O. Burlayenko ⁵⁴, J.T.P. Burr ³², C.D. Burton ¹¹, J.C. Burzynski ¹⁴²,
E.L. Busch ⁴¹, V. Büscher ¹⁰⁰, P.J. Bussey ⁵⁹, J.M. Butler ²⁵, C.M. Buttar ⁵⁹,
J.M. Butterworth ⁹⁶, W. Buttinger ¹³⁴, C.J. Buxo Vazquez ¹⁰⁷, A.R. Buzykaev ³⁷,
S. Cabrera Urbán ¹⁶³, L. Cadamuro ⁶⁶, D. Caforio ⁵⁸, H. Cai ¹²⁹, Y. Cai ^{14a,14e}, Y. Cai ^{14c},
V.M.M. Cairo ³⁶, O. Cakir ^{3a}, N. Calace ³⁶, P. Calafiura ^{17a}, G. Calderini ¹²⁷, P. Calfayan ⁶⁸,
G. Callea ⁵⁹, L.P. Caloba ^{83b}, D. Calvet ⁴⁰, S. Calvet ⁴⁰, T.P. Calvet ¹⁰², M. Calvetti ^{74a,74b},
R. Camacho Toro ¹²⁷, S. Camarda ³⁶, D. Camarero Munoz ²⁶, P. Camarri ^{76a,76b},
M.T. Camerlingo ^{72a,72b}, D. Cameron ³⁶, C. Camincher ¹⁶⁵, M. Campanelli ⁹⁶, A. Camplani ⁴²,
V. Canale ^{72a,72b}, A. Canesse ¹⁰⁴, J. Cantero ¹⁶³, Y. Cao ¹⁶², F. Capocasa ²⁶, M. Capua ^{43b,43a},
A. Carbone ^{71a,71b}, R. Cardarelli ^{76a}, J.C.J. Cardenas ⁸, F. Cardillo ¹⁶³, G. Carducci ^{43b,43a},
T. Carli ³⁶, G. Carlino ^{72a}, J.I. Carlotto ¹³, B.T. Carlson ^{129,q}, E.M. Carlson ^{165,156a},
L. Carminati ^{71a,71b}, A. Carnelli ¹³⁵, M. Carnesale ^{75a,75b}, S. Caron ¹¹³, E. Carquin ^{137f},
S. Carrá ^{71a}, G. Carratta ^{23b,23a}, F. Carrio Argos ^{33g}, J.W.S. Carter ¹⁵⁵, T.M. Carter ⁵²,
M.P. Casado ^{13,i}, M. Caspar ⁴⁸, F.L. Castillo ⁴, L. Castillo Garcia ¹³, V. Castillo Gimenez ¹⁶³,
N.F. Castro ^{130a,130e}, A. Catinaccio ³⁶, J.R. Catmore ¹²⁵, V. Cavaliere ²⁹, N. Cavalli ^{23b,23a},
V. Cavasinni ^{74a,74b}, Y.C. Cekmecelioglu ⁴⁸, E. Celebi ^{21a}, F. Celli ¹²⁶, M.S. Centonze ^{70a,70b},
V. Cepaitis ⁵⁶, K. Cerny ¹²², A.S. Cerqueira ^{83a}, A. Cerri ¹⁴⁶, L. Cerrito ^{76a,76b}, F. Cerutti ^{17a},
B. Cervato ¹⁴¹, A. Cervelli ^{23b}, G. Cesarini ⁵³, S.A. Cetin ⁸², D. Chakraborty ¹¹⁵, J. Chan ¹⁷⁰,
W.Y. Chan ¹⁵³, J.D. Chapman ³², E. Chapon ¹³⁵, B. Chargeishvili ^{149b}, D.G. Charlton ²⁰,
M. Chatterjee ¹⁹, C. Chauhan ¹³³, S. Chekanov ⁶, S.V. Chekulaev ^{156a}, G.A. Chelkov ^{38,a},
A. Chen ¹⁰⁶, B. Chen ¹⁵¹, B. Chen ¹⁶⁵, H. Chen ^{14c}, H. Chen ²⁹, J. Chen ^{62c}, J. Chen ¹⁴²,
M. Chen ¹²⁶, S. Chen ¹⁵³, S.J. Chen ^{14c}, X. Chen ^{62c,135}, X. Chen ^{14b,ae}, Y. Chen ^{62a},
C.L. Cheng ¹⁷⁰, H.C. Cheng ^{64a}, S. Cheong ¹⁴³, A. Cheplakov ³⁸, E. Cheremushkina ⁴⁸,
E. Cherepanova ¹¹⁴, R. Cherkaoui El Moursli ^{35e}, E. Cheu ⁷, K. Cheung ⁶⁵, L. Chevalier ¹³⁵,
V. Chiarella ⁵³, G. Chiarelli ^{74a}, N. Chiedde ¹⁰², G. Chiodini ^{70a}, A.S. Chisholm ²⁰,
A. Chitan ^{27b}, M. Chitishvili ¹⁶³, M.V. Chizhov ³⁸, K. Choi ¹¹, A.R. Chomont ^{75a,75b},

Y. Chou [id](#)¹⁰³, E.Y.S. Chow [id](#)¹¹³, T. Chowdhury [id](#)^{33g}, K.L. Chu [id](#)¹⁶⁹, M.C. Chu [id](#)^{64a}, X. Chu [id](#)^{14a,14e},
 J. Chudoba [id](#)¹³¹, J.J. Chwastowski [id](#)⁸⁷, D. Cieri [id](#)¹¹⁰, K.M. Ciesla [id](#)^{86a}, V. Cindro [id](#)⁹³, A. Ciocio [id](#)^{17a},
 F. Cirotto [id](#)^{72a,72b}, Z.H. Citron [id](#)^{169,k}, M. Citterio [id](#)^{71a}, D.A. Ciubotaru^{27b}, A. Clark [id](#)⁵⁶, P.J. Clark [id](#)⁵²,
 C. Clarry [id](#)¹⁵⁵, J.M. Clavijo Columbie [id](#)⁴⁸, S.E. Clawson [id](#)⁴⁸, C. Clement [id](#)^{47a,47b}, J. Clercx [id](#)⁴⁸,
 Y. Coadou [id](#)¹⁰², M. Cobal [id](#)^{69a,69c}, A. Coccaro [id](#)^{57b}, R.F. Coelho Barrue [id](#)^{130a},
 R. Coelho Lopes De Sa [id](#)¹⁰³, S. Coelli [id](#)^{71a}, A.E.C. Coimbra [id](#)^{71a,71b}, B. Cole [id](#)⁴¹, J. Collot [id](#)⁶⁰,
 P. Conde Muiño [id](#)^{130a,130g}, M.P. Connell [id](#)^{33c}, S.H. Connell [id](#)^{33c}, I.A. Connelly [id](#)⁵⁹, E.I. Conroy [id](#)¹²⁶,
 F. Conventi [id](#)^{72a,ag}, H.G. Cooke [id](#)²⁰, A.M. Cooper-Sarkar [id](#)¹²⁶, A. Cordeiro Oudot Choi [id](#)¹²⁷,
 L.D. Corpe [id](#)⁴⁰, M. Corradi [id](#)^{75a,75b}, F. Corriveau [id](#)^{104,w}, A. Cortes-Gonzalez [id](#)¹⁸, M.J. Costa [id](#)¹⁶³,
 F. Costanza [id](#)⁴, D. Costanzo [id](#)¹³⁹, B.M. Cote [id](#)¹¹⁹, G. Cowan [id](#)⁹⁵, K. Cranmer [id](#)¹⁷⁰,
 D. Cremonini [id](#)^{23b,23a}, S. Crépe-Renaudin [id](#)⁶⁰, F. Crescioli [id](#)¹²⁷, M. Cristinziani [id](#)¹⁴¹,
 M. Cristoforetti [id](#)^{78a,78b}, V. Croft [id](#)¹¹⁴, J.E. Crosby [id](#)¹²¹, G. Crosetti [id](#)^{43b,43a}, A. Cueto [id](#)⁹⁹,
 T. Cuhadar Donszelmann [id](#)¹⁶⁰, H. Cui [id](#)^{14a,14e}, Z. Cui [id](#)⁷, W.R. Cunningham [id](#)⁵⁹, F. Curcio [id](#)^{43b,43a},
 P. Czodrowski [id](#)³⁶, M.M. Czurylo [id](#)^{63b}, M.J. Da Cunha Sargedas De Sousa [id](#)^{57b,57a},
 J.V. Da Fonseca Pinto [id](#)^{83b}, C. Da Via [id](#)¹⁰¹, W. Dabrowski [id](#)^{86a}, T. Dado [id](#)⁴⁹, S. Dahbi [id](#)^{33g},
 T. Dai [id](#)¹⁰⁶, D. Dal Santo [id](#)¹⁹, C. Dallapiccola [id](#)¹⁰³, M. Dam [id](#)⁴², G. D'amen [id](#)²⁹, V. D'Amico [id](#)¹⁰⁹,
 J. Damp [id](#)¹⁰⁰, J.R. Dandoy [id](#)³⁴, M.F. Daneri [id](#)³⁰, M. Danninger [id](#)¹⁴², V. Dao [id](#)³⁶, G. Darbo [id](#)^{57b},
 S. Darmora [id](#)⁶, S.J. Das [id](#)^{29,ai}, S. D'Auria [id](#)^{71a,71b}, C. David [id](#)^{156b}, T. Davidek [id](#)¹³³,
 B. Davis-Purcell [id](#)³⁴, I. Dawson [id](#)⁹⁴, H.A. Day-hall [id](#)¹³², K. De [id](#)⁸, R. De Asmundis [id](#)^{72a},
 N. De Biase [id](#)⁴⁸, S. De Castro [id](#)^{23b,23a}, N. De Groot [id](#)¹¹³, P. de Jong [id](#)¹¹⁴, H. De la Torre [id](#)¹¹⁵,
 A. De Maria [id](#)^{14c}, A. De Salvo [id](#)^{75a}, U. De Sanctis [id](#)^{76a,76b}, F. De Santis [id](#)^{70a,70b}, A. De Santo [id](#)¹⁴⁶,
 J.B. De Vivie De Regie [id](#)⁶⁰, D.V. Dedovich³⁸, J. Degens [id](#)¹¹⁴, A.M. Deiana [id](#)⁴⁴, F. Del Corso [id](#)^{23b,23a},
 J. Del Peso [id](#)⁹⁹, F. Del Rio [id](#)^{63a}, L. Delagrangé [id](#)¹²⁷, F. Deliot [id](#)¹³⁵, C.M. Delitzsch [id](#)⁴⁹,
 M. Della Pietra [id](#)^{72a,72b}, D. Della Volpe [id](#)⁵⁶, A. Dell'Acqua [id](#)³⁶, L. Dell'Asta [id](#)^{71a,71b}, M. Delmastro [id](#)⁴,
 P.A. Delsart [id](#)⁶⁰, S. Demers [id](#)¹⁷², M. Demichev [id](#)³⁸, S.P. Denisov [id](#)³⁷, L. D'Eramo [id](#)⁴⁰,
 D. Derendarz [id](#)⁸⁷, F. Derue [id](#)¹²⁷, P. Dervan [id](#)⁹², K. Desch [id](#)²⁴, C. Deutsch [id](#)²⁴, F.A. Di Bello [id](#)^{57b,57a},
 A. Di Ciaccio [id](#)^{76a,76b}, L. Di Ciaccio [id](#)⁴, A. Di Domenico [id](#)^{75a,75b}, C. Di Donato [id](#)^{72a,72b},
 A. Di Girolamo [id](#)³⁶, G. Di Gregorio [id](#)³⁶, A. Di Luca [id](#)^{78a,78b}, B. Di Micco [id](#)^{77a,77b}, R. Di Nardo [id](#)^{77a,77b},
 C. Diaconu [id](#)¹⁰², M. Diamantopoulou [id](#)³⁴, F.A. Dias [id](#)¹¹⁴, T. Dias Do Vale [id](#)¹⁴², M.A. Diaz [id](#)^{137a,137b},
 F.G. Diaz Capriles [id](#)²⁴, M. Didenko [id](#)¹⁶³, E.B. Diehl [id](#)¹⁰⁶, L. Diehl [id](#)⁵⁴, S. Díez Cornell [id](#)⁴⁸,
 C. Díez Pardos [id](#)¹⁴¹, C. Dimitriadi [id](#)^{161,24}, A. Dimitrievska [id](#)^{17a}, J. Dingfelder [id](#)²⁴, I-M. Dinu [id](#)^{27b},
 S.J. Dittmeier [id](#)^{63b}, F. Dittus [id](#)³⁶, F. Djama [id](#)¹⁰², T. Djobava [id](#)^{149b}, J.I. Djuvsland [id](#)¹⁶,
 C. Doglioni [id](#)^{101,98}, A. Dohnalova [id](#)^{28a}, J. Dolejsi [id](#)¹³³, Z. Dolezal [id](#)¹³³, K.M. Dona [id](#)³⁹,
 M. Donadelli [id](#)^{83c}, B. Dong [id](#)¹⁰⁷, J. Donini [id](#)⁴⁰, A. D'Onofrio [id](#)^{72a,72b}, M. D'Onofrio [id](#)⁹²,
 J. Dopke [id](#)¹³⁴, A. Doria [id](#)^{72a}, N. Dos Santos Fernandes [id](#)^{130a}, P. Dougan [id](#)¹⁰¹, M.T. Dova [id](#)⁹⁰,
 A.T. Doyle [id](#)⁵⁹, M.A. Draguet [id](#)¹²⁶, E. Dreyer [id](#)¹⁶⁹, I. Drivas-koulouris [id](#)¹⁰, M. Drnevich [id](#)¹¹⁷,
 A.S. Drobac [id](#)¹⁵⁸, M. Drozdova [id](#)⁵⁶, D. Du [id](#)^{62a}, T.A. du Pree [id](#)¹¹⁴, F. Dubinin [id](#)³⁷, M. Dubovsky [id](#)^{28a},
 E. Duchovni [id](#)¹⁶⁹, G. Duckeck [id](#)¹⁰⁹, O.A. Ducu [id](#)^{27b}, D. Duda [id](#)⁵², A. Dudarev [id](#)³⁶, E.R. Duden [id](#)²⁶,
 M. D'uffizi [id](#)¹⁰¹, L. Duflo [id](#)⁶⁶, M. Dührssen [id](#)³⁶, C. Dülsen [id](#)¹⁷¹, A.E. Dumitriu [id](#)^{27b}, M. Dunford [id](#)^{63a},
 S. Dungs [id](#)⁴⁹, K. Dunne [id](#)^{47a,47b}, A. Duperrin [id](#)¹⁰², H. Duran Yildiz [id](#)^{3a}, M. Düren [id](#)⁵⁸,
 A. Durglishvili [id](#)^{149b}, B.L. Dwyer [id](#)¹¹⁵, G.I. Dyckes [id](#)^{17a}, M. Dyndal [id](#)^{86a}, B.S. Dziedzic [id](#)⁸⁷,
 Z.O. Earnshaw [id](#)¹⁴⁶, G.H. Eberwein [id](#)¹²⁶, B. Eckerova [id](#)^{28a}, S. Eggebrecht [id](#)⁵⁵,
 E. Egidio Purcino De Souza [id](#)¹²⁷, L.F. Ehrke [id](#)⁵⁶, G. Eigen [id](#)¹⁶, K. Einsweiler [id](#)^{17a}, T. Ekelof [id](#)¹⁶¹,
 P.A. Ekman [id](#)⁹⁸, S. El Farkh [id](#)^{35b}, Y. El Ghazali [id](#)^{35b}, H. El Jarrari [id](#)³⁶, A. El Moussaouy [id](#)¹⁰⁸,
 V. Ellajosyula [id](#)¹⁶¹, M. Ellert [id](#)¹⁶¹, F. Ellinghaus [id](#)¹⁷¹, N. Ellis [id](#)³⁶, J. Elmsheuser [id](#)²⁹, M. Elsing [id](#)³⁶,
 D. Emelianov [id](#)¹³⁴, Y. Enari [id](#)¹⁵³, I. Ene [id](#)^{17a}, S. Epari [id](#)¹³, J. Erdmann [id](#)⁴⁹, P.A. Erland [id](#)⁸⁷,
 M. Errenst [id](#)¹⁷¹, M. Escalier [id](#)⁶⁶, C. Escobar [id](#)¹⁶³, E. Etzion [id](#)¹⁵¹, G. Evans [id](#)^{130a}, H. Evans [id](#)⁶⁸,

L.S. Evans ^{id}95, M.O. Evans ^{id}146, A. Ezhilov ^{id}37, S. Ezzarqtouni ^{id}35a, F. Fabbri ^{id}59, L. Fabbri ^{id}23b,23a, G. Facini ^{id}96, V. Fadeyev ^{id}136, R.M. Fakhrutdinov ^{id}37, D. Fakoudis ^{id}100, S. Falciano ^{id}75a, L.F. Falda Ulhoa Coelho ^{id}36, P.J. Falke ^{id}24, J. Faltova ^{id}133, C. Fan ^{id}162, Y. Fan ^{id}14a, Y. Fang ^{id}14a,14e, M. Fanti ^{id}71a,71b, M. Faraj ^{id}69a,69b, Z. Farazpay ^{id}97, A. Farbin ^{id}8, A. Farilla ^{id}77a, T. Farooque ^{id}107, S.M. Farrington ^{id}52, F. Fassi ^{id}35e, D. Fassouliotis ^{id}9, M. Faucci Giannelli ^{id}76a,76b, W.J. Fawcett ^{id}32, L. Fayard ^{id}66, P. Federic ^{id}133, P. Federicova ^{id}131, O.L. Fedin ^{id}37,a, G. Fedotov ^{id}37, M. Feickert ^{id}170, L. Feligioni ^{id}102, D.E. Fellers ^{id}123, C. Feng ^{id}62b, M. Feng ^{id}14b, Z. Feng ^{id}114, M.J. Fenton ^{id}160, A.B. Fenyuk ^{id}37, L. Ferencz ^{id}48, R.A.M. Ferguson ^{id}91, S.I. Fernandez Luengo ^{id}137f, P. Fernandez Martinez ^{id}13, M.J.V. Fernoux ^{id}102, J. Ferrando ^{id}48, A. Ferrari ^{id}161, P. Ferrari ^{id}114,113, R. Ferrari ^{id}73a, D. Ferrere ^{id}56, C. Ferretti ^{id}106, F. Fiedler ^{id}100, P. Fiedler ^{id}132, A. Filipčič ^{id}93, E.K. Filmer ^{id}1, F. Filthaut ^{id}113, M.C.N. Fiolhais ^{id}130a,130c,c, L. Fiorini ^{id}163, W.C. Fisher ^{id}107, T. Fitschen ^{id}101, P.M. Fitzhugh ^{id}135, I. Fleck ^{id}141, P. Fleischmann ^{id}106, T. Flick ^{id}171, M. Flores ^{id}33d,ac, L.R. Flores Castillo ^{id}64a, L. Flores Sanz De Acedo ^{id}36, F.M. Follega ^{id}78a,78b, N. Fomin ^{id}16, J.H. Foo ^{id}155, B.C. Forland ^{id}68, A. Formica ^{id}135, A.C. Forti ^{id}101, E. Fortin ^{id}36, A.W. Fortman ^{id}61, M.G. Foti ^{id}17a, L. Fountas ^{id}9,j, D. Fournier ^{id}66, H. Fox ^{id}91, P. Francavilla ^{id}74a,74b, S. Francescato ^{id}61, S. Franchellucci ^{id}56, M. Franchini ^{id}23b,23a, S. Franchino ^{id}63a, D. Francis ^{id}36, L. Franco ^{id}113, V. Franco Lima ^{id}36, L. Franconi ^{id}48, M. Franklin ^{id}61, G. Frattari ^{id}26, A.C. Freegard ^{id}94, W.S. Freund ^{id}83b, Y.Y. Frid ^{id}151, J. Friend ^{id}59, N. Fritzsche ^{id}50, A. Froch ^{id}54, D. Froidevaux ^{id}36, J.A. Frost ^{id}126, Y. Fu ^{id}62a, S. Fuenzalida Garrido ^{id}137f, M. Fujimoto ^{id}102, K.Y. Fung ^{id}64a, E. Furtado De Simas Filho ^{id}83b, M. Furukawa ^{id}153, J. Fuster ^{id}163, A. Gabrielli ^{id}23b,23a, A. Gabrielli ^{id}155, P. Gadow ^{id}36, G. Gagliardi ^{id}57b,57a, L.G. Gagnon ^{id}17a, E.J. Gallas ^{id}126, B.J. Gallop ^{id}134, K.K. Gan ^{id}119, S. Ganguly ^{id}153, Y. Gao ^{id}52, F.M. Garay Walls ^{id}137a,137b, B. Garcia ^{id}29, C. García ^{id}163, A. Garcia Alonso ^{id}114, A.G. Garcia Caffaro ^{id}172, J.E. García Navarro ^{id}163, M. Garcia-Sciveres ^{id}17a, G.L. Gardner ^{id}128, R.W. Gardner ^{id}39, N. Garelli ^{id}158, D. Garg ^{id}80, R.B. Garg ^{id}143,n, J.M. Gargan ^{id}52, C.A. Garner ^{id}155, C.M. Garvey ^{id}33a, P. Gaspar ^{id}83b, V.K. Gassmann ^{id}158, G. Gaudio ^{id}73a, V. Gautam ^{id}13, P. Gauzzi ^{id}75a,75b, I.L. Gavrilenko ^{id}37, A. Gavriilyuk ^{id}37, C. Gay ^{id}164, G. Gaycken ^{id}48, E.N. Gazis ^{id}10, A.A. Geanta ^{id}27b, C.M. Gee ^{id}136, A. Gekow ^{id}119, C. Gemme ^{id}57b, M.H. Genest ^{id}60, S. Gentile ^{id}75a,75b, A.D. Gentry ^{id}112, S. George ^{id}95, W.F. George ^{id}20, T. Geralis ^{id}46, P. Gessinger-Befurt ^{id}36, M.E. Geyik ^{id}171, M. Ghani ^{id}167, M. Ghneimat ^{id}141, K. Ghorbanian ^{id}94, A. Ghosal ^{id}141, A. Ghosh ^{id}160, A. Ghosh ^{id}7, B. Giacobbe ^{id}23b, S. Giagu ^{id}75a,75b, T. Giani ^{id}114, P. Giannetti ^{id}74a, A. Giannini ^{id}62a, S.M. Gibson ^{id}95, M. Gignac ^{id}136, D.T. Gil ^{id}86b, A.K. Gilbert ^{id}86a, B.J. Gilbert ^{id}41, D. Gillberg ^{id}34, G. Gilles ^{id}114, N.E.K. Gillwald ^{id}48, L. Ginabat ^{id}127, D.M. Gingrich ^{id}2,af, M.P. Giordani ^{id}69a,69c, P.F. Giraud ^{id}135, G. Giugliarelli ^{id}69a,69c, D. Giugni ^{id}71a, F. Giuli ^{id}36, I. Gkialas ^{id}9,j, L.K. Gladilin ^{id}37, C. Glasman ^{id}99, G.R. Gledhill ^{id}123, G. Glemža ^{id}48, M. Glisic ^{id}123, I. Gnesi ^{id}43b,f, Y. Go ^{id}29,ai, M. Goblirsch-Kolb ^{id}36, B. Gocke ^{id}49, D. Godin ^{id}108, B. Gokturk ^{id}21a, S. Goldfarb ^{id}105, T. Golling ^{id}56, M.G.D. Gololo ^{id}33g, D. Golubkov ^{id}37, J.P. Gombas ^{id}107, A. Gomes ^{id}130a,130b, G. Gomes Da Silva ^{id}141, A.J. Gomez Delegido ^{id}163, R. Gonçalves ^{id}130a,130c, G. Gonella ^{id}123, L. Gonella ^{id}20, A. Gongadze ^{id}149c, F. Gonnella ^{id}20, J.L. Gonski ^{id}41, R.Y. González Andana ^{id}52, S. González de la Hoz ^{id}163, S. Gonzalez Fernandez ^{id}13, R. Gonzalez Lopez ^{id}92, C. Gonzalez Renteria ^{id}17a, M.V. Gonzalez Rodrigues ^{id}48, R. Gonzalez Suarez ^{id}161, S. Gonzalez-Sevilla ^{id}56, G.R. Gonzalvo Rodriguez ^{id}163, L. Goossens ^{id}36, B. Gorini ^{id}36, E. Gorini ^{id}70a,70b, A. Gorišek ^{id}93, T.C. Gosart ^{id}128, A.T. Goshaw ^{id}51, M.I. Gostkin ^{id}38, S. Goswami ^{id}121, C.A. Gottardo ^{id}36, S.A. Gotz ^{id}109, M. Goughri ^{id}35b, V. Goumarre ^{id}48, A.G. Goussiou ^{id}138, N. Govender ^{id}33c, I. Grabowska-Bold ^{id}86a, K. Graham ^{id}34, E. Gramstad ^{id}125, S. Grancagnolo ^{id}70a,70b, M. Grandi ^{id}146, C.M. Grant ^{id}1,135, P.M. Gravila ^{id}27f, F.G. Gravili ^{id}70a,70b, H.M. Gray ^{id}17a, M. Greco ^{id}70a,70b, C. Grefe ^{id}24, I.M. Gregor ^{id}48, P. Grenier ^{id}143, S.G. Grewe ^{id}110, C. Grieco ^{id}13, A.A. Grillo ^{id}136, K. Grimm ^{id}31, S. Grinstein ^{id}13,s, J.-F. Grivaz ^{id}66, E. Gross ^{id}169,

J. Grosse-Knetter ⁵⁵, C. Grud ¹⁰⁶, J.C. Grundy ¹²⁶, L. Guan ¹⁰⁶, W. Guan ²⁹, C. Gubbels ¹⁶⁴,
 J.G.R. Guerrero Rojas ¹⁶³, G. Guerrieri ^{69a,69c}, F. Guescini ¹¹⁰, R. Gugel ¹⁰⁰, J.A.M. Guhit ¹⁰⁶,
 A. Guida ¹⁸, E. Guilloton ^{167,134}, S. Guindon ³⁶, F. Guo ^{14a,14e}, J. Guo ^{62c}, L. Guo ⁴⁸,
 Y. Guo ¹⁰⁶, R. Gupta ⁴⁸, R. Gupta ¹²⁹, S. Gurbuz ²⁴, S.S. Gurdasani ⁵⁴, G. Gustavino ³⁶,
 M. Guth ⁵⁶, P. Gutierrez ¹²⁰, L.F. Gutierrez Zagazeta ¹²⁸, M. Gutsche ⁵⁰, C. Gutschow ⁹⁶,
 C. Gwenlan ¹²⁶, C.B. Gwilliam ⁹², E.S. Haaland ¹²⁵, A. Haas ¹¹⁷, M. Habedank ⁴⁸,
 C. Haber ^{17a}, H.K. Hadavand ⁸, A. Hadeef ⁵⁰, S. Hadzic ¹¹⁰, A.I. Hagan ⁹¹, J.J. Hahn ¹⁴¹,
 E.H. Haines ⁹⁶, M. Haleem ¹⁶⁶, J. Haley ¹²¹, J.J. Hall ¹³⁹, G.D. Hallewell ¹⁰², L. Halser ¹⁹,
 K. Hamano ¹⁶⁵, M. Hamer ²⁴, G.N. Hamity ⁵², E.J. Hampshire ⁹⁵, J. Han ^{62b}, K. Han ^{62a},
 L. Han ^{14c}, L. Han ^{62a}, S. Han ^{17a}, Y.F. Han ¹⁵⁵, K. Hanagaki ⁸⁴, M. Hance ¹³⁶,
 D.A. Hangal ^{41,ab}, H. Hanif ¹⁴², M.D. Hank ¹²⁸, R. Hankache ¹⁰¹, J.B. Hansen ⁴²,
 J.D. Hansen ⁴², P.H. Hansen ⁴², K. Hara ¹⁵⁷, D. Harada ⁵⁶, T. Harenberg ¹⁷¹, S. Harkusha ³⁷,
 M.L. Harris ¹⁰³, Y.T. Harris ¹²⁶, J. Harrison ¹³, N.M. Harrison ¹¹⁹, P.F. Harrison ¹⁶⁷,
 N.M. Hartman ¹¹⁰, N.M. Hartmann ¹⁰⁹, Y. Hasegawa ¹⁴⁰, R. Hauser ¹⁰⁷, C.M. Hawkes ²⁰,
 R.J. Hawkings ³⁶, Y. Hayashi ¹⁵³, S. Hayashida ¹¹¹, D. Hayden ¹⁰⁷, C. Hayes ¹⁰⁶,
 R.L. Hayes ¹¹⁴, C.P. Hays ¹²⁶, J.M. Hays ⁹⁴, H.S. Hayward ⁹², F. He ^{62a}, M. He ^{14a,14e},
 Y. He ¹⁵⁴, Y. He ⁴⁸, N.B. Heatley ⁹⁴, V. Hedberg ⁹⁸, A.L. Heggelund ¹²⁵, N.D. Hehir ^{94,*},
 C. Heidegger ⁵⁴, K.K. Heidegger ⁵⁴, W.D. Heidorn ⁸¹, J. Heilman ³⁴, S. Heim ⁴⁸, T. Heim ^{17a},
 J.G. Heinlein ¹²⁸, J.J. Heinrich ¹²³, L. Heinrich ^{110,ad}, J. Hejbal ¹³¹, L. Helary ⁴⁸, A. Held ¹⁷⁰,
 S. Hellesund ¹⁶, C.M. Helling ¹⁶⁴, S. Hellman ^{47a,47b}, R.C.W. Henderson ⁹¹, L. Henkelmann ³²,
 A.M. Henriques Correia ³⁶, H. Herde ⁹⁸, Y. Hernández Jiménez ¹⁴⁵, L.M. Herrmann ²⁴,
 T. Herrmann ⁵⁰, G. Herten ⁵⁴, R. Hertenberger ¹⁰⁹, L. Hervas ³⁶, M.E. Hespig ¹⁰⁰,
 N.P. Hessey ^{156a}, H. Hibi ⁸⁵, E. Hill ¹⁵⁵, S.J. Hillier ²⁰, J.R. Hinds ¹⁰⁷, F. Hinterkeuser ²⁴,
 M. Hirose ¹²⁴, S. Hirose ¹⁵⁷, D. Hirschbuehl ¹⁷¹, T.G. Hitchings ¹⁰¹, B. Hiti ⁹³, J. Hobbs ¹⁴⁵,
 R. Hobincu ^{27e}, N. Hod ¹⁶⁹, M.C. Hodgkinson ¹³⁹, B.H. Hodgkinson ³², A. Hoecker ³⁶,
 D.D. Hofer ¹⁰⁶, J. Hofer ⁴⁸, T. Holm ²⁴, M. Holzbock ¹¹⁰, L.B.A.H. Hommels ³²,
 B.P. Honan ¹⁰¹, J. Hong ^{62c}, T.M. Hong ¹²⁹, B.H. Hooberman ¹⁶², W.H. Hopkins ⁶, Y. Horii ¹¹¹,
 S. Hou ¹⁴⁸, A.S. Howard ⁹³, J. Howarth ⁵⁹, J. Hoya ⁶, M. Hrabovsky ¹²², A. Hrynevich ⁴⁸,
 T. Hryn'ova ⁴, P.J. Hsu ⁶⁵, S.-C. Hsu ¹³⁸, Q. Hu ^{62a}, Y.F. Hu ^{14a,14e}, S. Huang ^{64b},
 X. Huang ^{14c}, X. Huang ^{14a,14e}, Y. Huang ¹³⁹, Y. Huang ^{14a}, Z. Huang ¹⁰¹, Z. Hubacek ¹³²,
 M. Huebner ²⁴, F. Huegging ²⁴, T.B. Huffman ¹²⁶, C.A. Hugli ⁴⁸, M. Huhtinen ³⁶,
 S.K. Huiberts ¹⁶, R. Hulsken ¹⁰⁴, N. Huseynov ¹², J. Huston ¹⁰⁷, J. Huth ⁶¹, R. Hyneman ¹⁴³,
 G. Iacobucci ⁵⁶, G. Iakovidis ²⁹, I. Ibragimov ¹⁴¹, L. Iconomidou-Fayard ⁶⁶, P. Iengo ^{72a,72b},
 R. Iguchi ¹⁵³, T. Iizawa ¹²⁶, Y. Ikegami ⁸⁴, N. Ilic ¹⁵⁵, H. Imam ^{35a}, M. Ince Lezki ⁵⁶,
 T. Ingebretsen Carlson ^{47a,47b}, G. Introzzi ^{73a,73b}, M. Iodice ^{77a}, V. Ippolito ^{75a,75b}, R.K. Irwin ⁹²,
 M. Ishino ¹⁵³, W. Islam ¹⁷⁰, C. Issever ^{18,48}, S. Istin ^{21a,ak}, H. Ito ¹⁶⁸, J.M. Iturbe Ponce ^{64a},
 R. Iuppa ^{78a,78b}, A. Ivina ¹⁶⁹, J.M. Izen ⁴⁵, V. Izzo ^{72a}, P. Jacka ^{131,132}, P. Jackson ¹,
 R.M. Jacobs ⁴⁸, B.P. Jaeger ¹⁴², C.S. Jagfeld ¹⁰⁹, G. Jain ^{156a}, P. Jain ⁵⁴, K. Jakobs ⁵⁴,
 T. Jakoubek ¹⁶⁹, J. Jamieson ⁵⁹, K.W. Janas ^{86a}, M. Javurkova ¹⁰³, F. Jeanneau ¹³⁵,
 L. Jeanty ¹²³, J. Jejelava ^{149a,z}, P. Jenni ^{54,g}, C.E. Jessiman ³⁴, S. Jézéquel ⁴, C. Jia ^{62b}, J. Jia ¹⁴⁵,
 X. Jia ⁶¹, X. Jia ^{14a,14e}, Z. Jia ^{14c}, S. Jiggins ⁴⁸, J. Jimenez Pena ¹³, S. Jin ^{14c}, A. Jinaru ^{27b},
 O. Jinnouchi ¹⁵⁴, P. Johansson ¹³⁹, K.A. Johns ⁷, J.W. Johnson ¹³⁶, D.M. Jones ³², E. Jones ⁴⁸,
 P. Jones ³², R.W.L. Jones ⁹¹, T.J. Jones ⁹², H.L. Joos ^{55,36}, R. Joshi ¹¹⁹, J. Jovicevic ¹⁵,
 X. Ju ^{17a}, J.J. Junggeburth ¹⁰³, T. Junkermann ^{63a}, A. Juste Rozas ^{13,s}, M.K. Juzek ⁸⁷,
 S. Kabana ^{137e}, A. Kaczmarska ⁸⁷, M. Kado ¹¹⁰, H. Kagan ¹¹⁹, M. Kagan ¹⁴³, A. Kahn ⁴¹,
 A. Kahn ¹²⁸, C. Kahra ¹⁰⁰, T. Kaji ¹⁵³, E. Kajomovitz ¹⁵⁰, N. Kakati ¹⁶⁹, I. Kalaitzidou ⁵⁴,
 C.W. Kalderon ²⁹, A. Kamenshchikov ¹⁵⁵, N.J. Kang ¹³⁶, D. Kar ^{33g}, K. Karava ¹²⁶,

M.J. Kareem ^{156b}, E. Karentzos ⁵⁴, I. Karkanias ¹⁵², O. Karkout ¹¹⁴, S.N. Karpov ³⁸,
Z.M. Karpova ³⁸, V. Kartvelishvili ⁹¹, A.N. Karyukhin ³⁷, E. Kasimi ¹⁵², J. Katzy ⁴⁸,
S. Kaur ³⁴, K. Kawade ¹⁴⁰, M.P. Kawale ¹²⁰, C. Kawamoto ⁸⁸, T. Kawamoto ^{62a}, E.F. Kay ³⁶,
F.I. Kaya ¹⁵⁸, S. Kazakos ¹⁰⁷, V.F. Kazanin ³⁷, Y. Ke ¹⁴⁵, J.M. Keaveney ^{33a}, R. Keeler ¹⁶⁵,
G.V. Kehris ⁶¹, J.S. Keller ³⁴, A.S. Kelly ⁹⁶, J.J. Kempster ¹⁴⁶, K.E. Kennedy ⁴¹,
P.D. Kennedy ¹⁰⁰, O. Kepka ¹³¹, B.P. Kerridge ¹⁶⁷, S. Kersten ¹⁷¹, B.P. Kerševan ⁹³,
S. Keshri ⁶⁶, L. Keszeghova ^{28a}, S. Ketabchi Haghighat ¹⁵⁵, R.A. Khan ¹²⁹, M. Khandoga ¹²⁷,
A. Khanov ¹²¹, A.G. Kharlamov ³⁷, T. Kharlamova ³⁷, E.E. Khoda ¹³⁸, M. Kholodenko ³⁷,
T.J. Khoo ¹⁸, G. Khoraiuli ¹⁶⁶, J. Khubua ^{149b}, Y.A.R. Khwaira ⁶⁶, A. Kilgallon ¹²³,
D.W. Kim ^{47a,47b}, Y.K. Kim ³⁹, N. Kimura ⁹⁶, M.K. Kingston ⁵⁵, A. Kirchhoff ⁵⁵, C. Kirfel ²⁴,
F. Kirfel ²⁴, J. Kirk ¹³⁴, A.E. Kiryunin ¹¹⁰, C. Kitsaki ¹⁰, O. Kivernyk ²⁴, M. Klassen ^{63a},
C. Klein ³⁴, L. Klein ¹⁶⁶, M.H. Klein ¹⁰⁶, M. Klein ⁹², S.B. Klein ⁵⁶, U. Klein ⁹²,
P. Klimek ³⁶, A. Klimentov ²⁹, T. Klioutchnikova ³⁶, P. Kluit ¹¹⁴, S. Kluth ¹¹⁰, E. Kneringer ⁷⁹,
T.M. Knight ¹⁵⁵, A. Knue ⁴⁹, R. Kobayashi ⁸⁸, D. Kobylanski ¹⁶⁹, S.F. Koch ¹²⁶,
M. Kocian ¹⁴³, P. Kodyš ¹³³, D.M. Koeck ¹²³, P.T. Koenig ²⁴, T. Koffas ³⁴, O. Kolay ⁵⁰,
I. Koletsou ⁴, T. Komarek ¹²², K. Köneke ⁵⁴, A.X.Y. Kong ¹, T. Kono ¹¹⁸, N. Konstantinidis ⁹⁶,
P. Kontaxakis ⁵⁶, B. Konya ⁹⁸, R. Kopeliansky ⁶⁸, S. Koperny ^{86a}, K. Korcyl ⁸⁷, K. Kordas ^{152,e},
G. Koren ¹⁵¹, A. Korn ⁹⁶, S. Korn ⁵⁵, I. Korolkov ¹³, N. Korotkova ³⁷, B. Kortman ¹¹⁴,
O. Kortner ¹¹⁰, S. Kortner ¹¹⁰, W.H. Kostecka ¹¹⁵, V.V. Kostyukhin ¹⁴¹, A. Kotskechagia ¹³⁵,
A. Kotwal ⁵¹, A. Koulouris ³⁶, A. Kourkoumeli-Charalampidi ^{73a,73b}, C. Kourkoumelis ⁹,
E. Kourlitis ^{110,ad}, O. Kovanda ¹⁴⁶, R. Kowalewski ¹⁶⁵, W. Kozanecki ¹³⁵, A.S. Kozhin ³⁷,
V.A. Kramarenko ³⁷, G. Kramberger ⁹³, P. Kramer ¹⁰⁰, M.W. Krasny ¹²⁷, A. Krasznahorkay ³⁶,
J.W. Kraus ¹⁷¹, J.A. Kremer ⁴⁸, T. Kresse ⁵⁰, J. Kretschmar ⁹², K. Kreul ¹⁸, P. Krieger ¹⁵⁵,
S. Krishnamurthy ¹⁰³, M. Krivos ¹³³, K. Krizka ²⁰, K. Kroeninger ⁴⁹, H. Kroha ¹¹⁰, J. Kroll ¹³¹,
J. Kroll ¹²⁸, K.S. Krowpman ¹⁰⁷, U. Kruchonak ³⁸, H. Krüger ²⁴, N. Krumnack ⁸¹, M.C. Kruse ⁵¹,
O. Kuchinskaia ³⁷, S. Kuday ^{3a}, S. Kuehn ³⁶, R. Kuesters ⁵⁴, T. Kuhl ⁴⁸, V. Kukhtin ³⁸,
Y. Kulchitsky ^{37,a}, S. Kuleshov ^{137d,137b}, M. Kumar ^{33g}, N. Kumari ⁴⁸, P. Kumari ^{156b},
A. Kupco ¹³¹, T. Kupfer ⁴⁹, A. Kupich ³⁷, O. Kuprash ⁵⁴, H. Kurashige ⁸⁵, L.L. Kurchaninov ^{156a},
O. Kurdysh ⁶⁶, Y.A. Kurochkin ³⁷, A. Kurova ³⁷, M. Kuze ¹⁵⁴, A.K. Kvam ¹⁰³, J. Kvita ¹²²,
T. Kwan ¹⁰⁴, N.G. Kyriacou ¹⁰⁶, L.A.O. Laatu ¹⁰², C. Lacasta ¹⁶³, F. Lacava ^{75a,75b},
H. Lacker ¹⁸, D. Lacour ¹²⁷, N.N. Lad ⁹⁶, E. Ladygin ³⁸, B. Laforge ¹²⁷, T. Lagouri ^{137e},
F.Z. Lahbabi ^{35a}, S. Lai ⁵⁵, I.K. Lakomic ^{86a}, N. Lalloue ⁶⁰, J.E. Lambert ¹⁶⁵, S. Lammers ⁶⁸,
W. Lampl ⁷, C. Lampoudis ^{152,e}, A.N. Lancaster ¹¹⁵, E. Lançon ²⁹, U. Landgraf ⁵⁴,
M.P.J. Landon ⁹⁴, V.S. Lang ⁵⁴, R.J. Langenberg ¹⁰³, O.K.B. Langrekken ¹²⁵, A.J. Lankford ¹⁶⁰,
F. Lanni ³⁶, K. Lantzs ²⁴, A. Lanza ^{73a}, A. Lapertosa ^{57b,57a}, J.F. Laporte ¹³⁵, T. Lari ^{71a},
F. Lasagni Manghi ^{23b}, M. Lassnig ³⁶, V. Latonova ¹³¹, A. Laudrain ¹⁰⁰, A. Laurier ¹⁵⁰,
S.D. Lawlor ¹³⁹, Z. Lawrence ¹⁰¹, R. Lazaridou ¹⁶⁷, M. Lazzaroni ^{71a,71b}, B. Le ¹⁰¹,
E.M. Le Boulicaut ⁵¹, B. Leban ⁹³, A. Lebedev ⁸¹, M. LeBlanc ¹⁰¹, F. Ledroit-Guillon ⁶⁰,
A.C.A. Lee ⁹⁶, S.C. Lee ¹⁴⁸, S. Lee ^{47a,47b}, T.F. Lee ⁹², L.L. Leeuw ^{33c}, H.P. Lefebvre ⁹⁵,
M. Lefebvre ¹⁶⁵, C. Leggett ^{17a}, G. Lehmann Miotto ³⁶, M. Leigh ⁵⁶, W.A. Leight ¹⁰³,
W. Leinonen ¹¹³, A. Leisos ^{152,r}, M.A.L. Leite ^{83c}, C.E. Leitgeb ⁴⁸, R. Leitner ¹³³,
K.J.C. Leney ⁴⁴, T. Lenz ²⁴, S. Leone ^{74a}, C. Leonidopoulos ⁵², A. Leopold ¹⁴⁴, C. Leroy ¹⁰⁸,
R. Les ¹⁰⁷, C.G. Lester ³², M. Levchenko ³⁷, J. Levêque ⁴, D. Levin ¹⁰⁶, L.J. Levinson ¹⁶⁹,
M.P. Lewicki ⁸⁷, D.J. Lewis ⁴, A. Li ⁵, B. Li ^{62b}, C. Li ^{62a}, C-Q. Li ¹¹⁰, H. Li ^{62a}, H. Li ^{62b},
H. Li ^{14c}, H. Li ^{14b}, H. Li ^{62b}, J. Li ^{62c}, K. Li ¹³⁸, L. Li ^{62c}, M. Li ^{14a,14e}, Q.Y. Li ^{62a},
S. Li ^{14a,14e}, S. Li ^{62d,62c,d}, T. Li ⁵, X. Li ¹⁰⁴, Z. Li ¹²⁶, Z. Li ¹⁰⁴, Z. Li ^{14a,14e}, S. Liang ^{14a,14e},
Z. Liang ^{14a}, M. Liberatore ¹³⁵, B. Liberti ^{76a}, K. Lie ^{64c}, J. Lieber Marin ^{83b}, H. Lien ⁶⁸,

K. Lin ¹⁰⁷, R.E. Lindley ⁷, J.H. Lindon ², E. Lipeles ¹²⁸, A. Lipniacka ¹⁶, A. Lister ¹⁶⁴,
 J.D. Little ⁴, B. Liu ^{14a}, B.X. Liu ¹⁴², D. Liu ^{62d,62c}, J.B. Liu ^{62a}, J.K.K. Liu ³², K. Liu ^{62d,62c},
 M. Liu ^{62a}, M.Y. Liu ^{62a}, P. Liu ^{14a}, Q. Liu ^{62d,138,62c}, X. Liu ^{62a}, X. Liu ^{62b}, Y. Liu ^{14d,14e},
 Y.L. Liu ^{62b}, Y.W. Liu ^{62a}, J. Llorente Merino ¹⁴², S.L. Lloyd ⁹⁴, E.M. Lobodzinska ⁴⁸,
 P. Loch ⁷, T. Lohse ¹⁸, K. Lohwasser ¹³⁹, E. Loiacono ⁴⁸, M. Lokajicek ^{131,*}, J.D. Lomas ²⁰,
 J.D. Long ¹⁶², I. Longarini ¹⁶⁰, L. Longo ^{70a,70b}, R. Longo ¹⁶², I. Lopez Paz ⁶⁷,
 A. Lopez Solis ⁴⁸, N. Lorenzo Martinez ⁴, A.M. Lory ¹⁰⁹, G. Löschcke Centeno ¹⁴⁶, O. Loseva ³⁷,
 X. Lou ^{47a,47b}, X. Lou ^{14a,14e}, A. Lounis ⁶⁶, J. Love ⁶, P.A. Love ⁹¹, G. Lu ^{14a,14e}, M. Lu ⁸⁰,
 S. Lu ¹²⁸, Y.J. Lu ⁶⁵, H.J. Lubatti ¹³⁸, C. Luci ^{75a,75b}, F.L. Lucio Alves ^{14c}, A. Lucotte ⁶⁰,
 F. Luehring ⁶⁸, I. Luise ¹⁴⁵, O. Lukianchuk ⁶⁶, O. Lundberg ¹⁴⁴, B. Lund-Jensen ¹⁴⁴,
 N.A. Luongo ⁶, M.S. Lutz ¹⁵¹, A.B. Lux ²⁵, D. Lynn ²⁹, H. Lyons ⁹², R. Lysak ¹³¹, E. Lytken ⁹⁸,
 V. Lyubushkin ³⁸, T. Lyubushkina ³⁸, M.M. Lyukova ¹⁴⁵, H. Ma ²⁹, K. Ma ^{62a}, L.L. Ma ^{62b},
 W. Ma ^{62a}, Y. Ma ¹²¹, D.M. Mac Donell ¹⁶⁵, G. Maccarrone ⁵³, J.C. MacDonald ¹⁰⁰,
 P.C. Machado De Abreu Farias ^{83b}, R. Madar ⁴⁰, W.F. Mader ⁵⁰, T. Madula ⁹⁶, J. Maeda ⁸⁵,
 T. Maeno ²⁹, H. Maguire ¹³⁹, V. Maiboroda ¹³⁵, A. Maio ^{130a,130b,130d}, K. Maj ^{86a},
 O. Majersky ⁴⁸, S. Majewski ¹²³, N. Makovec ⁶⁶, V. Maksimovic ¹⁵, B. Malaescu ¹²⁷,
 Pa. Malecki ⁸⁷, V.P. Maleev ³⁷, F. Malek ⁶⁰, M. Mali ⁹³, D. Malito ⁹⁵, U. Mallik ⁸⁰,
 S. Maltezos ¹⁰, S. Malyukov ³⁸, J. Mamuzic ¹³, G. Mancini ⁵³, G. Manco ^{73a,73b}, J.P. Mandalia ⁹⁴,
 I. Mandić ⁹³, L. Manhaes de Andrade Filho ^{83a}, I.M. Maniatis ¹⁶⁹, J. Manjarres Ramos ^{102,aa},
 D.C. Mankad ¹⁶⁹, A. Mann ¹⁰⁹, B. Mansoulié ¹³⁵, S. Manzoni ³⁶, L. Mao ^{62c}, X. Mapekula ^{33c},
 A. Marantis ^{152,r}, G. Marchiori ⁵, M. Marcisovsky ¹³¹, C. Marcon ^{71a}, M. Marinescu ²⁰,
 S. Marium ⁴⁸, M. Marjanovic ¹²⁰, E.J. Marshall ⁹¹, Z. Marshall ^{17a}, S. Marti-Garcia ¹⁶³,
 T.A. Martin ¹⁶⁷, V.J. Martin ⁵², B. Martin dit Latour ¹⁶, L. Martinelli ^{75a,75b}, M. Martinez ^{13,s},
 P. Martinez Agullo ¹⁶³, V.I. Martinez Outschoorn ¹⁰³, P. Martinez Suarez ¹³, S. Martin-Haugh ¹³⁴,
 V.S. Martoiu ^{27b}, A.C. Martyniuk ⁹⁶, A. Marzin ³⁶, D. Mascione ^{78a,78b}, L. Masetti ¹⁰⁰,
 T. Mashimo ¹⁵³, J. Masik ¹⁰¹, A.L. Maslennikov ³⁷, L. Massa ^{23b}, P. Massarotti ^{72a,72b},
 P. Mastrandrea ^{74a,74b}, A. Mastroberardino ^{43b,43a}, T. Masubuchi ¹⁵³, T. Mathisen ¹⁶¹,
 J. Matousek ¹³³, N. Matsuzawa ¹⁵³, J. Maurer ^{27b}, B. Maček ⁹³, D.A. Maximov ³⁷, R. Mazini ¹⁴⁸,
 I. Maznas ¹⁵², M. Mazza ¹⁰⁷, S.M. Mazza ¹³⁶, E. Mazzeo ^{71a,71b}, C. Mc Ginn ²⁹,
 J.P. Mc Gowan ¹⁰⁴, S.P. Mc Kee ¹⁰⁶, C.C. McCracken ¹⁶⁴, E.F. McDonald ¹⁰⁵,
 A.E. McDougall ¹¹⁴, J.A. Mcfayden ¹⁴⁶, R.P. McGovern ¹²⁸, G. Mchedlidze ^{149b},
 R.P. Mckenzie ^{33g}, T.C. Mclachlan ⁴⁸, D.J. McLaughlin ⁹⁶, S.J. McMahon ¹³⁴,
 C.M. Mcpartland ⁹², R.A. McPherson ^{165,w}, S. Mehlhase ¹⁰⁹, A. Mehta ⁹², D. Melini ¹⁵⁰,
 B.R. Mellado Garcia ^{33g}, A.H. Melo ⁵⁵, F. Meloni ⁴⁸, A.M. Mendes Jacques Da Costa ¹⁰¹,
 H.Y. Meng ¹⁵⁵, L. Meng ⁹¹, S. Menke ¹¹⁰, M. Mentink ³⁶, E. Meoni ^{43b,43a}, G. Mercado ¹¹⁵,
 C. Merlassino ^{69a,69c}, L. Merola ^{72a,72b}, C. Meroni ^{71a,71b}, G. Merz ¹⁰⁶, J. Metcalfe ⁶, A.S. Mete ⁶,
 C. Meyer ⁶⁸, J-P. Meyer ¹³⁵, R.P. Middleton ¹³⁴, L. Mijović ⁵², G. Mikenberg ¹⁶⁹,
 M. Mikestikova ¹³¹, M. Mikuž ⁹³, H. Mildner ¹⁰⁰, A. Milic ³⁶, C.D. Milke ⁴⁴, D.W. Miller ³⁹,
 L.S. Miller ³⁴, A. Milov ¹⁶⁹, D.A. Milstead ^{47a,47b}, T. Min ^{14c}, A.A. Minaenko ³⁷,
 I.A. Minashvili ^{149b}, L. Mince ⁵⁹, A.I. Mincer ¹¹⁷, B. Mindur ^{86a}, M. Mineev ³⁸, Y. Mino ⁸⁸,
 L.M. Mir ¹³, M. Miralles Lopez ¹⁶³, M. Mironova ^{17a}, A. Mishima ¹⁵³, M.C. Missio ¹¹³,
 A. Mitra ¹⁶⁷, V.A. Mitsou ¹⁶³, Y. Mitsumori ¹¹¹, O. Miu ¹⁵⁵, P.S. Miyagawa ⁹⁴,
 T. Mkrtychyan ^{63a}, M. Mlinarevic ⁹⁶, T. Mlinarevic ⁹⁶, M. Mlynarikova ³⁶, S. Mobius ¹⁹,
 P. Moder ⁴⁸, P. Mogg ¹⁰⁹, M.H. Mohamed Farook ¹¹², A.F. Mohammed ^{14a,14e}, S. Mohapatra ⁴¹,
 G. Mokgatitswane ^{33g}, L. Moleri ¹⁶⁹, B. Mondal ¹⁴¹, S. Mondal ¹³², K. Mönig ⁴⁸,
 E. Monnier ¹⁰², L. Monsonis Romero ¹⁶³, J. Montejo Berlingen ¹³, M. Montella ¹¹⁹,
 F. Montereali ^{77a,77b}, F. Monticelli ⁹⁰, S. Monzani ^{69a,69c}, N. Morange ⁶⁶,

A.L. Moreira De Carvalho [ID130a](#), M. Moreno Llácer [ID163](#), C. Moreno Martinez [ID56](#), P. Morettini [ID57b](#),
 S. Morgenstern [ID36](#), M. Morii [ID61](#), M. Morinaga [ID153](#), A.K. Morley [ID36](#), F. Morodei [ID75a,75b](#),
 L. Morvaj [ID36](#), P. Moschovakos [ID36](#), B. Moser [ID36](#), M. Mosidze [ID149b](#), T. Moskalets [ID54](#),
 P. Moskvitina [ID113](#), J. Moss [ID31.1](#), E.J.W. Moyse [ID103](#), O. Mtintsilana [ID33g](#), S. Muanza [ID102](#),
 J. Mueller [ID129](#), D. Muenstermann [ID91](#), R. Müller [ID19](#), G.A. Mullier [ID161](#), A.J. Mullin³², J.J. Mullin¹²⁸,
 D.P. Mungo [ID155](#), D. Munoz Perez [ID163](#), F.J. Munoz Sanchez [ID101](#), M. Murin [ID101](#), W.J. Murray [ID167,134](#),
 A. Murrone [ID71a,71b](#), M. Muškinja [ID17a](#), C. Mwewa [ID29](#), A.G. Myagkov [ID37,a](#), A.J. Myers [ID8](#),
 G. Myers [ID68](#), M. Myska [ID132](#), B.P. Nachman [ID17a](#), O. Nackenhorst [ID49](#), A. Nag [ID50](#), K. Nagai [ID126](#),
 K. Nagano [ID84](#), J.L. Nagle [ID29,ai](#), E. Nagy [ID102](#), A.M. Nairz [ID36](#), Y. Nakahama [ID84](#), K. Nakamura [ID84](#),
 K. Nakkalil [ID5](#), H. Nanjo [ID124](#), R. Narayan [ID44](#), E.A. Narayanan [ID112](#), I. Naryshkin [ID37](#), M. Naseri [ID34](#),
 S. Nasri [ID159](#), C. Nass [ID24](#), G. Navarro [ID22a](#), J. Navarro-Gonzalez [ID163](#), R. Nayak [ID151](#), A. Nayaz [ID18](#),
 P.Y. Nechaeva [ID37](#), F. Nechansky [ID48](#), L. Nedic [ID126](#), T.J. Neep [ID20](#), A. Negri [ID73a,73b](#), M. Negrini [ID23b](#),
 C. Nellist [ID114](#), C. Nelson [ID104](#), K. Nelson [ID106](#), S. Nemecek [ID131](#), M. Nessi [ID36,h](#), M.S. Neubauer [ID162](#),
 F. Neuhaus [ID100](#), J. Neundorf [ID48](#), R. Newhouse [ID164](#), P.R. Newman [ID20](#), C.W. Ng [ID129](#), Y.W.Y. Ng [ID48](#),
 B. Ngair [ID35e](#), H.D.N. Nguyen [ID108](#), R.B. Nickerson [ID126](#), R. Nicolaidou [ID135](#), J. Nielsen [ID136](#),
 M. Niemeyer [ID55](#), J. Niermann [ID55,36](#), N. Nikiforou [ID36](#), V. Nikolaenko [ID37,a](#), I. Nikolic-Audit [ID127](#),
 K. Nikolopoulos [ID20](#), P. Nilsson [ID29](#), I. Ninca [ID48](#), H.R. Nindhito [ID56](#), G. Ninio [ID151](#), A. Nisati [ID75a](#),
 N. Nishu [ID2](#), R. Nisius [ID110](#), J-E. Nitschke [ID50](#), E.K. Nkadimeng [ID33g](#), T. Nobe [ID153](#), D.L. Noel [ID32](#),
 T. Nommensen [ID147](#), M.B. Norfolk [ID139](#), R.R.B. Norisam [ID96](#), B.J. Norman [ID34](#), M. Noury [ID35a](#),
 J. Novak [ID93](#), T. Novak [ID48](#), L. Novotny [ID132](#), R. Novotny [ID112](#), L. Nozka [ID122](#), K. Ntekas [ID160](#),
 N.M.J. Nunes De Moura Junior [ID83b](#), E. Nurse⁹⁶, J. Ocariz [ID127](#), A. Ochi [ID85](#), I. Ochoa [ID130a](#),
 S. Oerdek [ID48](#), J.T. Offermann [ID39](#), A. Ogrodnik [ID133](#), A. Oh [ID101](#), C.C. Ohm [ID144](#), H. Oide [ID84](#),
 R. Oishi [ID153](#), M.L. Ojeda [ID48](#), M.W. O’Keefe⁹², Y. Okumura [ID153](#), L.F. Oleiro Seabra [ID130a](#),
 S.A. Olivares Pino [ID137d](#), D. Oliveira Damazio [ID29](#), D. Oliveira Goncalves [ID83a](#), J.L. Oliver [ID160](#),
 Ö.O. Öncel [ID54](#), A.P. O’Neill [ID19](#), A. Onofre [ID130a,130e](#), P.U.E. Onyisi [ID11](#), M.J. Oreglia [ID39](#),
 G.E. Orellana [ID90](#), D. Orestano [ID77a,77b](#), N. Orlando [ID13](#), R.S. Orr [ID155](#), V. O’Shea [ID59](#),
 L.M. Osojnak [ID128](#), R. Ospanov [ID62a](#), G. Otero y Garzon [ID30](#), H. Otono [ID89](#), P.S. Ott [ID63a](#),
 G.J. Ottino [ID17a](#), M. Ouchrif [ID35d](#), J. Ouellette [ID29](#), F. Ould-Saada [ID125](#), M. Owen [ID59](#), R.E. Owen [ID134](#),
 K.Y. Oyulmaz [ID21a](#), V.E. Ozcan [ID21a](#), F. Ozturk [ID87](#), N. Ozturk [ID8](#), S. Ozturk [ID82](#), H.A. Pacey [ID126](#),
 A. Pacheco Pages [ID13](#), C. Padilla Aranda [ID13](#), G. Padovano [ID75a,75b](#), S. Pagan Griso [ID17a](#),
 G. Palacino [ID68](#), A. Palazzo [ID70a,70b](#), S. Palestini [ID36](#), J. Pan [ID172](#), T. Pan [ID64a](#), D.K. Panchal [ID11](#),
 C.E. Pandini [ID114](#), J.G. Panduro Vazquez [ID95](#), H.D. Pandya [ID1](#), H. Pang [ID14b](#), P. Pani [ID48](#),
 G. Panizzo [ID69a,69c](#), L. Paolozzi [ID56](#), C. Papadatos [ID108](#), S. Parajuli [ID44](#), A. Paramonov [ID6](#),
 C. Paraskevopoulos [ID10](#), D. Paredes Hernandez [ID64b](#), K.R. Park [ID41](#), T.H. Park [ID155](#), M.A. Parker [ID32](#),
 F. Parodi [ID57b,57a](#), E.W. Parrish [ID115](#), V.A. Parrish [ID52](#), J.A. Parsons [ID41](#), U. Parzefall [ID54](#),
 B. Pascual Dias [ID108](#), L. Pascual Dominguez [ID151](#), E. Pasqualucci [ID75a](#), S. Passaggio [ID57b](#), F. Pastore [ID95](#),
 P. Pasuwan [ID47a,47b](#), P. Patel [ID87](#), U.M. Patel [ID51](#), J.R. Pater [ID101](#), T. Pauly [ID36](#), J. Pearkes [ID143](#),
 M. Pedersen [ID125](#), R. Pedro [ID130a](#), S.V. Peleganchuk [ID37](#), O. Penc [ID36](#), E.A. Pender [ID52](#),
 K.E. Penski [ID109](#), M. Penzin [ID37](#), B.S. Peralva [ID83d](#), A.P. Pereira Peixoto [ID60](#), L. Pereira Sanchez [ID47a,47b](#),
 D.V. Perepelitsa [ID29,ai](#), E. Perez Codina [ID156a](#), M. Perganti [ID10](#), L. Perini [ID71a,71b,*](#), H. Pernegger [ID36](#),
 O. Perrin [ID40](#), K. Peters [ID48](#), R.F.Y. Peters [ID101](#), B.A. Petersen [ID36](#), T.C. Petersen [ID42](#), E. Petit [ID102](#),
 V. Petousis [ID132](#), C. Petridou [ID152,e](#), A. Petrukhin [ID141](#), M. Pettee [ID17a](#), N.E. Pettersson [ID36](#),
 A. Petukhov [ID37](#), K. Petukhova [ID133](#), R. Pezoa [ID137f](#), L. Pezzotti [ID36](#), G. Pezzullo [ID172](#), T.M. Pham [ID170](#),
 T. Pham [ID105](#), P.W. Phillips [ID134](#), G. Piacquadio [ID145](#), E. Pianori [ID17a](#), F. Piazza [ID123](#), R. Piegai [ID30](#),
 D. Pietreanu [ID27b](#), A.D. Pilkington [ID101](#), M. Pinamonti [ID69a,69c](#), J.L. Pinfeld [ID2](#),
 B.C. Pinheiro Pereira [ID130a](#), A.E. Pinto Pinoargote [ID100,135](#), L. Pintucci [ID69a,69c](#), K.M. Piper [ID146](#),
 A. Pirttikoski [ID56](#), D.A. Pizzi [ID34](#), L. Pizzimento [ID64b](#), A. Pizzini [ID114](#), M.-A. Pleier [ID29](#), V. Plesanovs⁵⁴,

V. Pleskot ¹³³, E. Plotnikova³⁸, G. Poddar ⁴, R. Poettgen ⁹⁸, L. Poggioli ¹²⁷, I. Pokharel ⁵⁵, S. Polacek ¹³³, G. Polesello ^{73a}, A. Poley ^{142,156a}, R. Polifka ¹³², A. Polini ^{23b}, C.S. Pollard ¹⁶⁷, Z.B. Pollock ¹¹⁹, V. Polychronakos ²⁹, E. Pompa Pacchi ^{75a,75b}, D. Ponomarenko ¹¹³, L. Pontecorvo ³⁶, S. Popa ^{27a}, G.A. Popeneciu ^{27d}, A. Poreba ³⁶, D.M. Portillo Quintero ^{156a}, S. Pospisil ¹³², M.A. Postill ¹³⁹, P. Postolache ^{27c}, K. Potamianos ¹⁶⁷, P.A. Potepa ^{86a}, I.N. Potrap ³⁸, C.J. Potter ³², H. Potti ¹, T. Poulsen ⁴⁸, J. Poveda ¹⁶³, M.E. Pozo Astigarraga ³⁶, A. Prades Ibanez ¹⁶³, J. Pretel ⁵⁴, D. Price ¹⁰¹, M. Primavera ^{70a}, M.A. Principe Martin ⁹⁹, R. Privara ¹²², T. Procter ⁵⁹, M.L. Proffitt ¹³⁸, N. Proklova ¹²⁸, K. Prokofiev ^{64c}, G. Proto ¹¹⁰, S. Protopopescu ²⁹, J. Proudfoot ⁶, M. Przybycien ^{86a}, W.W. Przygoda ^{86b}, J.E. Puddefoot ¹³⁹, D. Pudzha ³⁷, D. Pyatiizbyantseva ³⁷, J. Qian ¹⁰⁶, D. Qichen ¹⁰¹, Y. Qin ¹⁰¹, T. Qiu ⁵², A. Quadt ⁵⁵, M. Queitsch-Maitland ¹⁰¹, G. Quetant ⁵⁶, R.P. Quinn ¹⁶⁴, G. Rabanal Bolanos ⁶¹, D. Rafanoharana ⁵⁴, F. Ragusa ^{71a,71b}, J.L. Rainbolt ³⁹, J.A. Raine ⁵⁶, S. Rajagopalan ²⁹, E. Ramakoti ³⁷, I.A. Ramirez-Berend ³⁴, K. Ran ^{48,14e}, N.P. Rapheeha ^{33g}, H. Rasheed ^{27b}, V. Raskina ¹²⁷, D.F. Rassloff ^{63a}, A. Rastogi ^{17a}, S. Rave ¹⁰⁰, B. Ravina ⁵⁵, I. Ravinovich ¹⁶⁹, M. Raymond ³⁶, A.L. Read ¹²⁵, N.P. Readioff ¹³⁹, D.M. Rebuzzi ^{73a,73b}, G. Redlinger ²⁹, A.S. Reed ¹¹⁰, K. Reeves ²⁶, J.A. Reidelsturz ¹⁷¹, D. Reikher ¹⁵¹, A. Rej ⁴⁹, C. Rembser ³⁶, A. Renardi ⁴⁸, M. Renda ^{27b}, M.B. Rendel¹¹⁰, F. Renner ⁴⁸, A.G. Rennie ¹⁶⁰, A.L. Rescia ⁴⁸, S. Resconi ^{71a}, M. Ressegotti ^{57b,57a}, S. Rettie ³⁶, J.G. Reyes Rivera ¹⁰⁷, E. Reynolds ^{17a}, O.L. Rezanova ³⁷, P. Reznicek ¹³³, N. Ribaric ⁹¹, E. Ricci ^{78a,78b}, R. Richter ¹¹⁰, S. Richter ^{47a,47b}, E. Richter-Was ^{86b}, M. Ridel ¹²⁷, S. Ridouani ^{35d}, P. Rieck ¹¹⁷, P. Riedler ³⁶, E.M. Riefel ^{47a,47b}, J.O. Rieger ¹¹⁴, M. Rijssenbeek ¹⁴⁵, A. Rimoldi ^{73a,73b}, M. Rimoldi ³⁶, L. Rinaldi ^{23b,23a}, T.T. Rinn ²⁹, M.P. Rinnagel ¹⁰⁹, G. Ripellino ¹⁶¹, I. Riu ¹³, P. Rivadeneira ⁴⁸, J.C. Rivera Vergara ¹⁶⁵, F. Rizatdinova ¹²¹, E. Rizvi ⁹⁴, B.A. Roberts ¹⁶⁷, B.R. Roberts ^{17a}, S.H. Robertson ^{104,w}, D. Robinson ³², C.M. Robles Gajardo^{137f}, M. Robles Manzano ¹⁰⁰, A. Robson ⁵⁹, A. Rocchi ^{76a,76b}, C. Roda ^{74a,74b}, S. Rodriguez Bosca ^{63a}, Y. Rodriguez Garcia ^{22a}, A. Rodriguez Rodriguez ⁵⁴, A.M. Rodríguez Vera ^{156b}, S. Roe³⁶, J.T. Roemer ¹⁶⁰, A.R. Roepe-Gier ¹³⁶, J. Roggel ¹⁷¹, O. Røhne ¹²⁵, R.A. Rojas ¹⁰³, C.P.A. Roland ¹²⁷, J. Roloff ²⁹, A. Romaniouk ³⁷, E. Romano ^{73a,73b}, M. Romano ^{23b}, A.C. Romero Hernandez ¹⁶², N. Rompotis ⁹², L. Roos ¹²⁷, S. Rosati ^{75a}, B.J. Rosser ³⁹, E. Rossi ¹²⁶, E. Rossi ^{72a,72b}, L.P. Rossi ^{57b}, L. Rossini ⁵⁴, R. Rosten ¹¹⁹, M. Rotaru ^{27b}, B. Rottler ⁵⁴, C. Rougier ^{102,aa}, D. Rousseau ⁶⁶, D. Rousso ³², A. Roy ¹⁶², S. Roy-Garand ¹⁵⁵, A. Rozanov ¹⁰², Z.M.A. Rozario ⁵⁹, Y. Rozen ¹⁵⁰, X. Ruan ^{33g}, A. Rubio Jimenez ¹⁶³, A.J. Ruby ⁹², V.H. Ruelas Rivera ¹⁸, T.A. Ruggeri ¹, A. Ruggiero ¹²⁶, A. Ruiz-Martinez ¹⁶³, A. Rummeler ³⁶, Z. Rurikova ⁵⁴, N.A. Rusakovich ³⁸, H.L. Russell ¹⁶⁵, G. Russo ^{75a,75b}, J.P. Rutherford ⁷, S. Rutherford Colmenares ³², K. Rybacki⁹¹, M. Rybar ¹³³, E.B. Rye ¹²⁵, A. Ryzhov ⁴⁴, J.A. Sabater Iglesias ⁵⁶, P. Sabatini ¹⁶³, H.F-W. Sadrozinski ¹³⁶, F. Safai Tehrani ^{75a}, B. Safarzadeh Samani ¹³⁴, M. Safdari ¹⁴³, S. Saha ¹⁶⁵, M. Sahinsoy ¹¹⁰, A. Saibel ¹⁶³, M. Saimpert ¹³⁵, M. Saito ¹⁵³, T. Saito ¹⁵³, D. Salamani ³⁶, A. Salnikov ¹⁴³, J. Salt ¹⁶³, A. Salvador Salas ¹⁵¹, D. Salvatore ^{43b,43a}, F. Salvatore ¹⁴⁶, A. Salzburger ³⁶, D. Sammel ⁵⁴, D. Sampsonidis ^{152,e}, D. Sampsonidou ¹²³, J. Sánchez ¹⁶³, A. Sanchez Pineda ⁴, V. Sanchez Sebastian ¹⁶³, H. Sandaker ¹²⁵, C.O. Sander ⁴⁸, J.A. Sandesara ¹⁰³, M. Sandhoff ¹⁷¹, C. Sandoval ^{22b}, D.P.C. Sankey ¹³⁴, T. Sano ⁸⁸, A. Sansoni ⁵³, L. Santi ^{75a,75b}, C. Santoni ⁴⁰, H. Santos ^{130a,130b}, S.N. Santpur ^{17a}, A. Santra ¹⁶⁹, K.A. Saoucha ^{116b}, J.G. Saraiva ^{130a,130d}, J. Sardain ⁷, O. Sasaki ⁸⁴, K. Sato ¹⁵⁷, C. Sauer^{63b}, F. Sauerburger ⁵⁴, E. Sauvan ⁴, P. Savard ^{155,af}, R. Sawada ¹⁵³, C. Sawyer ¹³⁴, L. Sawyer ⁹⁷, I. Sayago Galvan¹⁶³, C. Sbarra ^{23b}, A. Sbrizzi ^{23b,23a}, T. Scanlon ⁹⁶, J. Schaarschmidt ¹³⁸, P. Schacht ¹¹⁰, U. Schäfer ¹⁰⁰, A.C. Schaffer ^{66,44}, D. Schaile ¹⁰⁹, R.D. Schamberger ¹⁴⁵, C. Scharf ¹⁸, M.M. Schefer ¹⁹,

V.A. Schegelsky [ID37](#), D. Scheirich [ID133](#), F. Schenck [ID18](#), M. Schernau [ID160](#), C. Scheulen [ID55](#), C. Schiavi [ID57b,57a](#), E.J. Schioppa [ID70a,70b](#), M. Schioppa [ID43b,43a](#), B. Schlag [ID143,n](#), K.E. Schleicher [ID54](#), S. Schlenker [ID36](#), J. Schmeing [ID171](#), M.A. Schmidt [ID171](#), K. Schmieden [ID100](#), C. Schmitt [ID100](#), N. Schmitt [ID100](#), S. Schmitt [ID48](#), L. Schoeffel [ID135](#), A. Schoening [ID63b](#), P.G. Scholer [ID54](#), E. Schopf [ID126](#), M. Schott [ID100](#), J. Schovancova [ID36](#), S. Schramm [ID56](#), F. Schroeder [ID171](#), T. Schroer [ID56](#), H-C. Schultz-Coulon [ID63a](#), M. Schumacher [ID54](#), B.A. Schumm [ID136](#), Ph. Schune [ID135](#), A.J. Schuy [ID138](#), H.R. Schwartz [ID136](#), A. Schwartzman [ID143](#), T.A. Schwarz [ID106](#), Ph. Schwemling [ID135](#), R. Schwienhorst [ID107](#), A. Sciandra [ID136](#), G. Sciolla [ID26](#), F. Scuri [ID74a](#), C.D. Sebastiani [ID92](#), K. Sedlaczek [ID115](#), P. Seema [ID18](#), S.C. Seidel [ID112](#), A. Seiden [ID136](#), B.D. Seidlitz [ID41](#), C. Seitz [ID48](#), J.M. Seixas [ID83b](#), G. Sekhniaidze [ID72a](#), S.J. Sekula [ID44](#), L. Selem [ID60](#), N. Semprini-Cesari [ID23b,23a](#), D. Sengupta [ID56](#), V. Senthilkumar [ID163](#), L. Serin [ID66](#), L. Serkin [ID69a,69b](#), M. Sessa [ID76a,76b](#), H. Severini [ID120](#), F. Sforza [ID57b,57a](#), A. Sfyrta [ID56](#), E. Shabalina [ID55](#), R. Shaheen [ID144](#), J.D. Shahinian [ID128](#), D. Shaked Renous [ID169](#), L.Y. Shan [ID14a](#), M. Shapiro [ID17a](#), A. Sharma [ID36](#), A.S. Sharma [ID164](#), P. Sharma [ID80](#), S. Sharma [ID48](#), P.B. Shatalov [ID37](#), K. Shaw [ID146](#), S.M. Shaw [ID101](#), A. Shcherbakova [ID37](#), Q. Shen [ID62c,5](#), D.J. Sheppard [ID142](#), P. Sherwood [ID96](#), L. Shi [ID96](#), X. Shi [ID14a](#), C.O. Shimmin [ID172](#), J.D. Shinner [ID95](#), I.P.J. Shipsey [ID126](#), S. Shirabe [ID56,h](#), M. Shiyakova [ID38,u](#), J. Shlomi [ID169](#), M.J. Shochet [ID39](#), J. Shojaii [ID105](#), D.R. Shope [ID125](#), B. Shrestha [ID120](#), S. Shrestha [ID119,aj](#), E.M. Shrif [ID33g](#), M.J. Shroff [ID165](#), P. Sicho [ID131](#), A.M. Sickles [ID162](#), E. Sideras Haddad [ID33g](#), A.C. Sidley [ID114](#), A. Sidoti [ID23b](#), F. Siegert [ID50](#), Dj. Sijacki [ID15](#), F. Sili [ID90](#), J.M. Silva [ID20](#), M.V. Silva Oliveira [ID29](#), S.B. Silverstein [ID47a](#), S. Simion [ID66](#), R. Simoniello [ID36](#), E.L. Simpson [ID59](#), H. Simpson [ID146](#), L.R. Simpson [ID106](#), N.D. Simpson [ID98](#), S. Simsek [ID82](#), S. Sindhu [ID55](#), P. Sinervo [ID155](#), S. Singh [ID155](#), S. Sinha [ID48](#), S. Sinha [ID101](#), M. Sioli [ID23b,23a](#), I. Siral [ID36](#), E. Sitnikova [ID48](#), S.Yu. Sivoklov [ID37,*](#), J. Sjölin [ID47a,47b](#), A. Skaf [ID55](#), E. Skorda [ID20](#), P. Skubic [ID120](#), M. Slawinska [ID87](#), V. Smakhtin [ID169](#), B.H. Smart [ID134](#), J. Smiesko [ID36](#), S.Yu. Smirnov [ID37](#), Y. Smirnov [ID37](#), L.N. Smirnova [ID37,a](#), O. Smirnova [ID98](#), A.C. Smith [ID41](#), E.A. Smith [ID39](#), H.A. Smith [ID126](#), J.L. Smith [ID92](#), R. Smith [ID143](#), M. Smizanska [ID91](#), K. Smolek [ID132](#), A.A. Snesarev [ID37](#), S.R. Snider [ID155](#), H.L. Snoek [ID114](#), S. Snyder [ID29](#), R. Sobie [ID165,w](#), A. Soffer [ID151](#), C.A. Solans Sanchez [ID36](#), E.Yu. Soldatov [ID37](#), U. Soldevila [ID163](#), A.A. Solodkov [ID37](#), S. Solomon [ID26](#), A. Soloshenko [ID38](#), K. Solovieva [ID54](#), O.V. Solovyanov [ID40](#), V. Solovyev [ID37](#), P. Sommer [ID36](#), A. Sonay [ID13](#), W.Y. Song [ID156b](#), J.M. Sonneveld [ID114](#), A. Sopczak [ID132](#), A.L. Soppio [ID96](#), F. Sopkova [ID28b](#), I.R. Sotarriva Alvarez [ID154](#), V. Sothilingam [ID63a](#), O.J. Soto Sandoval [ID137c,137b](#), S. Sottocornola [ID68](#), R. Soualah [ID116b](#), Z. Soumami [ID35e](#), D. South [ID48](#), N. Soybelman [ID169](#), S. Spagnolo [ID70a,70b](#), M. Spalla [ID110](#), D. Sperlich [ID54](#), G. Spigo [ID36](#), S. Spinali [ID91](#), D.P. Spiteri [ID59](#), M. Spousta [ID133](#), E.J. Staats [ID34](#), A. Stabile [ID71a,71b](#), R. Stamen [ID63a](#), A. Stampekis [ID20](#), M. Standke [ID24](#), E. Stanecka [ID87](#), M.V. Stange [ID50](#), B. Stanislaus [ID17a](#), M.M. Stanitzki [ID48](#), B. Stapf [ID48](#), E.A. Starchenko [ID37](#), G.H. Stark [ID136](#), J. Stark [ID102,aa](#), D.M. Starke [ID156b](#), P. Staroba [ID131](#), P. Starovoitov [ID63a](#), S. Stärz [ID104](#), R. Staszewski [ID87](#), G. Stavropoulos [ID46](#), J. Steentoft [ID161](#), P. Steinberg [ID29](#), B. Stelzer [ID142,156a](#), H.J. Stelzer [ID129](#), O. Stelzer-Chilton [ID156a](#), H. Stenzel [ID58](#), T.J. Stevenson [ID146](#), G.A. Stewart [ID36](#), J.R. Stewart [ID121](#), M.C. Stockton [ID36](#), G. Stoicea [ID27b](#), M. Stolarski [ID130a](#), S. Stonjek [ID110](#), A. Straessner [ID50](#), J. Strandberg [ID144](#), S. Strandberg [ID47a,47b](#), M. Stratmann [ID171](#), M. Strauss [ID120](#), T. Streblner [ID102](#), P. Strizenc [ID28b](#), R. Ströhmer [ID166](#), D.M. Strom [ID123](#), R. Stroynowski [ID44](#), A. Strubig [ID47a,47b](#), S.A. Stucci [ID29](#), B. Stugu [ID16](#), J. Stupak [ID120](#), N.A. Styles [ID48](#), D. Su [ID143](#), S. Su [ID62a](#), W. Su [ID62d](#), X. Su [ID62a,66](#), K. Sugizaki [ID153](#), V.V. Sulim [ID37](#), M.J. Sullivan [ID92](#), D.M.S. Sultan [ID78a,78b](#), L. Sultanaliev [ID37](#), S. Sultansoy [ID3b](#), T. Sumida [ID88](#), S. Sun [ID106](#), S. Sun [ID170](#), O. Sunneborn Gudnadottir [ID161](#), N. Sur [ID102](#), M.R. Sutton [ID146](#), H. Suzuki [ID157](#), M. Svatos [ID131](#), M. Swiatlowski [ID156a](#), T. Swirski [ID166](#), I. Sykora [ID28a](#), M. Sykora [ID133](#), T. Sykora [ID133](#), D. Ta [ID100](#), K. Tackmann [ID48,t](#), A. Taffard [ID160](#), R. Tafirout [ID156a](#), J.S. Tafuya Vargas [ID66](#), E.P. Takeva [ID52](#),

Y. Takubo ⁸⁴, M. Talby ¹⁰², A.A. Talyshev ³⁷, K.C. Tam ^{64b}, N.M. Tamir ¹⁵¹, A. Tanaka ¹⁵³,
 J. Tanaka ¹⁵³, R. Tanaka ⁶⁶, M. Tanasini ^{57b,57a}, Z. Tao ¹⁶⁴, S. Tapia Araya ^{137f},
 S. Tapprogge ¹⁰⁰, A. Tarek Abouelfadl Mohamed ¹⁰⁷, S. Tarem ¹⁵⁰, K. Tariq ^{14a}, G. Tarna ^{102,27b},
 G.F. Tartarelli ^{71a}, P. Tas ¹³³, M. Tasevsky ¹³¹, E. Tassi ^{43b,43a}, A.C. Tate ¹⁶², G. Tateno ¹⁵³,
 Y. Tayalati ^{35e,v}, G.N. Taylor ¹⁰⁵, W. Taylor ^{156b}, A.S. Tee ¹⁷⁰, R. Teixeira De Lima ¹⁴³,
 P. Teixeira-Dias ⁹⁵, J.J. Teoh ¹⁵⁵, K. Terashi ¹⁵³, J. Terron ⁹⁹, S. Terzo ¹³, M. Testa ⁵³,
 R.J. Teuscher ^{155,w}, A. Thaler ⁷⁹, O. Theiner ⁵⁶, N. Themistokleous ⁵², T. Thevenaux-Pelzer ¹⁰²,
 O. Thielmann ¹⁷¹, D.W. Thomas ⁹⁵, J.P. Thomas ²⁰, E.A. Thompson ^{17a}, P.D. Thompson ²⁰,
 E. Thomson ¹²⁸, Y. Tian ⁵⁵, V. Tikhomirov ^{37,a}, Yu.A. Tikhonov ³⁷, S. Timoshenko ³⁷,
 D. Timoshyn ¹³³, E.X.L. Ting ¹, P. Tipton ¹⁷², A. Tishelman-Charny ²⁹, S.H. Tlou ^{33g},
 A. Tnourji ⁴⁰, K. Todome ¹⁵⁴, S. Todorova-Nova ¹³³, S. Todt ⁵⁰, M. Togawa ⁸⁴, J. Tojo ⁸⁹,
 S. Tokár ^{28a}, K. Tokushuku ⁸⁴, O. Toldaiev ⁶⁸, R. Tombs ³², M. Tomoto ^{84,111},
 L. Tompkins ^{143,n}, K.W. Topolnicki ^{86b}, E. Torrence ¹²³, H. Torres ^{102,aa}, E. Torró Pastor ¹⁶³,
 M. Toscani ³⁰, C. Toscirci ³⁹, M. Tost ¹¹, D.R. Tovey ¹³⁹, A. Traeet ¹⁶, I.S. Trandafir ^{27b},
 T. Trefzger ¹⁶⁶, A. Tricoli ²⁹, I.M. Trigger ^{156a}, S. Trincaz-Duvoid ¹²⁷, D.A. Trischuk ²⁶,
 B. Trocmé ⁶⁰, C. Troncon ^{71a}, L. Truong ^{33c}, M. Trzebinski ⁸⁷, A. Trzupek ⁸⁷, F. Tsai ¹⁴⁵,
 M. Tsai ¹⁰⁶, A. Tsiamis ^{152,e}, P.V. Tsiareshka ³⁷, S. Tsigaridas ^{156a}, A. Tsirigotis ^{152,r},
 V. Tsiskaridze ¹⁵⁵, E.G. Tskhadadze ^{149a}, M. Tsopoulou ^{152,e}, Y. Tsujikawa ⁸⁸, I.I. Tsukerman ³⁷,
 V. Tsulaia ^{17a}, S. Tsuno ⁸⁴, K. Tsuri ¹¹⁸, D. Tsybychev ¹⁴⁵, Y. Tu ^{64b}, A. Tudorache ^{27b},
 V. Tudorache ^{27b}, A.N. Tuna ⁶¹, S. Turchikhin ^{57b,57a}, I. Turk Cakir ^{3a}, R. Turra ^{71a},
 T. Turtuvshin ^{38,x}, P.M. Tuts ⁴¹, S. Tzamarias ^{152,e}, P. Tzanis ¹⁰, E. Tzovara ¹⁰⁰, F. Ukegawa ¹⁵⁷,
 P.A. Ulloa Poblete ^{137c,137b}, E.N. Umaka ²⁹, G. Unal ³⁶, M. Unal ¹¹, A. Undrus ²⁹, G. Unel ¹⁶⁰,
 J. Urban ^{28b}, P. Urquijo ¹⁰⁵, P. Urrejola ^{137a}, G. Usai ⁸, R. Ushioda ¹⁵⁴, M. Usman ¹⁰⁸,
 Z. Uysal ^{21b}, V. Vacek ¹³², B. Vachon ¹⁰⁴, K.O.H. Vadla ¹²⁵, T. Vafeiadis ³⁶, A. Vaitkus ⁹⁶,
 C. Valderanis ¹⁰⁹, E. Valdes Santurio ^{47a,47b}, M. Valente ^{156a}, S. Valentinetti ^{23b,23a}, A. Valero ¹⁶³,
 E. Valiente Moreno ¹⁶³, A. Vallier ^{102,aa}, J.A. Valls Ferrer ¹⁶³, D.R. Van Arneeman ¹¹⁴,
 T.R. Van Daalen ¹³⁸, A. Van Der Graaf ⁴⁹, P. Van Gemmeren ⁶, M. Van Rijnbach ^{125,36},
 S. Van Stroud ⁹⁶, I. Van Vulpen ¹¹⁴, M. Vanadia ^{76a,76b}, W. Vandelli ³⁶, M. Vandenbroucke ¹³⁵,
 E.R. Vandewall ¹²¹, D. Vannicola ¹⁵¹, L. Vannoli ^{57b,57a}, R. Vari ^{75a}, E.W. Varnes ⁷,
 C. Varni ^{17b}, T. Varol ¹⁴⁸, D. Varouchas ⁶⁶, L. Varriale ¹⁶³, K.E. Varvell ¹⁴⁷, M.E. Vasile ^{27b},
 L. Vaslin ⁸⁴, G.A. Vasquez ¹⁶⁵, A. Vasyukov ³⁸, F. Vazeille ⁴⁰, T. Vazquez Schroeder ³⁶,
 J. Veatch ³¹, V. Vecchio ¹⁰¹, M.J. Veen ¹⁰³, I. Veliscek ¹²⁶, L.M. Veloce ¹⁵⁵, F. Veloso ^{130a,130c},
 S. Veneziano ^{75a}, A. Ventura ^{70a,70b}, S. Ventura Gonzalez ¹³⁵, A. Verbytskyi ¹¹⁰,
 M. Verducci ^{74a,74b}, C. Vergis ²⁴, M. Verissimo De Araujo ^{83b}, W. Verkerke ¹¹⁴,
 J.C. Vermeulen ¹¹⁴, C. Vernieri ¹⁴³, M. Vessella ¹⁰³, M.C. Vetterli ^{142,af}, A. Vgenopoulos ^{152,e},
 N. Viaux Maira ^{137f}, T. Vickey ¹³⁹, O.E. Vickey Boeriu ¹³⁹, G.H.A. Viehhauser ¹²⁶, L. Vigani ^{63b},
 M. Villa ^{23b,23a}, M. Villaplana Perez ¹⁶³, E.M. Villhauer ⁵², E. Vilucchi ⁵³, M.G. Vinciter ³⁴,
 G.S. Virdee ²⁰, A. Vishwakarma ⁵², A. Visibile ¹¹⁴, C. Vittori ³⁶, I. Vivarelli ¹⁴⁶,
 E. Voevodina ¹¹⁰, F. Vogel ¹⁰⁹, J.C. Voigt ⁵⁰, P. Vokac ¹³², Yu. Volkotrub ^{86a}, J. Von Ahnen ⁴⁸,
 E. Von Toerne ²⁴, B. Vormwald ³⁶, V. Vorobel ¹³³, K. Vorobev ³⁷, M. Vos ¹⁶³, K. Voss ¹⁴¹,
 J.H. Vossebeld ⁹², M. Vozak ¹¹⁴, L. Vozdecky ⁹⁴, N. Vranjes ¹⁵, M. Vranjes Milosavljevic ¹⁵,
 M. Vreeswijk ¹¹⁴, R. Vuillermet ³⁶, O. Vujanovic ¹⁰⁰, I. Vukotic ³⁹, S. Wada ¹⁵⁷, C. Wagner ¹⁰³,
 J.M. Wagner ^{17a}, W. Wagner ¹⁷¹, S. Wahdan ¹⁷¹, H. Wahlberg ⁹⁰, M. Wakida ¹¹¹, J. Walder ¹³⁴,
 R. Walker ¹⁰⁹, W. Walkowiak ¹⁴¹, A. Wall ¹²⁸, T. Wamorkar ⁶, A.Z. Wang ¹³⁶, C. Wang ¹⁰⁰,
 C. Wang ^{62c}, H. Wang ^{17a}, J. Wang ^{64a}, R.-J. Wang ¹⁰⁰, R. Wang ⁶¹, R. Wang ⁶,
 S.M. Wang ¹⁴⁸, S. Wang ^{62b}, T. Wang ^{62a}, W.T. Wang ⁸⁰, W. Wang ^{14a}, X. Wang ^{14c},
 X. Wang ¹⁶², X. Wang ^{62c}, Y. Wang ^{62d}, Y. Wang ^{14c}, Z. Wang ¹⁰⁶, Z. Wang ^{62d,51,62c},

Z. Wang ¹⁰⁶, A. Warburton ¹⁰⁴, R.J. Ward ²⁰, N. Warrack ⁵⁹, A.T. Watson ²⁰, H. Watson ⁵⁹, M.F. Watson ²⁰, E. Watton ^{59,134}, G. Watts ¹³⁸, B.M. Waugh ⁹⁶, C. Weber ²⁹, H.A. Weber ¹⁸, M.S. Weber ¹⁹, S.M. Weber ^{63a}, C. Wei ^{62a}, Y. Wei ¹²⁶, A.R. Weidberg ¹²⁶, E.J. Weik ¹¹⁷, J. Weingarten ⁴⁹, M. Weirich ¹⁰⁰, C. Weiser ⁵⁴, C.J. Wells ⁴⁸, T. Wenaus ²⁹, B. Wendland ⁴⁹, T. Wengler ³⁶, N.S. Wenke ¹¹⁰, N. Wermes ²⁴, M. Wessels ^{63a}, A.M. Wharton ⁹¹, A.S. White ⁶¹, A. White ⁸, M.J. White ¹, D. Whiteson ¹⁶⁰, L. Wickremasinghe ¹²⁴, W. Wiedenmann ¹⁷⁰, C. Wiel ⁵⁰, M. Wielers ¹³⁴, C. Wiglesworth ⁴², D.J. Wilbern ¹²⁰, H.G. Wilkens ³⁶, D.M. Williams ⁴¹, H.H. Williams ¹²⁸, S. Williams ³², S. Willocq ¹⁰³, B.J. Wilson ¹⁰¹, P.J. Windischhofer ³⁹, F.I. Winkel ³⁰, F. Winklmeier ¹²³, B.T. Winter ⁵⁴, J.K. Winter ¹⁰¹, M. Wittgen ¹⁴³, M. Wobisch ⁹⁷, Z. Wolffs ¹¹⁴, J. Wollrath ¹⁶⁰, M.W. Wolter ⁸⁷, H. Wolters ^{130a,130c}, A.F. Wongel ⁴⁸, E.L. Woodward ⁴¹, S.D. Worm ⁴⁸, B.K. Wosiek ⁸⁷, K.W. Woźniak ⁸⁷, S. Wozniowski ⁵⁵, K. Wraight ⁵⁹, C. Wu ²⁰, J. Wu ^{14a,14e}, M. Wu ^{64a}, M. Wu ¹¹³, S.L. Wu ¹⁷⁰, X. Wu ⁵⁶, Y. Wu ^{62a}, Z. Wu ¹³⁵, J. Wuerzinger ^{110,ad}, T.R. Wyatt ¹⁰¹, B.M. Wynne ⁵², S. Xella ⁴², L. Xia ^{14c}, M. Xia ^{14b}, J. Xiang ^{64c}, M. Xie ^{62a}, X. Xie ^{62a}, S. Xin ^{14a,14e}, A. Xiong ¹²³, J. Xiong ^{17a}, D. Xu ^{14a}, H. Xu ^{62a}, L. Xu ^{62a}, R. Xu ¹²⁸, T. Xu ¹⁰⁶, Y. Xu ^{14b}, Z. Xu ⁵², Z. Xu ^{14c}, B. Yabsley ¹⁴⁷, S. Yacoob ^{33a}, Y. Yamaguchi ¹⁵⁴, E. Yamashita ¹⁵³, H. Yamauchi ¹⁵⁷, T. Yamazaki ^{17a}, Y. Yamazaki ⁸⁵, J. Yan ^{62c}, S. Yan ¹²⁶, Z. Yan ²⁵, H.J. Yang ^{62c,62d}, H.T. Yang ^{62a}, S. Yang ^{62a}, T. Yang ^{64c}, X. Yang ³⁶, X. Yang ^{14a}, Y. Yang ⁴⁴, Y. Yang ^{62a}, Z. Yang ^{62a}, W-M. Yao ^{17a}, Y.C. Yap ⁴⁸, H. Ye ^{14c}, H. Ye ⁵⁵, J. Ye ^{14a}, S. Ye ²⁹, X. Ye ^{62a}, Y. Yeh ⁹⁶, I. Yeletsikh ³⁸, B.K. Yeo ^{17b}, M.R. Yexley ⁹⁶, P. Yin ⁴¹, K. Yorita ¹⁶⁸, S. Younas ^{27b}, C.J.S. Young ³⁶, C. Young ¹⁴³, C. Yu ^{14a,14e,ah}, Y. Yu ^{62a}, M. Yuan ¹⁰⁶, R. Yuan ^{62b}, L. Yue ⁹⁶, M. Zaazoua ^{62a}, B. Zabinski ⁸⁷, E. Zaid ⁵², Z.K. Zak ⁸⁷, T. Zakareishvili ^{149b}, N. Zakharchuk ³⁴, S. Zambito ⁵⁶, J.A. Zamora Saa ^{137d,137b}, J. Zang ¹⁵³, D. Zanzi ⁵⁴, O. Zaplatilek ¹³², C. Zeitnitz ¹⁷¹, H. Zeng ^{14a}, J.C. Zeng ¹⁶², D.T. Zenger Jr ²⁶, O. Zenin ³⁷, T. Ženiš ^{28a}, S. Zenz ⁹⁴, S. Zerradi ^{35a}, D. Zerwas ⁶⁶, M. Zhai ^{14a,14e}, B. Zhang ^{14c}, D.F. Zhang ¹³⁹, J. Zhang ^{62b}, J. Zhang ⁶, K. Zhang ^{14a,14e}, L. Zhang ^{14c}, P. Zhang ^{14a,14e}, R. Zhang ¹⁷⁰, S. Zhang ¹⁰⁶, S. Zhang ⁴⁴, T. Zhang ¹⁵³, X. Zhang ^{62c}, X. Zhang ^{62b}, Y. Zhang ^{62c,5}, Y. Zhang ⁹⁶, Y. Zhang ^{14c}, Z. Zhang ^{17a}, Z. Zhang ⁶⁶, H. Zhao ¹³⁸, T. Zhao ^{62b}, Y. Zhao ¹³⁶, Z. Zhao ^{62a}, A. Zhemchugov ³⁸, J. Zheng ^{14c}, K. Zheng ¹⁶², X. Zheng ^{62a}, Z. Zheng ¹⁴³, D. Zhong ¹⁶², B. Zhou ¹⁰⁶, H. Zhou ⁷, N. Zhou ^{62c}, Y. Zhou ⁷, C.G. Zhu ^{62b}, J. Zhu ¹⁰⁶, Y. Zhu ^{62c}, Y. Zhu ^{62a}, X. Zhuang ^{14a}, K. Zhukov ³⁷, V. Zhulanov ³⁷, N.I. Zimine ³⁸, J. Zinsser ^{63b}, M. Ziolkowski ¹⁴¹, L. Živković ¹⁵, A. Zoccoli ^{23b,23a}, K. Zoch ⁶¹, T.G. Zorbas ¹³⁹, O. Zormpa ⁴⁶, W. Zou ⁴¹, L. Zwalinski ³⁶.

¹Department of Physics, University of Adelaide, Adelaide; Australia.

²Department of Physics, University of Alberta, Edmonton AB; Canada.

^{3(a)}Department of Physics, Ankara University, Ankara; ^(b)Division of Physics, TOBB University of Economics and Technology, Ankara; Türkiye.

⁴LAPP, Université Savoie Mont Blanc, CNRS/IN2P3, Annecy; France.

⁵APC, Université Paris Cité, CNRS/IN2P3, Paris; France.

⁶High Energy Physics Division, Argonne National Laboratory, Argonne IL; United States of America.

⁷Department of Physics, University of Arizona, Tucson AZ; United States of America.

⁸Department of Physics, University of Texas at Arlington, Arlington TX; United States of America.

⁹Physics Department, National and Kapodistrian University of Athens, Athens; Greece.

¹⁰Physics Department, National Technical University of Athens, Zografou; Greece.

¹¹Department of Physics, University of Texas at Austin, Austin TX; United States of America.

¹²Institute of Physics, Azerbaijan Academy of Sciences, Baku; Azerbaijan.

- ¹³Institut de Física d'Altes Energies (IFAE), Barcelona Institute of Science and Technology, Barcelona; Spain.
- ¹⁴(^a)Institute of High Energy Physics, Chinese Academy of Sciences, Beijing; (^b)Physics Department, Tsinghua University, Beijing; (^c)Department of Physics, Nanjing University, Nanjing; (^d)School of Science, Shenzhen Campus of Sun Yat-sen University; (^e)University of Chinese Academy of Science (UCAS), Beijing; China.
- ¹⁵Institute of Physics, University of Belgrade, Belgrade; Serbia.
- ¹⁶Department for Physics and Technology, University of Bergen, Bergen; Norway.
- ¹⁷(^a)Physics Division, Lawrence Berkeley National Laboratory, Berkeley CA; (^b)University of California, Berkeley CA; United States of America.
- ¹⁸Institut für Physik, Humboldt Universität zu Berlin, Berlin; Germany.
- ¹⁹Albert Einstein Center for Fundamental Physics and Laboratory for High Energy Physics, University of Bern, Bern; Switzerland.
- ²⁰School of Physics and Astronomy, University of Birmingham, Birmingham; United Kingdom.
- ²¹(^a)Department of Physics, Bogazici University, Istanbul; (^b)Department of Physics Engineering, Gaziantep University, Gaziantep; (^c)Department of Physics, Istanbul University, Istanbul; Türkiye.
- ²²(^a)Facultad de Ciencias y Centro de Investigaciones, Universidad Antonio Nariño, Bogotá; (^b)Departamento de Física, Universidad Nacional de Colombia, Bogotá; Colombia.
- ²³(^a)Dipartimento di Fisica e Astronomia A. Righi, Università di Bologna, Bologna; (^b)INFN Sezione di Bologna; Italy.
- ²⁴Physikalisches Institut, Universität Bonn, Bonn; Germany.
- ²⁵Department of Physics, Boston University, Boston MA; United States of America.
- ²⁶Department of Physics, Brandeis University, Waltham MA; United States of America.
- ²⁷(^a)Transilvania University of Brasov, Brasov; (^b)Horia Hulubei National Institute of Physics and Nuclear Engineering, Bucharest; (^c)Department of Physics, Alexandru Ioan Cuza University of Iasi, Iasi; (^d)National Institute for Research and Development of Isotopic and Molecular Technologies, Physics Department, Cluj-Napoca; (^e)University Politehnica Bucharest, Bucharest; (^f)West University in Timisoara, Timisoara; (^g)Faculty of Physics, University of Bucharest, Bucharest; Romania.
- ²⁸(^a)Faculty of Mathematics, Physics and Informatics, Comenius University, Bratislava; (^b)Department of Subnuclear Physics, Institute of Experimental Physics of the Slovak Academy of Sciences, Kosice; Slovak Republic.
- ²⁹Physics Department, Brookhaven National Laboratory, Upton NY; United States of America.
- ³⁰Universidad de Buenos Aires, Facultad de Ciencias Exactas y Naturales, Departamento de Física, y CONICET, Instituto de Física de Buenos Aires (IFIBA), Buenos Aires; Argentina.
- ³¹California State University, CA; United States of America.
- ³²Cavendish Laboratory, University of Cambridge, Cambridge; United Kingdom.
- ³³(^a)Department of Physics, University of Cape Town, Cape Town; (^b)iThemba Labs, Western Cape; (^c)Department of Mechanical Engineering Science, University of Johannesburg, Johannesburg; (^d)National Institute of Physics, University of the Philippines Diliman (Philippines); (^e)University of South Africa, Department of Physics, Pretoria; (^f)University of Zululand, KwaDlangezwa; (^g)School of Physics, University of the Witwatersrand, Johannesburg; South Africa.
- ³⁴Department of Physics, Carleton University, Ottawa ON; Canada.
- ³⁵(^a)Faculté des Sciences Ain Chock, Réseau Universitaire de Physique des Hautes Energies - Université Hassan II, Casablanca; (^b)Faculté des Sciences, Université Ibn-Tofail, Kénitra; (^c)Faculté des Sciences Semlalia, Université Cadi Ayyad, LPHEA-Marrakech; (^d)LPMR, Faculté des Sciences, Université Mohamed Premier, Oujda; (^e)Faculté des sciences, Université Mohammed V, Rabat; (^f)Institute of Applied Physics, Mohammed VI Polytechnic University, Ben Guerir; Morocco.

- ³⁶CERN, Geneva; Switzerland.
- ³⁷Affiliated with an institute covered by a cooperation agreement with CERN.
- ³⁸Affiliated with an international laboratory covered by a cooperation agreement with CERN.
- ³⁹Enrico Fermi Institute, University of Chicago, Chicago IL; United States of America.
- ⁴⁰LPC, Université Clermont Auvergne, CNRS/IN2P3, Clermont-Ferrand; France.
- ⁴¹Nevis Laboratory, Columbia University, Irvington NY; United States of America.
- ⁴²Niels Bohr Institute, University of Copenhagen, Copenhagen; Denmark.
- ⁴³(^a)Dipartimento di Fisica, Università della Calabria, Rende;(^b)INFN Gruppo Collegato di Cosenza, Laboratori Nazionali di Frascati; Italy.
- ⁴⁴Physics Department, Southern Methodist University, Dallas TX; United States of America.
- ⁴⁵Physics Department, University of Texas at Dallas, Richardson TX; United States of America.
- ⁴⁶National Centre for Scientific Research "Demokritos", Agia Paraskevi; Greece.
- ⁴⁷(^a)Department of Physics, Stockholm University;(^b)Oskar Klein Centre, Stockholm; Sweden.
- ⁴⁸Deutsches Elektronen-Synchrotron DESY, Hamburg and Zeuthen; Germany.
- ⁴⁹Fakultät Physik , Technische Universität Dortmund, Dortmund; Germany.
- ⁵⁰Institut für Kern- und Teilchenphysik, Technische Universität Dresden, Dresden; Germany.
- ⁵¹Department of Physics, Duke University, Durham NC; United States of America.
- ⁵²SUPA - School of Physics and Astronomy, University of Edinburgh, Edinburgh; United Kingdom.
- ⁵³INFN e Laboratori Nazionali di Frascati, Frascati; Italy.
- ⁵⁴Physikalisches Institut, Albert-Ludwigs-Universität Freiburg, Freiburg; Germany.
- ⁵⁵II. Physikalisches Institut, Georg-August-Universität Göttingen, Göttingen; Germany.
- ⁵⁶Département de Physique Nucléaire et Corpusculaire, Université de Genève, Genève; Switzerland.
- ⁵⁷(^a)Dipartimento di Fisica, Università di Genova, Genova;(^b)INFN Sezione di Genova; Italy.
- ⁵⁸II. Physikalisches Institut, Justus-Liebig-Universität Giessen, Giessen; Germany.
- ⁵⁹SUPA - School of Physics and Astronomy, University of Glasgow, Glasgow; United Kingdom.
- ⁶⁰LPSC, Université Grenoble Alpes, CNRS/IN2P3, Grenoble INP, Grenoble; France.
- ⁶¹Laboratory for Particle Physics and Cosmology, Harvard University, Cambridge MA; United States of America.
- ⁶²(^a)Department of Modern Physics and State Key Laboratory of Particle Detection and Electronics, University of Science and Technology of China, Hefei;(^b)Institute of Frontier and Interdisciplinary Science and Key Laboratory of Particle Physics and Particle Irradiation (MOE), Shandong University, Qingdao;(^c)School of Physics and Astronomy, Shanghai Jiao Tong University, Key Laboratory for Particle Astrophysics and Cosmology (MOE), SKLPPC, Shanghai;(^d)Tsung-Dao Lee Institute, Shanghai;(^e)School of Physics and Microelectronics, Zhengzhou University; China.
- ⁶³(^a)Kirchhoff-Institut für Physik, Ruprecht-Karls-Universität Heidelberg, Heidelberg;(^b)Physikalisches Institut, Ruprecht-Karls-Universität Heidelberg, Heidelberg; Germany.
- ⁶⁴(^a)Department of Physics, Chinese University of Hong Kong, Shatin, N.T., Hong Kong;(^b)Department of Physics, University of Hong Kong, Hong Kong;(^c)Department of Physics and Institute for Advanced Study, Hong Kong University of Science and Technology, Clear Water Bay, Kowloon, Hong Kong; China.
- ⁶⁵Department of Physics, National Tsing Hua University, Hsinchu; Taiwan.
- ⁶⁶IJCLab, Université Paris-Saclay, CNRS/IN2P3, 91405, Orsay; France.
- ⁶⁷Centro Nacional de Microelectrónica (IMB-CNM-CSIC), Barcelona; Spain.
- ⁶⁸Department of Physics, Indiana University, Bloomington IN; United States of America.
- ⁶⁹(^a)INFN Gruppo Collegato di Udine, Sezione di Trieste, Udine;(^b)ICTP, Trieste;(^c)Dipartimento Politecnico di Ingegneria e Architettura, Università di Udine, Udine; Italy.
- ⁷⁰(^a)INFN Sezione di Lecce;(^b)Dipartimento di Matematica e Fisica, Università del Salento, Lecce; Italy.
- ⁷¹(^a)INFN Sezione di Milano;(^b)Dipartimento di Fisica, Università di Milano, Milano; Italy.

- 72^(a) INFN Sezione di Napoli; ^(b) Dipartimento di Fisica, Università di Napoli, Napoli; Italy.
- 73^(a) INFN Sezione di Pavia; ^(b) Dipartimento di Fisica, Università di Pavia, Pavia; Italy.
- 74^(a) INFN Sezione di Pisa; ^(b) Dipartimento di Fisica E. Fermi, Università di Pisa, Pisa; Italy.
- 75^(a) INFN Sezione di Roma; ^(b) Dipartimento di Fisica, Sapienza Università di Roma, Roma; Italy.
- 76^(a) INFN Sezione di Roma Tor Vergata; ^(b) Dipartimento di Fisica, Università di Roma Tor Vergata, Roma; Italy.
- 77^(a) INFN Sezione di Roma Tre; ^(b) Dipartimento di Matematica e Fisica, Università Roma Tre, Roma; Italy.
- 78^(a) INFN-TIFPA; ^(b) Università degli Studi di Trento, Trento; Italy.
- 79 Universität Innsbruck, Department of Astro and Particle Physics, Innsbruck; Austria.
- 80 University of Iowa, Iowa City IA; United States of America.
- 81 Department of Physics and Astronomy, Iowa State University, Ames IA; United States of America.
- 82 Istinye University, Sariyer, Istanbul; Türkiye.
- 83^(a) Departamento de Engenharia Elétrica, Universidade Federal de Juiz de Fora (UFJF), Juiz de Fora; ^(b) Universidade Federal do Rio De Janeiro COPPE/EE/IF, Rio de Janeiro; ^(c) Instituto de Física, Universidade de São Paulo, São Paulo; ^(d) Rio de Janeiro State University, Rio de Janeiro; Brazil.
- 84 KEK, High Energy Accelerator Research Organization, Tsukuba; Japan.
- 85 Graduate School of Science, Kobe University, Kobe; Japan.
- 86^(a) AGH University of Krakow, Faculty of Physics and Applied Computer Science, Krakow; ^(b) Marian Smoluchowski Institute of Physics, Jagiellonian University, Krakow; Poland.
- 87 Institute of Nuclear Physics Polish Academy of Sciences, Krakow; Poland.
- 88 Faculty of Science, Kyoto University, Kyoto; Japan.
- 89 Research Center for Advanced Particle Physics and Department of Physics, Kyushu University, Fukuoka ; Japan.
- 90 Instituto de Física La Plata, Universidad Nacional de La Plata and CONICET, La Plata; Argentina.
- 91 Physics Department, Lancaster University, Lancaster; United Kingdom.
- 92 Oliver Lodge Laboratory, University of Liverpool, Liverpool; United Kingdom.
- 93 Department of Experimental Particle Physics, Jožef Stefan Institute and Department of Physics, University of Ljubljana, Ljubljana; Slovenia.
- 94 School of Physics and Astronomy, Queen Mary University of London, London; United Kingdom.
- 95 Department of Physics, Royal Holloway University of London, Egham; United Kingdom.
- 96 Department of Physics and Astronomy, University College London, London; United Kingdom.
- 97 Louisiana Tech University, Ruston LA; United States of America.
- 98 Fysiska institutionen, Lunds universitet, Lund; Sweden.
- 99 Departamento de Física Teórica C-15 and CIAFF, Universidad Autónoma de Madrid, Madrid; Spain.
- 100 Institut für Physik, Universität Mainz, Mainz; Germany.
- 101 School of Physics and Astronomy, University of Manchester, Manchester; United Kingdom.
- 102 CPPM, Aix-Marseille Université, CNRS/IN2P3, Marseille; France.
- 103 Department of Physics, University of Massachusetts, Amherst MA; United States of America.
- 104 Department of Physics, McGill University, Montreal QC; Canada.
- 105 School of Physics, University of Melbourne, Victoria; Australia.
- 106 Department of Physics, University of Michigan, Ann Arbor MI; United States of America.
- 107 Department of Physics and Astronomy, Michigan State University, East Lansing MI; United States of America.
- 108 Group of Particle Physics, University of Montreal, Montreal QC; Canada.
- 109 Fakultät für Physik, Ludwig-Maximilians-Universität München, München; Germany.
- 110 Max-Planck-Institut für Physik (Werner-Heisenberg-Institut), München; Germany.

- ¹¹¹Graduate School of Science and Kobayashi-Maskawa Institute, Nagoya University, Nagoya; Japan.
- ¹¹²Department of Physics and Astronomy, University of New Mexico, Albuquerque NM; United States of America.
- ¹¹³Institute for Mathematics, Astrophysics and Particle Physics, Radboud University/Nikhef, Nijmegen; Netherlands.
- ¹¹⁴Nikhef National Institute for Subatomic Physics and University of Amsterdam, Amsterdam; Netherlands.
- ¹¹⁵Department of Physics, Northern Illinois University, DeKalb IL; United States of America.
- ¹¹⁶^(a)New York University Abu Dhabi, Abu Dhabi;^(b)University of Sharjah, Sharjah; United Arab Emirates.
- ¹¹⁷Department of Physics, New York University, New York NY; United States of America.
- ¹¹⁸Ochanomizu University, Otsuka, Bunkyo-ku, Tokyo; Japan.
- ¹¹⁹Ohio State University, Columbus OH; United States of America.
- ¹²⁰Homer L. Dodge Department of Physics and Astronomy, University of Oklahoma, Norman OK; United States of America.
- ¹²¹Department of Physics, Oklahoma State University, Stillwater OK; United States of America.
- ¹²²Palacký University, Joint Laboratory of Optics, Olomouc; Czech Republic.
- ¹²³Institute for Fundamental Science, University of Oregon, Eugene, OR; United States of America.
- ¹²⁴Graduate School of Science, Osaka University, Osaka; Japan.
- ¹²⁵Department of Physics, University of Oslo, Oslo; Norway.
- ¹²⁶Department of Physics, Oxford University, Oxford; United Kingdom.
- ¹²⁷LPNHE, Sorbonne Université, Université Paris Cité, CNRS/IN2P3, Paris; France.
- ¹²⁸Department of Physics, University of Pennsylvania, Philadelphia PA; United States of America.
- ¹²⁹Department of Physics and Astronomy, University of Pittsburgh, Pittsburgh PA; United States of America.
- ¹³⁰^(a)Laboratório de Instrumentação e Física Experimental de Partículas - LIP, Lisboa;^(b)Departamento de Física, Faculdade de Ciências, Universidade de Lisboa, Lisboa;^(c)Departamento de Física, Universidade de Coimbra, Coimbra;^(d)Centro de Física Nuclear da Universidade de Lisboa, Lisboa;^(e)Departamento de Física, Universidade do Minho, Braga;^(f)Departamento de Física Teórica y del Cosmos, Universidad de Granada, Granada (Spain);^(g)Departamento de Física, Instituto Superior Técnico, Universidade de Lisboa, Lisboa; Portugal.
- ¹³¹Institute of Physics of the Czech Academy of Sciences, Prague; Czech Republic.
- ¹³²Czech Technical University in Prague, Prague; Czech Republic.
- ¹³³Charles University, Faculty of Mathematics and Physics, Prague; Czech Republic.
- ¹³⁴Particle Physics Department, Rutherford Appleton Laboratory, Didcot; United Kingdom.
- ¹³⁵IRFU, CEA, Université Paris-Saclay, Gif-sur-Yvette; France.
- ¹³⁶Santa Cruz Institute for Particle Physics, University of California Santa Cruz, Santa Cruz CA; United States of America.
- ¹³⁷^(a)Departamento de Física, Pontificia Universidad Católica de Chile, Santiago;^(b)Millennium Institute for Subatomic physics at high energy frontier (SAPHIR), Santiago;^(c)Instituto de Investigación Multidisciplinario en Ciencia y Tecnología, y Departamento de Física, Universidad de La Serena;^(d)Universidad Andres Bello, Department of Physics, Santiago;^(e)Instituto de Alta Investigación, Universidad de Tarapacá, Arica;^(f)Departamento de Física, Universidad Técnica Federico Santa María, Valparaíso; Chile.
- ¹³⁸Department of Physics, University of Washington, Seattle WA; United States of America.
- ¹³⁹Department of Physics and Astronomy, University of Sheffield, Sheffield; United Kingdom.
- ¹⁴⁰Department of Physics, Shinshu University, Nagano; Japan.

- ¹⁴¹Department Physik, Universität Siegen, Siegen; Germany.
- ¹⁴²Department of Physics, Simon Fraser University, Burnaby BC; Canada.
- ¹⁴³SLAC National Accelerator Laboratory, Stanford CA; United States of America.
- ¹⁴⁴Department of Physics, Royal Institute of Technology, Stockholm; Sweden.
- ¹⁴⁵Departments of Physics and Astronomy, Stony Brook University, Stony Brook NY; United States of America.
- ¹⁴⁶Department of Physics and Astronomy, University of Sussex, Brighton; United Kingdom.
- ¹⁴⁷School of Physics, University of Sydney, Sydney; Australia.
- ¹⁴⁸Institute of Physics, Academia Sinica, Taipei; Taiwan.
- ¹⁴⁹^(a)E. Andronikashvili Institute of Physics, Iv. Javakhishvili Tbilisi State University, Tbilisi;^(b)High Energy Physics Institute, Tbilisi State University, Tbilisi;^(c)University of Georgia, Tbilisi; Georgia.
- ¹⁵⁰Department of Physics, Technion, Israel Institute of Technology, Haifa; Israel.
- ¹⁵¹Raymond and Beverly Sackler School of Physics and Astronomy, Tel Aviv University, Tel Aviv; Israel.
- ¹⁵²Department of Physics, Aristotle University of Thessaloniki, Thessaloniki; Greece.
- ¹⁵³International Center for Elementary Particle Physics and Department of Physics, University of Tokyo, Tokyo; Japan.
- ¹⁵⁴Department of Physics, Tokyo Institute of Technology, Tokyo; Japan.
- ¹⁵⁵Department of Physics, University of Toronto, Toronto ON; Canada.
- ¹⁵⁶^(a)TRIUMF, Vancouver BC;^(b)Department of Physics and Astronomy, York University, Toronto ON; Canada.
- ¹⁵⁷Division of Physics and Tomonaga Center for the History of the Universe, Faculty of Pure and Applied Sciences, University of Tsukuba, Tsukuba; Japan.
- ¹⁵⁸Department of Physics and Astronomy, Tufts University, Medford MA; United States of America.
- ¹⁵⁹United Arab Emirates University, Al Ain; United Arab Emirates.
- ¹⁶⁰Department of Physics and Astronomy, University of California Irvine, Irvine CA; United States of America.
- ¹⁶¹Department of Physics and Astronomy, University of Uppsala, Uppsala; Sweden.
- ¹⁶²Department of Physics, University of Illinois, Urbana IL; United States of America.
- ¹⁶³Instituto de Física Corpuscular (IFIC), Centro Mixto Universidad de Valencia - CSIC, Valencia; Spain.
- ¹⁶⁴Department of Physics, University of British Columbia, Vancouver BC; Canada.
- ¹⁶⁵Department of Physics and Astronomy, University of Victoria, Victoria BC; Canada.
- ¹⁶⁶Fakultät für Physik und Astronomie, Julius-Maximilians-Universität Würzburg, Würzburg; Germany.
- ¹⁶⁷Department of Physics, University of Warwick, Coventry; United Kingdom.
- ¹⁶⁸Waseda University, Tokyo; Japan.
- ¹⁶⁹Department of Particle Physics and Astrophysics, Weizmann Institute of Science, Rehovot; Israel.
- ¹⁷⁰Department of Physics, University of Wisconsin, Madison WI; United States of America.
- ¹⁷¹Fakultät für Mathematik und Naturwissenschaften, Fachgruppe Physik, Bergische Universität Wuppertal, Wuppertal; Germany.
- ¹⁷²Department of Physics, Yale University, New Haven CT; United States of America.
- ^a Also Affiliated with an institute covered by a cooperation agreement with CERN.
- ^b Also at An-Najah National University, Nablus; Palestine.
- ^c Also at Borough of Manhattan Community College, City University of New York, New York NY; United States of America.
- ^d Also at Center for High Energy Physics, Peking University; China.
- ^e Also at Center for Interdisciplinary Research and Innovation (CIRI-AUTH), Thessaloniki; Greece.
- ^f Also at Centro Studi e Ricerche Enrico Fermi; Italy.
- ^g Also at CERN, Geneva; Switzerland.

- h* Also at Département de Physique Nucléaire et Corpusculaire, Université de Genève, Genève; Switzerland.
- i* Also at Departament de Física de la Universitat Autònoma de Barcelona, Barcelona; Spain.
- j* Also at Department of Financial and Management Engineering, University of the Aegean, Chios; Greece.
- k* Also at Department of Physics, Ben Gurion University of the Negev, Beer Sheva; Israel.
- l* Also at Department of Physics, California State University, Sacramento; United States of America.
- m* Also at Department of Physics, King's College London, London; United Kingdom.
- n* Also at Department of Physics, Stanford University, Stanford CA; United States of America.
- o* Also at Department of Physics, University of Fribourg, Fribourg; Switzerland.
- p* Also at Department of Physics, University of Thessaly; Greece.
- q* Also at Department of Physics, Westmont College, Santa Barbara; United States of America.
- r* Also at Hellenic Open University, Patras; Greece.
- s* Also at Institutio Catalana de Recerca i Estudis Avancats, ICREA, Barcelona; Spain.
- t* Also at Institut für Experimentalphysik, Universität Hamburg, Hamburg; Germany.
- u* Also at Institute for Nuclear Research and Nuclear Energy (INRNE) of the Bulgarian Academy of Sciences, Sofia; Bulgaria.
- v* Also at Institute of Applied Physics, Mohammed VI Polytechnic University, Ben Guerir; Morocco.
- w* Also at Institute of Particle Physics (IPP); Canada.
- x* Also at Institute of Physics and Technology, Mongolian Academy of Sciences, Ulaanbaatar; Mongolia.
- y* Also at Institute of Physics, Azerbaijan Academy of Sciences, Baku; Azerbaijan.
- z* Also at Institute of Theoretical Physics, Ilia State University, Tbilisi; Georgia.
- aa* Also at L2IT, Université de Toulouse, CNRS/IN2P3, UPS, Toulouse; France.
- ab* Also at Lawrence Livermore National Laboratory, Livermore; United States of America.
- ac* Also at National Institute of Physics, University of the Philippines Diliman (Philippines); Philippines.
- ad* Also at Technical University of Munich, Munich; Germany.
- ae* Also at The Collaborative Innovation Center of Quantum Matter (CICQM), Beijing; China.
- af* Also at TRIUMF, Vancouver BC; Canada.
- ag* Also at Università di Napoli Parthenope, Napoli; Italy.
- ah* Also at University of Chinese Academy of Sciences (UCAS), Beijing; China.
- ai* Also at University of Colorado Boulder, Department of Physics, Colorado; United States of America.
- aj* Also at Washington College, Chestertown, MD; United States of America.
- ak* Also at Yeditepe University, Physics Department, Istanbul; Türkiye.
- * Deceased